COMPONENT AND FAULT IDENTIFICATION IN A MACHINE STRUCTURE USING AN ACOUSTIC SIGNAL

by

AFARIN ORDUBADI

MSc. Polytechnic Institute of New York
(1976)

SUBMITTED IN PARTIAL FULFILLMENT
OF THE REQUIREMENTS FOR THE
DEGREE OF

DOCTOR OF SCIENCE

at the

MASSACHUSETTS INSTITUTE OF TECHNOLOGY

May 1980

Signature of Author Signature redacted
Department of Mechanical Engineering
May 2, 1980

Certified by Signature redacted
Richard H. Lyon
Thesis Supervisor

Accepted by Signature redacted
Warren Rohsenow
Chairman, Departmental Committee

COMPONENT AND FAULT IDENTIFICATION IN A MACHINE STRUCURE USING AN ACOUSTIC SIGNAL

by

AFARIN ORDUBADI

Submitted to the Department of Mechanical Engineering
on May 16, 1980 in partial fulfillment
of the requirements for the Degree of Doctor of Science in
Mechanical Engineering

ABSTRACT

Analytical approach to vibration signature analysis for fault detection has been considered impractical because of the difficulties in defining a sufficiently accurate vibration transfer function, VTF. The feasibility of such analysis has been demonstrated in this study by accurate reconstruction of the cylinder pressure of a diesel engine using measured acceleration on the block.

Determining VTF in structures with complicated geometries requires understanding the exact vibration transfer mechanisms in the machine structures. The vibration on the surface of the machine is the result of traveling wave propagation in the structure as well as formation of resonances because of the reflections from the engine boundaries and interfaces. The VTF of both modes of vibration transfer for the diesel engine studied was modeled. The VTF was measured on a non-running engine and an operating engine. This latter VTF was modified to result in three other VTFs; one representing multipath propagation, one single path propagation, and one a simple resonance.

The five VTFs were used for estimating cylinder pressure from engine block acceleration measured at several operating conditions of the engine. The accuracy of reconstructed cylinder pressures was determined by comparing it with the measured cylinder pressure. The accuracy was evaluated quantitatively using several performance indices.

The estimated cylinder pressures using measured VTF on non-running and operating engine was satisfactory. However, the most accurate estimate of cylinder pressure was obtained by using the modified VTF which represents multipath propagation. This VTF remained unchanged during a reasonable period of engine life under normal wear and was insensitive to variations resulting from re-assembly of the engines.

Simulated leak of an engine injector and the location of a faulty cylinder was detected using the above method. A technique to separate the effect of secondary vibration sources such as piston slap in engines is suggested. The results of this study can be generalized for machines other than engines. Possibilities for on-line application of this method is discussed.

Thesis Supervisor: Richard H. Lyon
Title: Professor, Department of Mechanical Engineering

ACKNOWLEDGEMENT

In the years to come, I'll remember MIT with pride and a warm feeling toward all the people who helped me during the course of my studies. I am grateful to all of them.

I am honored to have worked with Professor Richard H. Lyon, his wise guidance and intelligent criticism made the research a rewarding experience for me.

I am grateful for the enthusiasm and active participation of members of my doctorate committee; Dr. Richard R. DeJong, Prof. H. Paynter and Prof. P. Houpt. Their creative suggestions contributed substantially to the results of this study.

I would like to express my gratitude to J. W. Slack, III, for his technical advice and assistance and in particular for his friendship and moral support, and to M. Toscano for her numerous administrative help and editing and typing the manuscript of this thesis.

The assistance of W. Finley, W. S. Laird, A. Felch and N. Parsons in operating the engine and data acquisition is greatly appreciated.

I am grateful to Prof. K. N. Stevens and Dr. R. DeJong

for providing me the access to computer facilities at RLE and Cambridge Collaborative, Inc. and to G. M. Glass for helping me in using the latter facility.

The encouragement of my family, and especially my mother throughout these years is greatly appreciated.

Finally, there is a special thanks due to Jeanne R. Pamilla, without her I would have never come this far.

This research was partially supported by an ONAC-EPA sub-contract from Cambridge Collaborative Inc. to MIT.

TABLE OF CONTENTS

TABLE OF CONTENTS (CONTINUED)

TABLE OF CONTENTS (CONTINUED)

LIST OF FIGURES

LIST OF FIGURES (CONTINUED)

LIST OF FIGURES (CONTINUED)

LIST OF FIGURES (CONTINUED)

LIST OF FIGURES (CONTINUED)

GLOSSARY OF SYMBOLS

$A(\omega)$	Acceleration
DVTF	Vibration transfer function of operating engine
$E(\omega)$	Error
$F(\omega)$	Force
FT	Fourier transform
$I(\omega)$	input inertance
$P(\omega)$	Cylinder pressure
R	Correlation
S	Sample variance
T	Sampling period
SVTF	Vibration transfer function measured on non-running engine
VTF	Vibration transfer function
a(n)	Acceleration
c_b	Bending phase speed
C_{ph}	Phase speed
f(n)	Force
f	Frequency
h(n)	Impulse response
j	$\sqrt{-1}$
k	Wavenumber
n	Sample number

GLOSSARY OF SYMBOLS (CONTINUED)

$p(n)$	Cylinder pressure
$p_1(n)$	Compression cycle
$p_2(n)$	Combustion cycle
t	Time
$u(n)$	Unit step
$v(n)$	Variance
$w(n)$	Weighting function
$\alpha(\omega)$	Ratio of vibration transfer function for piston slap to vibration transfer function for combustion force
$\beta(\omega)$	The ratio of piston slap to combustion
$\delta(n)$	Kronecker delta
η	Damping loss factor
ε	Error
ρ_s	Surface density
ρ_{x_1,x_2}	Correlation coefficient of two signals x_1 and x_2
ω	Radian frequency
SUBSCRIPTS	
c	Combustion forces
d	Direct propagation
r	Reverberant field
p	Piston Slap

GLOSSARY SYMBOLS (CONTINUED)

Superscript

~	Estimated signal
^	Cepstrum

DEFINITIONS

Following definitions has been used in this report.

Cepstrum(^): of a signal is the inverse fourier transform of logarithm of fourier transform of the signal $\hat{x}(n) = FT^{-1}(\ell n\ F\ T(x(n))$.

Convolution(*): of two signals, $x_1(n)$, and $x_2(n)$, $y(n)$ is defined as:

$$y(n) = x_1(n)*x_2(n) = \sum_{k=-\infty}^{n} x_1(k)x_2(k-n).$$

Data record: A finite sequence used for processing.

Discrete time, sample number, n,: Integer multiples of sampling period T.

Linear time system, LTI: A linear system for which if $y(n)$ is the response to input $x(n)$, then the response to $x(n-k)$ is $y(n-k)$.

Linear constant coefficient difference equation: A subclass of LTI systems for which input and output are related by a M^{th} order difference equation. The impulse response of the system is then represented as the sum of M exponentials

$$h(n) = \sum_{k=0}^{M-1} (b_k)^n .$$

DEFINITIONS (CONTINUED)

Minimum Phase Signal/ System:	A stable system/signal with stable inverse.
Signal:	A functional that conveys information.
Sequence, x(n):	A signal that is defined only for n integer multiples of a sampling period, T. A sequence or discrete time signal may arise by sampling a continuous signal or may be generated directly from a digial process.

CHAPTER I: INTRODUCTION

Early detection of failures within a system is important in preventing further damage to the system and other possible hazardous consequences. Fault detection and monitoring have been the subject of much research in system dynamics and control. In complicated systems, direct access to a particular part of the system is not often possible or practical. In such cases, a *transformed* version of the output signal of the subystem under study is measured at the periphy of the system and is used in monitoring its operation.

If the transformation is broad band and linear, the transformed signal is a replica of the original signal, e.g., the transformation of a mechanical signal to an electrical signal in a transducer. The measured signal is equivalent to the output signal and can be used directly to control the operation of the system. In practice, the transformation is often narrow band, complicated and sometimes nonlinear, such as acoustic emission of signals from cracks. In this case, in order to use the observed signal for monitoring or fault detection, the effect of the transformation must be either minimized (recovery of original signal), or the changes in the observed signal must be related to the abnormalities that occur in the original signal.

The observable manifestation of the output signal of a system is sometimes called the *signature of the system.* When a particular event occurs within the system, the changes in the normal pattern of the system signature is called *signature of the event.* This system signature can be of any physical nature; optical, electrical, acoustical, etc.

Traditionally, the acoustical signatures of physical systems are considered good indicators of the operations of the system. Just as doctors use heart beats to diagnose the status of a patient's health, mechanics "listen" to an engine in order to detect its problems. The vibration signal of a mechanical structure is the result of fluctuating forces acting within the system and the changes in the signature represent the changes in these forces. The radiation of vibration from surfaces of the machine produces an acoustical signal.

Two methods are used in detection of faults through vibration signals; analytical and data base pattern recognition. The analytical approach is one which relates the features in the observed signal to system changes by determining the transformation between the original signal/event and the observed signal. The transfer function TF, of the transformation can be used to recover the original output signal. The major difficulty in using this method is in defining the transfer function in a complex system.

In the data base pattern recognition method, a set of features in the signature which are related to the faults in the system are identified experimentally. Based on measurements taken on "normal" and "faulty" systems, several criteria are established for discriminating between the two. This method is very useful when the exact transformation between the original signal and its signature is not known, is difficult to find, or when the transformation is nonlinear. The disadvantages of the data base method are that accuracy of results require collecting a large amount of data. In addition, the processing usually involves manipulation of large matrices. Also, the uncertainty in associating a particular feature to a particular fault may never be as small as desired. However, the development of fast computers with large memories has made this method very popular.

In seismology, signature analysis has been used to recover the seismic wavelets from the measured vibration signal excited by a source hundreds of miles away. The vibration signal is transferred through the earth. In these studies, the earth is modeled as a layered medium. The properties of impulse response of the earth is determined. This impulse response is used to deconvolve the received vibration and to recover the seismic wavelets. The success of these studies show that when the TF of the *path* system is known, the analytical approach to vibration signature analysis is feasible. In most machines, determining the vibration transfer

function, VTF, is difficult as a result of the complicated geometry of the machine.

The relationship between fluctuating forces in a machine and vibration of its surface have been the subject of many studies in machinery noise control. The main purpose of these studies is in modifying the vibration trasfer path to reduce the surface vibration and, therefore, the radiated noise. For these studies, an approximate estimation of the magnitude of the VTF is sufficient. Usually, an error of 3 to 5 dB in magnitude is acceptable and the phase characteristics are neglected. Because of the uncertainty in defining the mechanism of the VTF and the contaminating effect of different sources on surface vibration, some researchers have stated that recovery of input forces from surface vibration is not practical [1].

Most studies on vibration signature analysis have been concentrated on the data base method. Some of these studies, aimed at finding features to detect particular failure(s) had limited success, especially in monitoring flight instrumentation and nuclear reactors [2]. However, it is reported that some of the heavily financed programs that attempt to collect a huge amount of data regarding features to detect faults have failed as a result of a lack of proper analysis.

The aim of this study is to show that modeling an acoustical system with an accurate input-output relationship is feasible. Determining a vibration transfer function, VTF, for machine that is accurate enough for fault diagnosis purposes does not vary from one run to another is the goal. Such a VTF should be linear, insensitive to practical variation of the machine properties in assembly and remains unchanged during a reasonable period of life of the machine under normal wear. This VTF can be used either in reconstruction of the internal forces of the machine from its surface vibration, or in reflecting the changes in the forces as a result of malfunction on the surface vibration.

The approach of this research is to define a VTF for the machine, to use the VTF in recovery of the input signal from the vibration at the surface, and to evaluate the procedure by comparing the estimated and measured inputs. When there are ambiguities involved in modeling the VTF, several VTFs based on different possible models are determined and the performance of each in accurate reconstruction of input under different operating conditions of the machine are evaluated and compared. This approach not only identifies the best VTF for fault diagnosis, but gives an insight to vibration transfer mechanisms in the machine. This method is suitable for studying a variety of machine structures such as engines, turbines, airplanes, sewing machines, etc. In addition,

the acoustic signature of other physical and biological systems can be analyzed using this method, .e.g., heart beats.

The particular system under study for this research was a four-cylinder naturally aspirated diesel engine. The particular "input" of interest to the system is the combustion force; the observed signal or "output" is the block acceleration and the TF is the VTF of the engine between a cylinder and a fixed observation point on the engine. In addition to diagnosis of malfunction in cylinder pressure, the possibility of localizing the faulty component by the above method is investigated. Some of the faults in the engine operation which affect the combustion force or equivalent cylinder pressure, are injector malfunctions and deposits inside the cylinders. In addition, there are malfunctions which are reflected in piston slap, such as piston ring malfunction. The VTF of a machine also changes as a result of a drastic change in mechanical properties such as a crack at the components of the engine which transfer vibration.

The vibration produced by combustion force is transferred to the block through two paths: piston-crankshaft-bearing path and the path through the head [3]. The acceleration at any point on the engine block is the result of propagated waves as well as the re-

flections from boundaries of the system. The VTF of the engine should represent both the directly propagated waves as well as the echoes. In this study, two types of VTF, one representing propagation mode, and the other, resonance mode of the engine vibration transfer and the combination of both types of VTF are considered. The performance of these VTFs in estimating cylinder pressure is evaluated. Both types of VTF are common in most machine structures.

This study is not concerned with the particular problem of fault diagnosis in diesel engines. Rather it uses the engine to demonstrate the feasibility of fault diagnosis in machine structures using vibration signal(s). The engine is a typical example of a machine, and many of the problems encountered in defining VTF and recovering the input forces in engine are similar to those that exist in other complicated mechanical systems. The signal processing techniques used were all general. The classical linear filtering methods which do not rely on any particular properties of the signal were used extensively.

The first Chapter of this report is concerned with review of the previous studies done on related subjects. Chapter II is concerned with modeling the system, input signal and different VTFs. The measurement and processing techniques to obtain VTF on running and non-running engines as well as the determined VTFs is discussed in Chapter III. In all, five VTFs were measured or derived from the data.

In Chapter IV, the deconvolution of acceleration signals with the measured/constructed VTFs to obtain estimates of the input cylinder pressure is studied. These estimated pressure signals are compared with the measured pressure signal to evaluate the accuracy of estimation and the performance of the VTF. The application of this method in fault diagnosis in engines, an algorithm to eliminate the effect of sources other than combustion as well as practical considerations in implementing the method are the subjects of Chapter V.

1.1 Several Studies in Acoustics Signatures Analysis

Acoustics signature of a machine has been used to detect the status of the machine for many years. Development of high quality transducers and real time spectrum analysis has made this type of analysis more feasible for industrial usage. In this section some of the studies on acoustics signatures analysis are mentioned.

The relationship between excessive vibration of a rotary machine and problems such as machine imbalances, misalignments and improper installation has been studied in classical mechanics. In the past twenty years, industrial usage of vibration level for detection of these faults have increased and several vibration criteria has been developed (4).

Fault diagnosis using vibration level is limited to detection of malfunctions that effect first few harmonics of the exciting forces. A recent study by NASA is concerned with detection of bearing failures using high frequency acoustics emission of the bearings [5].

Early detection of failures in nuclear reactors is essential. Monitoring the core components of a reactor using the noise emission of these components has been studied extensively [6]. These studies were focused on finding a data base pattern recognition scheme for automatic monitoring of the plant.

Statistical and pattern recognition scheme were also used in quality control of gear boxes. The level and spectrum of the noise generated by the gear box was used to distinguish the faulty gears by an electronic device [7].

As a result of research in speech processing, many new processing techniques such as cepstrum analysis (see definition) has been developed. The usage of this new technique in detection of gear malfunction has been proposed [8].

The changes in transfer characteristics and mechanical impedance of components were also used in diagnosing their failure

One of these studies were concerned with the relationship between the failure of a bearing and its seal and the input inertance of the bearing support [9]. In another study on off shore platforms, the dynamic response of the platform were used to detect its structural problems [10].

Undoubtedly the most extensive research on acoustic signature analysis to date has been in the fields of seismology and geophysics. In the past 20 years development of fast computers and the field of digital signal processing has helped the growth of research in these fields.

In seismology, reconstruction of seismic wavelets occurred hundreds of miles from the observation point is desired. It has been shown that when the general characteristics of the path system, in this case, earth,is known, reconstruction of wavelets is possible [11]. In geophysics, accurate determination of the impulse response of the earth is desired for detection of minerals and specially petroleum.

The idea of analytical approach to vibration signature analysis has been initiated by the results of recent studies on correlation between the exciting forces in a machine and is generated noise as well as the research in modeling vibration transfer function [3]. Studies on relation between generated noise of a diesel engine and engine operating condition have shown a high

degree of correlation between the two [12].

CHAPTER II: MODELING THE SYSTEM

The machine used for this study is a John Deere Model 419 diesel engine. The engine has four cylinders and is four-stroke, naturally aspirated, and directly injected. The balancing shafts on the engine decrease inertial forces. The "input" signal to the system is defined to be the combustion force, the "output" is the acceleration on the engine block, and the "transfer function" is the vibration transfer function, VTF, between the combustion force and the engine block acceleration.

In addition to the combustion force, there are other sources of excitation in the engine, such as piston slap and the opening and closing of the valves. The most important of these forces is piston slap [13]. Piston slap is more of an impulse-like excitation than is the combustion force pulse.

All of the excitation forces are sequential, i.e., the cylinders fire one after another, and the acceleration caused by the excitation of one cylinder attenuates before the next cylinder fires. The secondary sources are also sequential. Generally, their time of occurrence is different from that of the combustion force.

The vibration caused by the combustion force propagates throughout the system via piston, crank shaft and bearings, and the engine head. The engine is not an infinite system; therefore,

acceleration at any point on the engine block is the result of direct vibration propagation as well as reflections from the boundaries of the system. The engine may be modeled as a "reverberant" system if the engine of the reflected vibration waves is higher than that of the directly propagated waves. If the directly propagated vibration energy is dominant, the reverberant vibration is neglected and hence the vibration transfer is treated as a multipath wave propagation in a dispersive medium.

Modeling the engine as a system and the conditions under which it may be simplified to a single input-single output system is the subject of this Chapter. In addition, the characteristics of the combustion force or equivalent cylinder pressure will be studied. The vibration transfer in the engine and the techniques to measure it as well as the effects of secondary sources on VTF will be discussed.

2.1 Modeling the System

The engine, in general, is a multi-input, multi-output system. Its inputs are combustion and other forces, and its output(s) are vibration (acceleration) of a given point(s) on the block. If the study of acceleration at a particular fixed observation point is desired, then the system is single output. The combustion force is sequential and the acceleration, excited by the firing of any cylinder, is attenuated before the firing of the next cylinder occurs.

If combustion is the dominant force, in a short time frame of about 180° crank angle, the engine is treated as having a single input.

As the pistons move, the vibration transfer path of the engine varies slightly. However, the following assumptions are made:

(a) Although the combustion force is not impulsive, the duration of the force signal is short compared with the engine cycle [14].

(b) The variation in the transfer function during occurrence of cylinder pressure is negligible [15].

Under the above assumptions, we will regard the engine as a linear time invariant system with a single input and a single output. The output acceleration at any observation point, a(n), is the convolution of input force, f(n), and the system impulse response $h_c(n)$ to the force. In a short time window, N_0, equal to one-half of an engine revolution (180° crank angle), the acceleration is:

$$a(n) = h_c(n) * f(n) \qquad N_1 \leq n \leq N_1 + N_0 \tag{2.1}$$

where n, discrete time (sample number) is equal to t/T and T is sampling period, N_1 is the firing time of a particular cylinder, and the convolution of two signals is defined as:

$$a(n) = \sum_{j=0}^{h} f(j)\, h_c(n-j)$$

In order to account for the effect of all of the cylinders, a(n) is defined as:

$$a(n) = \sum_{i=1}^{4} h_{ci}(n) * f_i(n) \qquad (2.2)$$

where $f_i(n)$ is the force inserted by the cylinder i and $h_i(n)$ is the impulse response of the system to a force applied at cylinder i. The force f_i is proportional to pressure in cylinder i when cylinder fires; once every full cycle of engine, which in a four stroke engine is two revolutions. The force is zero otherwise. In each engine full cycle f_i is:

$$f_i \quad \alpha \quad \text{cylinder pressure} \quad (k-1)\, N_o < n < kN_o$$
$$k = 1,2,3,4 \qquad (2.3)$$
$$0 \quad \text{otherwise}$$

where k is an integer that defines the firing order. For the John Deere engine under study, the firing order is 1-3-4-2. Therefore, the relation between i and k is as follows:

for	k = 1	i = 1
	k = 2	i = 3
	k = 3	i = 4
	k = 4	i = 2

To account for variation in the transfer path during combustion h(n) may be defined as *time-invariant*. In measuring VTF on non-running engine, h(n) is assumed to be time invariant.

The effect of forces other than combustion may be taken into account by modifying Eq. (2.2) to result in Eq. (2.4):

$$a(n) = \sum_{i=1}^{4} \sum_{k=1}^{P} f_{ik}(n) * h_{ik}(n) + \phi(n) \qquad (2.4)$$

where f_{ik} is the excitation force, h_{ik} is the time variant impulse response of VTF between observation point and diffferent force inputs

and $\phi(n)$ is noise. The f_{ik}'s are of the general form of Eq. 2.3.

2.2 The Excitation -- Cylinder Pressure

The combustion in the cylinder is the principal excitation force in an operating engine under load. This force is associated with cylinder pressure of the operating engine:

$$f(n) = \int_A p(n)\, dA$$

where A is the area of the piston top and $p(n)$ and $f(n)$ are cylinder pressure and the combustion force.

The variation of the cylinder pressure has the following five stages [16]:

(1) The Compression Cycle. During the early part of the process, before the injector opens, the air in the cylinder is compressed and pressure rises slowly.

(2) Ignition Delay. After the injector valve opens, the fuel is injected into the cylinder; however, the temperature is not high enough to cause ignition. The pressure may *drop* in this stage.

(3) Heat Release. Combustion occurs and pressure rises very rapidly (knocking).

(4) Slow Burning. After a period of rapid pressure rise, fuel burns slowly, pressure rises slightly or stays steady.

(5) Pressure Drop. The expansion cycle begins and pressure drops rapidly.

The total pressure cycle last for about 90° crank angle. Typically, the pressure cycle starts at 20° crank angle before top dead center, TDC, and ends 60° to 70° crank angle after TDC (Fig. 2.1).

The pressure signal may be divided into two parts: compression and combustion. The compression cycle varies slowly with crank angle. The combustion cycle has a short duration and fluctuates rapidly. The operating condition of the engine affects the compression and the combustion cycles as well as the relative timing between the two. One cycle of the pressure signal, p(n) may be defined as:

$$p(n) = A_1 p_1(n) + A_2 p_2(n)\ u(n-n_\ell) \qquad (2.5a)$$

where $p_1(n)$ is compression cycle, $p_2(n)$ is the combustion cycle, A_1 and A_2 are gain factors, n_ℓ in the initiation of combustion and u(m) is the step function

$$u(m) = \begin{matrix} 1 & 0 \leq m \\ 0 & m \leq 0 \end{matrix}$$

TABLE 2.1: PARAMETERIC REPRESENTATION OF CYLINDER PRESSURE

A: at 1500 rpm
N_S = 256

Load (%) Full load	Compression Cycle					Combustion Cycle				
	A_1 (bar)	a_o	a_1	a_2	a_3	A_2 (bar)	n_ℓ	b_o	b_2 mag.	b_2 phase (rad x 10^3)
100	25	.7	.98	.8	.8	50	41	.7	.98	3.14
60	24.3	.7	.96	.8	.82	46	51	.7	.98	3.77
0	21.8	.7	.97	.8	.85	14	72	.7	.98	6.01
B: at 2500 rpm N_S = 160										
50	50	.7	.98	.83	.82	37.14	32	.7	.93	9.4
0	32.8	.7	.46	.81	.86	14.2	56	.7	.95	6.3

*b_2 is a complex number

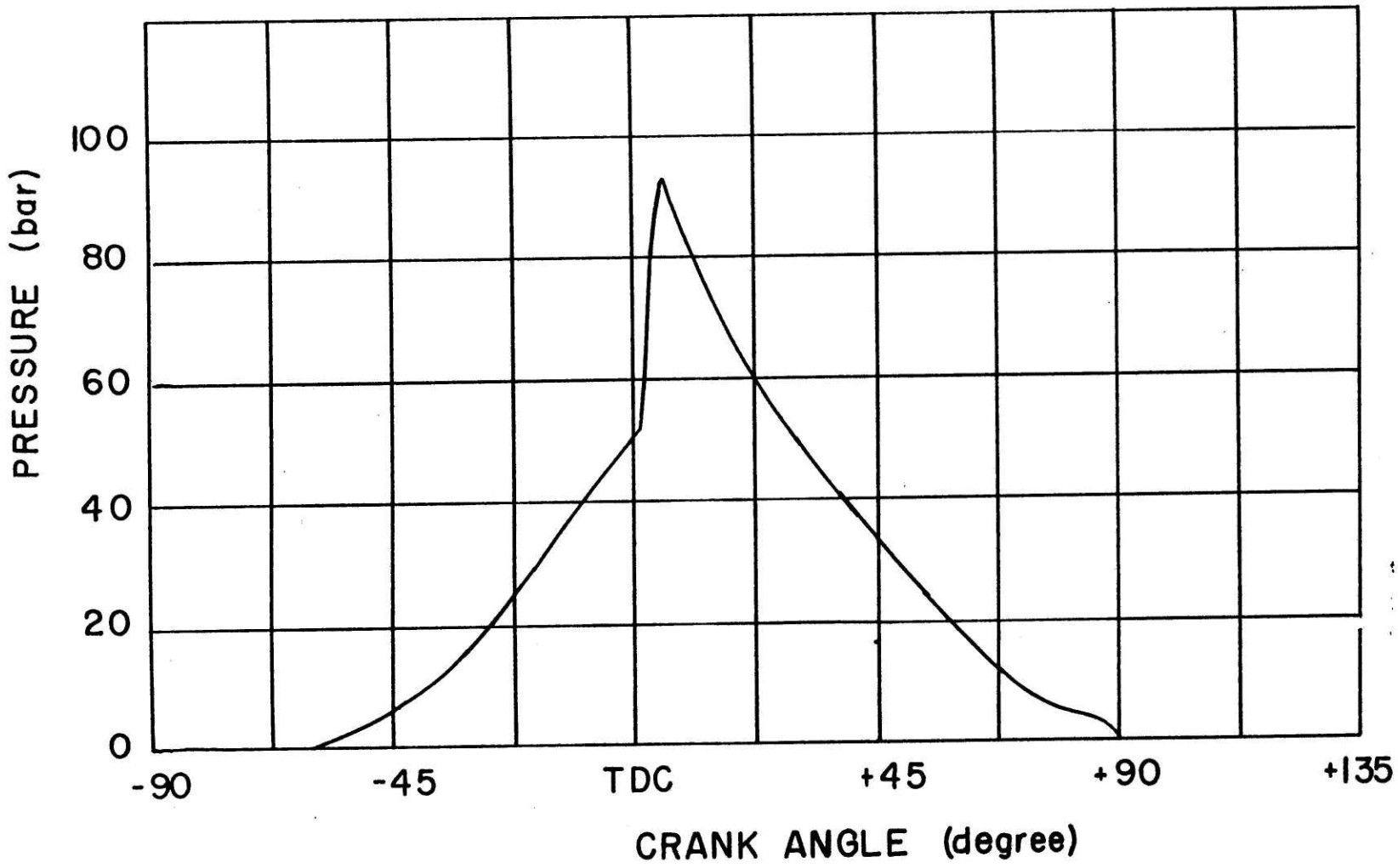

Figure 2.1: Theoretical Cylinder Pressure Trace for a Diesel Engine

The parameters A_1, A_2, $p_2(n)$ and n_ℓ are affected by the operating condition of the engine and its abnormalities. Detection of these parameters are important in diagnosing engine malfunction, e.g., the presence of deposits in the cylinder will decrease both A_1 and A_2; incorrect injector timing will effect n_ℓ; abnormalities in injection system will change $p_2(n)$ and n_ℓ. The parameters are also affected by the load on the engine under normal conditions (see Chapter III). The measurements, as well as a literature study [17] indicate that the shape of the compression cycle does not change significantly with the operating condition of the engine.

For the John Deere engine, p(n) at different operating conditions may be modeled from the measured cylinder pressure. The compression cycle, $p_1(n)$ is modeled by measuring the cylinder pressure when the injector is shut off, therefore, no combustion occurs. The other parameters are found by measuring cylinder pressure of the engine, operating at 1500 rpm and no load, as well as at 60% and 90% of full load.

The compression cycle, $p_1(n)$ is modeled with the first four harmonics of firing frequency ω_f (Fig. 2.2). The signal is not minimum phase and is rotated in time [18]:

$$p_1(n) = \sum_{k=1}^{3} a_k \exp\left[j\omega_f k T(n-n_s)\right] + a_0 \qquad (2.6)$$

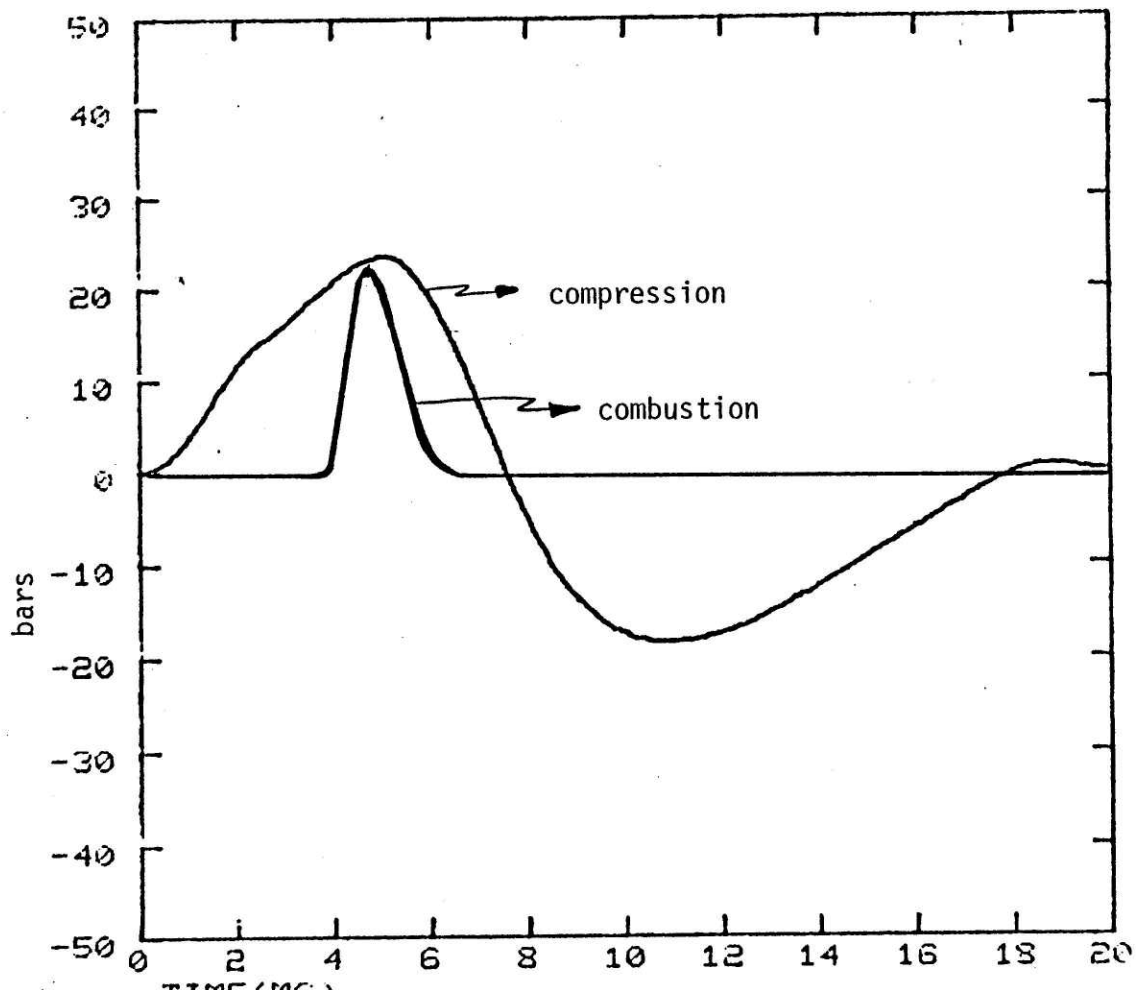

FIG. 2.2:- COMPRESSION AND COMBUSTION CYCLES OF CYLINDER PRESSURE

$p_2(n)$ is modeled with two poles and is minimum phase.

$$p_2(n) = (b_1)^n + b_o \tag{2.7}$$

The measured values of a_k's, b_k's and A_1 and A_2 for the engine operating at 1500 rpm under different loads is given in Table 2.1.

Changing speed will change the fundamental frequency of cylinder pressure. For $p_1(n)$ all frequency components will shift, but the combustion cycle $p_2(n)$ does not change significantly. The parameters found for the cylinder pressure measured at 2500 rpm is also given in Table 2.1.

Equation 2.5 is not a unique mathematical representation of the cylinder pressure. Another possible model for cylinder pressure results from studying the *cepstrum* of the signal [18]. The cepstrum of a signal is the inverse fourier transform of the logarithm of its fourier transform. The cepstra of cylinder pressure under different loads (Fig. 2.3) depend on load for sample number, n, less than 100 and especially for 25 <n< 75. This observation suggests that the cepstrum of cylinder pressure, $\hat{p}(n)$ can be modeled as the sum of two functions, $\hat{p}_\alpha(n)$ and $\hat{p}_\beta(n)$ of which only $\hat{p}_\alpha(n)$ depends on load:

$$\hat{p}(n) = \hat{p}_\alpha(n) + \hat{p}_\beta(n) \tag{2.8}$$

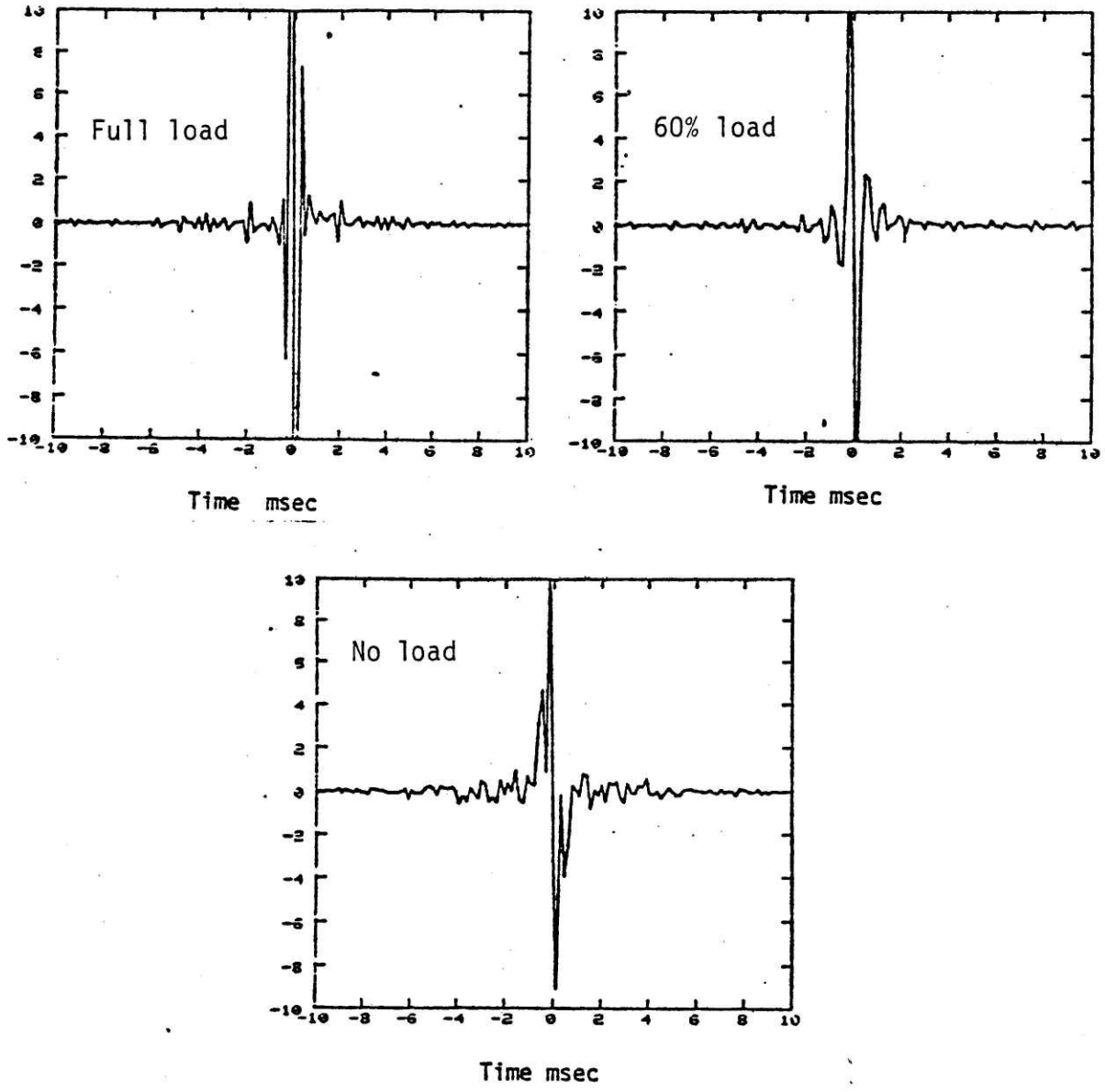

Figure 2.3 Cepstrum of Measured Cylinder Pressure for John Deere Deisel Engine

(a) Full load

(b) 60% load

(c) No load

where

$$\hat{p}_{\alpha}(n) = 0 \text{ for } n \geq 75$$

$$\hat{p}_{\beta}(n) = 0 \text{ for } n \leq 75.$$

The two signals can be easily separated by windowing $\hat{p}(n)$.

If $\hat{p}_{\alpha}(n)$ and $\hat{p}_{\beta}(n)$ were the cepstra of the signals $\hat{p}_{\alpha}(a)$ and $p_{\beta}(n)$, taking the inverse cepstrum of both sides of Equation 2.6 will result in representing p(n) by convolution of the two signals $p_{\alpha}(n)$ and $p_{\beta}(n)$:

$$p(n) = p_{\alpha}(n) * p_{\beta}(n) \tag{2.9}$$

$p_{\alpha}(n)$ is shown in Fig. 2.4.

The physical significance of $p_{\alpha}(n)$ and $p_{\beta}(n)$ is not clear at the present time. The spectrum of $p_{\alpha}(n)$ varies slowly with frequency while the spectrum of $p_{\beta}(n)$ is similar to that of a combination filter and is periodic in frequency. This type of representation is useful in cepstral analysis of the acceleration (Section 5.4) Although cepstral domain analysis is a promising technique in diagnosing faults in engines, a better knowledge of pressure signal is necessary before cepstral analysis can be applied successfully to fault detection problems. Special emphasis in understanding

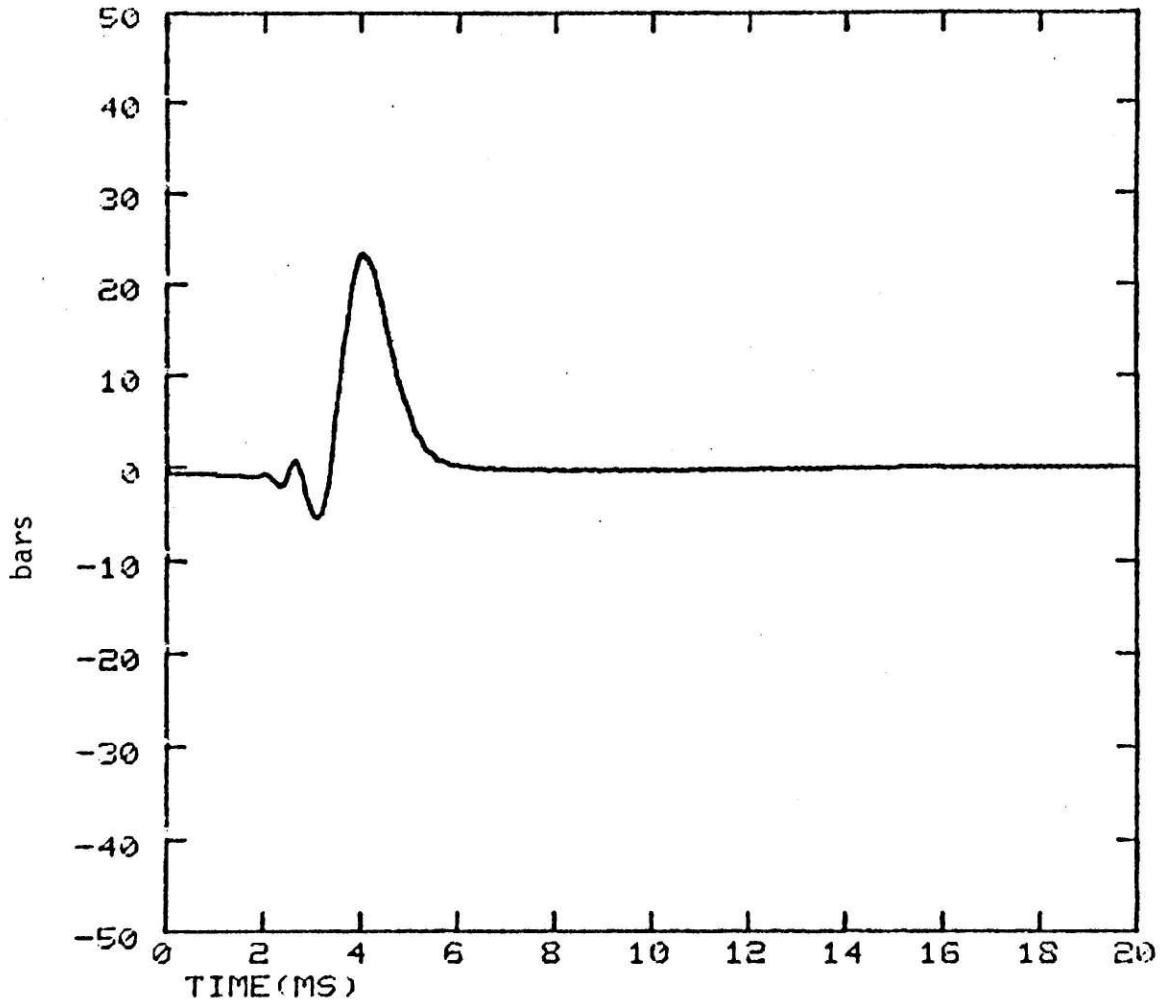

FIG. 2.4:- CEPSTRALLY WNDOWED CYLINDER PRESS. -- SAMP.# ≤ 75
PRESSURE MEASURED ON ENGINE OPERATING AT FULL LOAD

the combustion process and modeling variation of cylinder pressure with the operating condition is required.

2.3 Vibration Propagation

The vibration induced by the combustion force propagates through the engine to the block. The two major paths of propagation are: the piston-crank shaft-bearings and the head. The engine is both dispersive and finite. The reflections from the boundaries of the system form standing wave patterns and a reverberant field results. Acceleration at any point on the engine block is the sum of the directly propagated and reflected waves.

The average length of the directly propagated waves are shorter than that of the reflected ones. If boundaries of the system are far from the observation point and the system is moderately damped, directly propagated vibration is dominant. Similarly, when a medium with slow phase speed is excited by a transient force, the early part of resulting vibration is the directly propagated wave. However, if the attenuation in such a medium is low, as the number of reflections (echoes) increase and the medium responds as a reverberant system. Direct and reverberant vibration is analogous to transient and steady responses of a system.

The impulse response of the engine to the combustion force, $h_c(n)$ in Eq. 2.1 may be written as the sum of two impulse responses; one for propagated waves, $h_d(n)$, and one for the resonant response, $h_r(n)$

$$h_c(n) = h_d(n) + h_r(n) \tag{2.10}$$

Eq. 2.1 will thus change to:

$$a(n) = p(n)*h_d(n) + p(n)*h_r(n) = a_d + a_r$$

where a_d and a_r are the "direct" and "reverberant" accelerations. In the frequency domain, the response to combustion forces, $H_c(\omega)$ will be

$$H_c(\omega) = H_d(\omega) + H_r(\omega)$$

where $H_d(\omega)$ and $H_r(\omega)$ have the forms of the transfer functions of an infinite dispersive medium and a finite reverberant system, respectively.

2.3.1 Input Inertance

Both $H_d(\omega)$ and $H_r(\omega)$ are modeled as the product of an input inertance and a vibration transfer function. The input inertance $I(\omega)$ defines the ratio of input acceleration to the input

force. The acceleration transfer function, AT , is the relationship between input and received accelerations:

$$H(\omega) = I(\omega) \cdot AT(\omega) \tag{2.11}$$

where

$$I(\omega) = \frac{A_{in}(\omega)}{F_{in}(\omega)}$$

and

$$AT(\omega) = \frac{A_{out}(\omega)}{A_{in}(\omega)}$$

where $A_{in}(\omega)$, $A_{out}(\omega)$ and $A_{out}(\omega)$ and $F_{in}(\omega)$ are Fourier transforms of input, output accelerations and input force, respectively.

The effect of system boundaries on input inertance is neglected and $I(\omega)$ is assumed to be the same for both vibration transfer modes of the engine; direct and reverberent. Measurements support this assumption (see Chapter III).

Predicting input inertance of the engine requires the knowledge of the reaction of the excitation surfaces to the combustion force. The force acts on the piston top and head simultaneously. Major problems in finding $I(\omega)$ are in defining geometrical distribution of cylinder pressure and the local reaction of piston top and head to the pressure. A theoretical solution to these problems is beyond the scope of this thesis. Measuring the

input inertance for piston path as well as head (Chapter III) showed that:

(a) Input inertance to both paths are similar

(b) At low frequencies, below 1 kHz, $I(\omega)$ behaves as a stiffness. The behavior of the input inertance at frequencies above 3 kHz approaches that of a mass. In the region 1 to 3 kHz, $I(\omega)$ has two very damped resonances at 1500 Hz and 2500 Hz.

(c) In addition to these two resonances, input inertance to the piston path shows a damped resonance at 3 kHz.

In general, input inertance of the engine is similar to that of a thick finite plate [19].

2.4 Wave Propagation in the Engine

The vibration generated at the piston/cylinder top propagates through many paths. The acceleration at any point on the block is the sum of the vibration transmitted through these paths, each with a different length and arrival time. Each path may contain several sections, each with a different phase speed. In addition, several types of waves, such as longitudinal, bending or torsional, may be excited simultaneously and propagated in each path or section of a path.

The transfer function at a distance x_i from the source $VT(\omega,x_i) = |VT(\omega,x_i)|\, e^{-j\phi(\omega,x_i)}$ where $|VT(\omega,x_i)|$ denotes the magnitude and $\phi(\omega,x_i)$ is the phase of transform function. The phase of transfer function is:

$$\phi(\omega,x_i) = kx_i \qquad (2.12)$$

where the wavenumber k equals ω/c_{ph} and c_{ph} is phase speed.

Bending waves are likely to be the dominant waves propagated below 2500 Hz in the engine. The phase speed of being waves C_b is:

$$c_b = \left(\frac{B}{\rho_s}\right)^{1/4} \omega^{1/2}$$

where ρ_s is the surface density of the medium, and $B = (Eh^3/12(1-\nu^2))$ is the bending rigidity for a plate, where E is Young's modulus, h is the plate thickness and ν is Poisson's ratio.

The phase of the transfer function for bending wave propagation is:

$$\phi(\omega,x_i) = \left(\frac{\rho_s}{B}\right)^{1/4} x_i\omega^{1/2} \qquad (2.13)$$

The magnitude of vibration transfer function, at distance x_i from the source, $|VT(\omega,x_i)|$, depends on the damping loss factor, η of the medium and geometrical spreading:

$$|VT(\omega,x_i)| = \Gamma \exp(4.27\, c_b x_i \eta/w) \qquad (2.14)$$

where Γ is a function of the geometry of the system.

The propagation impulse response $h_p(n,x_i)$ is the inverse Fourier transform of $VT(\omega,x_i)$. The impulse response for discrete time, n, is $h_d(n,x_i) = h_d(t=nT,x_i)$ when n is an integer and T is the sampling period. Neglecting frequency dependence of the magnitude:

$$h_d(n,x_i) \propto \frac{(\rho_s/B)^{1/4}}{2\sqrt{\pi}\, T^3} \cdot n^{-3/2} \exp\left(\frac{-(\rho_s/B)^{1/2} x_i^2}{4\, T\, n}\right) \qquad (2.15)$$

The phase of transfer function and impulse response for several distances of .5, 1, 1.5, and 2 meters are plotted in Fig. 2.5. The propagation impulse response of the engine point on the engine block is the sum of impulse responses of different direct paths. The paths are those that are permissible by the engine geometry:

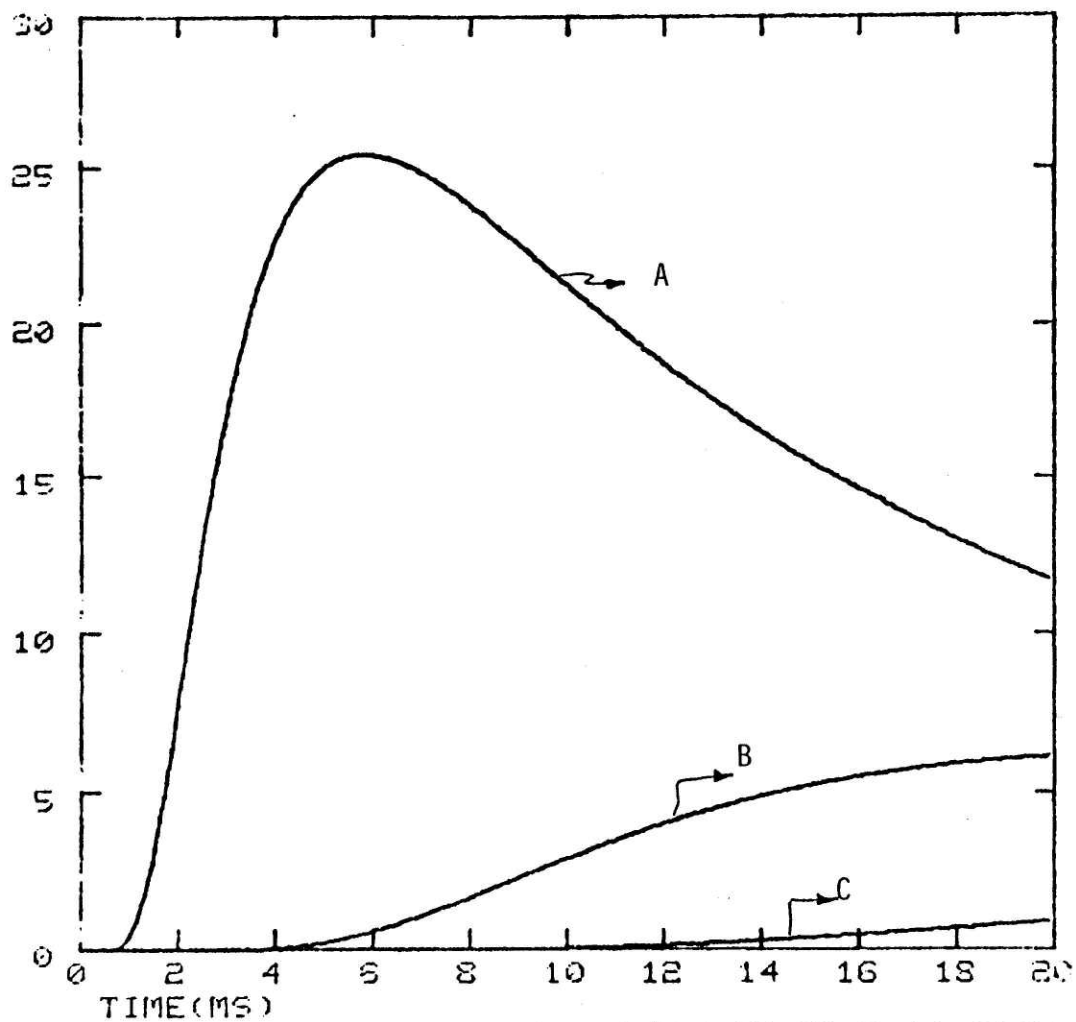

FIG. 2.5:- PROPAGATION IMPULSE RESPONSE IN 3/16 INCH THICK STEEL PLATE AT A DISTANCE OF (A) .5 M, (B) 1 M, (C) 1.5 M

The impulse response of a point on the engine block is the sum of impulse responses of different paths. The paths are those that are permissible by the engine geometry:

$$h_p(n) = \sum_i h_p(n,x_i) \quad . \tag{2.16}$$

The path lengths vary between the shortest path permissible by geometry x_s, and the longest path x_e, possible in the time window, t_w, $x_e \leq t_w c_b$. The vibration propagated through the piston path is typically transferred via different bearings, therefore, the path may be determined. Propagation through the head is much more complicated.

2.5 The Resonant Response and the Modes of the Engine

The transfer function of a resonant system, $H(\omega)$ may be represented by its resonances and anti-resonances:

$$H(\omega) = \frac{\Gamma_i((\omega_i-\omega)^2 + j\omega r_i)}{\Gamma_j((\omega_j-\omega)^2 + j\omega r_j)} \tag{2.17}$$

where ω_i and ω_j are anti-resonance (zero) and resonance (pole) frequencies and r_i and r_j are losses in these frequencies. The relation between r_α and damping loss factor η is

$$r_\alpha = \eta\, \omega_\alpha \quad . \tag{2.18}$$

Poles and zeroes of the engine depend on its resonance modes and mode shapes. In general, calculating these modes for an engine is complicated. Modeling the engine as a cascade of two port subsystems, each having simple modes and mode shapes, is a good way to analyze the complicated system. These subsystems are the parts of the engine which participate in transmitting the vibration, such as piston, crank shaft, bearing and the block.

If the transfer function for a dispersive medium is added to Eq. 2.17, total VTF, $H_r(\omega,x)$ results:

$$H_r(\omega,x) = \Gamma e^{j\phi_t(\omega,x)} + \frac{\prod_i ((\omega_i-\omega)^2 + j\omega r_i)}{\prod_j ((\omega_j-\omega)^2 + j\omega r_j)} \qquad (2.19)$$

The phase shift ϕ_t in general is a continuous and monotically varying function of frequency. Experimental measurements of vibration trasnfer function, VTF, is consistent with this model and shows a monotonically increasing phase.

The transfer function $H(\omega,x)$ as represented by Eq. 2.17 is a minimum phase function. Therefore, its phase and magnitude are the Hilbert transform of each other [18]. The knowledge of either of the two, phase or magnitude, will define the other.

2.6 Additional Sources of Excitation in Engine -- Piston Slap

Sources of vibration in an engine other than the combustion pulse are inertial forces, piston slap, valve opening/closing and other mechanical noises. The most important of these *secondary* forces at frequencies higher than several times firing frequency is piston slap. The characteristics of piston slap and the transfer paths between the force and the engine block has been and continues to be studied [20]. Some of the properties of piston slap are:

(a) Piston slap is an approximately impulsive source with a broad band spectrum.

(b) The magnitude of the force depends on speed, but its dependence to load is much less than that of the combustion force.

(c) Piston slap occurs 10° to 20° crank angle *after* TDC.

(d) The dominant transfer path for piston slap is through the top of the block.

These properties can be used to reduce the effect of piston slap; (b) and (d) are useful in selecting an operating condition and an observation point where the effect of piston slap on measured acceleration is minimal, and (a) and (c) suggest processing techniques to separate the effect of piston slap from combustion.

Eq. 2.4 for two sources of excitation; combustion p(n) and piston slap, s(n) becomes

$$a(n) = p(n) * h_p(n) + s(n) * h_s(n) \qquad (2.20)$$

Piston slap can be used in diagnosis of faults in an engine, e.g., in the detection of a damaged ring. However, such an application requires better acknowledge of the piston slap and its transfer function. In this study, piston slap is treated as a *noise* rather than a *signal*. Reducing the effect of piston slap on meausured acceleration by proper selection of observation points and operating conditions as well as using special processing techniques will be discussed.

2.7 Cepstral Analysis and Echo Removal

The impulse response of the engine to combustion forces $h_c(h)$ may be defined as the convolution of an impulse response representing the propagation in the medium, $h_d(n)$, and a series of pulses representing multiple propagation paths and the reflections, $h_r(n)$;

$$h_c(n) = h_d(n) * h_r(n) \qquad (2.21)$$

where

$$h_r(n) = 1 + \sum_k \alpha_k \, \delta(n-n_k) \qquad n_k = \text{integer} \qquad (2.22)$$

The $h_d(n)$ for a dispersive media is the same as Eq. 2.15. In the frequency domain the relationship between the Fourier transforms of $h_c(n)$, $h_d(n)$ and $h_r(n)$ or $H_c(\omega)$, $H_d(\omega)$ and $H_r(\omega)$ are:

$$H_c(\omega) = H_d(\omega)\, H_r(\omega)$$

$$H_c(\omega) = H_d(\omega)\, [1 + \sum_k \alpha_k\, e^{-j\omega n_k}] \qquad (2.23)$$

Taking complex logarithm for both sides results in

$$\ln H_c(\omega) = \ln H_p(\omega) + \ln [1 + \sum_k \alpha_k\, e^{j\omega n_k}] \qquad (2.24)$$

The inverse Fourier transforms for both sides are the cepstra of the three impulse responses: $\hat{h}_c(n)$, $\hat{h}_r(n)$ and $\hat{h}_d(n)$ [18]

$$\hat{h}_c(n) = \hat{h}_r(n) + \hat{h}_d(n) \qquad (2.25)$$

The cepstrum of a series of pulses is itself a series of pulses [11]. Therefore, $\hat{h}_d(n)$ has the form:

$$\hat{h}_d(n) = 1 + \sum_k r_k\, \delta(n-n_k)\ . \qquad (2.26)$$

The $\hat{h}_d(n)$ tends to occupy the high time portion of the $\hat{h}_c(n)$ while $\hat{h}_p(n)$ is more concentrated around the origin. It should be noted that

the cepstrum of impulse response of a dispersive medium of the form of Eq. 2.15 spreads into the high time portion. However, the energy of the cepstrum is small when the value of n is large.

Eq. 2.25 suggests a very effective way to distinguish between reflected and propagated impulse responses. If n_k's are known, a cepstral domain filter may be designed to eliminate $\hat{h}_d(n)$. This method is likely to be useful in removing reflected waves. The acceleration on the engine block results from combining 2.26 and 2.1 in cepstrum domain:

$$a(n) = b(n) * h_r(n) * h_d(n) \qquad (2.27)$$

The cepstrum of the cylinder pressure p(n) spreads over both low and high time regions. Therefore, windowing a(n) will not deconvolve the signal. However, we will see that a combination of cepstral windowing/filtering and short time fast deconvolution gives good results in estimation of the combustion force and detection of fault in cylinder pressure.

CHAPTER III: EXPERIMENTAL ESTIMATION OF THE VIBRATION TRANSFER FUNCTION

Determining the vibration transfer function, VTF, of a complicated system such as an engine requires the thorough knowledge of transfer mechanisms and paths. One way to determine the VTF is to measure it. The measurements can be done by externally exciting the non-running engine with a known force and measuring block acceleration. On an operating engine, the VTF may be found by simultaneous measurements of cylinder pressure and block acceleration.

In this chapter, measuring VTF on both non-running and operating engine will be discussed. The data on the operating engine was also used to estimate the combustion force from block acceleration.

The engine under study was a John Deere 4219 diesel. The engine has four cylinders with direct injection and is naturally aspirated. The VTF of operating engine, DVTF1 has been estimated under several load/speed conditions.

The VTF of the non-running engine, SVTF, was estimated by exciting the engine on the piston and measuring both the applied force and the resultant acceleration. The SVTF between all four cylinders and a number of observation points was measured.

The cylinder pressure of the operating engine and the block acceleration were also measured in synchronization with a timing mark at TDC of piston #1. This set of data provided the timing information between the pressure/acceleration and the crank position.

The errors associated with measuring VTF on a non-running engine are as follows:

(a) The excitation force applied to the engine, e.g., by a shaker, is usually a point source, while the combustion force is distribution over the piston and the top of combustion chamber.

(b) The VTF is measured for one crank position, i.e., TDC.

(c) The behavior of VTF may be affected by the changes in the environmental condition of the operating engine such as temperature-and motion-caused stress and flow of different fluids.

Experiments have shown that changes in crank angle position of up to 40° does not affect the VTF significantly. The errors caused by applying the point force may be reduced by measuring VTF for several force locations and averaging the VTF.

Measuring VTF on an operating engine eliminates the errors discussed. Unfortunately, the VTF determined on a running engine, DVTF, is contaminated by the effect of *secondary* vibration sources, especially piston slap. Reducing the effect of piston slap requires studying the characteristics of piston slap and the VTF associated with it, VTP.

All of the measurements were recorded on a two channel Nagra tape recorder (see Appendix A). Data was processed on a Data General Nova computer with a 10 bit A/D converter. The sampling rate was 12.5 kHz. To avoid aliasing, the data was low pass filtered at 4 kHz.

In addition to the two measured VTF's, variations in DVTF1 resulted in three other VTFs; one representing multipath direct propagation, DVTF2; one representing single path direct propagation, DVTF3; and one representing simple resonance DVTF4. (See Table 3.1).

Four pairs of observation points were selected on the engine block (Fig. 3.1). The two points of each pair were on alternate cylinders, i.e., one and three or two and four. Two of the pairs: 1 and 2, were on the right engine block; the other two pairs were on the left engine block. The first pair of points: 1a and 1b were on the top of the engine block where the vibration will most likely be transferred through the head. The second pair of points were on the skirt of the engine, directly

TABLE III-I

DESCRIPTION OF DIFFERENT VIBRATION TRANSFER FUNCTIONS,VTF

VTF	Description
SVTF	VTF measured on non-running engine
DVTF1	VTF measured on operating engine
DVTF2	Represents multipath propagation, derived from data
DVTF3	Represents single path propagation derived from data
DVTF4	Represents simple resonance, derived from data

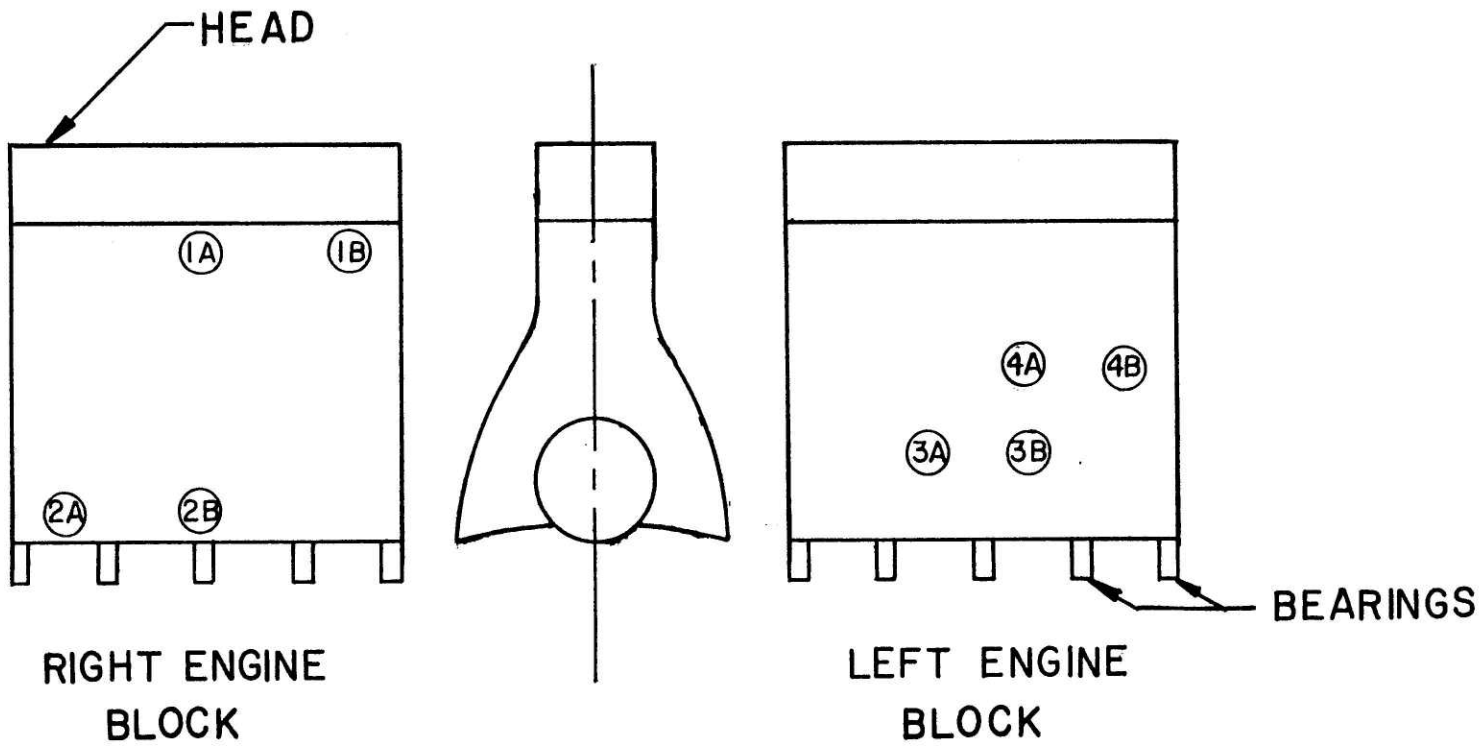

Figure 3.1: Observation Points on Engine

on the bearings, where the piston path should be dominant. The other pairs were on the middle of the engine block. The VTF from all four cylinder/pistons were measured to all observation points.

3.1 The Vibration Transfer Function of the Non-Running Engine

Two major vibration transfer paths in the engine are through the piston-crank-shaft bearing and the cylinder head. The SVTF of both paths were measured. The total SVTF was obtained by adding the two paths together.

When the non-running engine is excited by a force, $F(\omega)$, the acceleration in frequency domain, $A(\omega)$ is:

$$F(\omega) = A(\omega)\, H(\omega) \qquad (3.1)$$

The $H(\omega)$ defined in Eq. 3.1 is for an applied point force. To estimate the cylinder pressure, $H(\omega)$ should be corrected for the piston surface.

To excite the non-running engine, either an impulsive source or white noise is used. Using an impulse to measure the impulse response is especially appropriate in studying the propagation transfer function. Using white noise excitation will emphasize steady state or the resonance response. However, the phase information in this type of measurement may be used to modify the measured transfer function if the frequency dependence of phase speed of the medium is known.

The SVTF of the transfer path through the piston was measured with the head removed. The excitation force was applied to the top of the piston and this force and block acceleration were measured. The SVTF of the transfer path through the head was measured using reciprocity; the force was applied to the observation point and the acceleration was measured inside the cylinder top. For this experiment, the piston was removed to eliminate the vibration transfer through the piston path. In addition to the VTF of the transfer paths, input inertance of the pistons and observation points were measured.

The force was applied by a hand-held Wilcoxon shaker. The shaker was excited by band-limited white noise. The band pass filter was used to shape the force spectrum in order to ensure high signal-to-noise ratio over the frequency bands of interest; 10 Hz to 4 kHz. The acceleration was picked up by a two gram B&K accelerometer. The force was measured by the impedance head attached to the shaker.

The experimental set-up is shown in Fig. 3.2. The engine was set on a bed plate with resilient mounts. Both force and acceleration signals were amplified. A two channel Ithaco step amplifier/attenuator was used to adjust signal levels for recording. The two signals were monitored on a Nicolet spectrum analyzer.

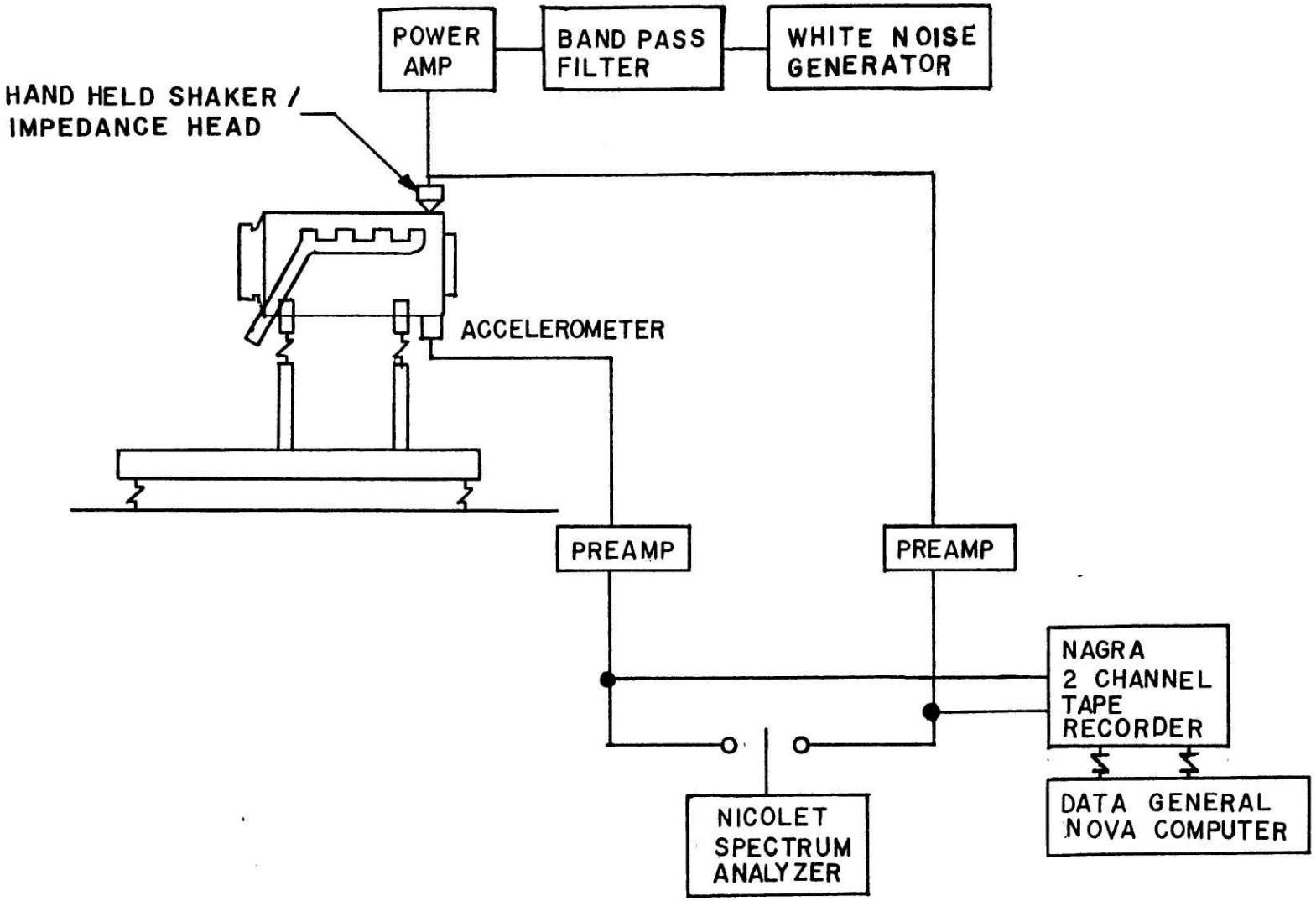

Figure 3.2: Experimental Set-Up to Measure Vibration Transfer Function of Non-Running Engine

The system was calibrated at each measurement session. First, a 100 Hz calibration signal was used to calibrate the accelerometer and the circuitry associated with it. Then, the input inertance of a known mass (1.8 kg) was measured. Both signals were recorded and were used to check the system calibration while processing on the computer.

3.1.1 Processing technique

The engine is assumed to be a linear, time-invariant system. When the system is excited by a random stationary force, a random stationary acceleration results. The estimate of the force power spectrum density is $\tilde{G}_{ff}$, acceleration power spectrum density is $\tilde{G}_{aa}$ and the cross-spectrum density between force and acceleration is $\tilde{G}_{af}$. The relationship between the estimated magnitude and phase of VTF, $|\tilde{H}_{VT}|$, $\tilde{\phi}_{VT}$, and $\tilde{G}_{aa}$, $\tilde{G}_{af}$, and $\tilde{G}_{ff}$ is [21]:

$$|\tilde{H}_{VT}|^2 = \frac{\tilde{G}_{aa}}{\tilde{G}_{ff}} \qquad (3.2)$$

$$\exp(-j\phi_{VT}) = \frac{\tilde{G}_{af}}{\tilde{G}_{ff}} \times \frac{1}{|\tilde{H}_{VT}|}$$

The power and cross spectra may be computed by the Cooley-Tukey method [24]. A standard radix 2 FFT was used to calculate Fourier transforms. The FFT length was 512 points. A cosine window

was used to taper the first and last 10% of each data record. The estimated spectrum was the average of 20 measurements. The normal standard error of estimation, ε_r, was:

$$\varepsilon_r = \sqrt{\frac{1}{20}} \simeq .22, \tag{3.3}$$

The variance of error associated with FFT routine, σ^2_{FFT} is [22]:

$$\sigma^2_{FFT} = P(m)\ \sigma^2_a \tag{3.4}$$

where σ^2_a is the variance of the data and P(m) is:

$$P(m) = 0.5\ (5m-6)\ \sigma^2_E + 0.25\ (25m^2-51\ m+18)\ \mu^2$$

where m is $\log_2 N$, N is FFT length, and μ and σ^2_E are the mean and variance of rounding error.

Therefore,

$$\sigma_{FFT} \simeq .5 \times 10^{-6}$$

which is negligible compared with ε_r.

3.1.2 The path through the piston

To estimate the SVTF of this path, the engine head was removed. The piston under study was brought to TDC position. The input inertance, $I(\omega)$, of all four pistons was measured. The SVTF of all four pistons to 8 points of observation was measured.

Some of the typical results of points 2a and 1a are shown in Figs. 3.3 and 3.4.

The input inertance for pistons in the frequency range below 1500 Hz behaves as a pure stiffness (Fig. 3.5). Above 1500 Hz, it shows a very damped ($\sigma \simeq .12$) resonance at 2500 Hz. This resonance may be associated with piston or piston-crank shaft combination. The $I(\omega)$ of all four pistons are similar. All of the SVTFs show a high pass filtering behavior, which may be associated with the input inertance. The envelope of magnitude for all SVTFs is similar and resembles the $I(\omega)$, but the detail of the resonance peaks as expected, are different. The magnitude of the SVTF is comparable to that of the transfer function for an all zero filter. The magnitude of SVTF between point 2a and different pistons shows a broad peak at 1500 Hz. The peak seems to be associated with a group of modes. The phase of SVTFs show a monotonically increasing characteristic.

3.1.3 The path through the head

Measuring SVTF of this path directly requires exciting the engine from inside the cylinder, which is very difficult. Therefore,

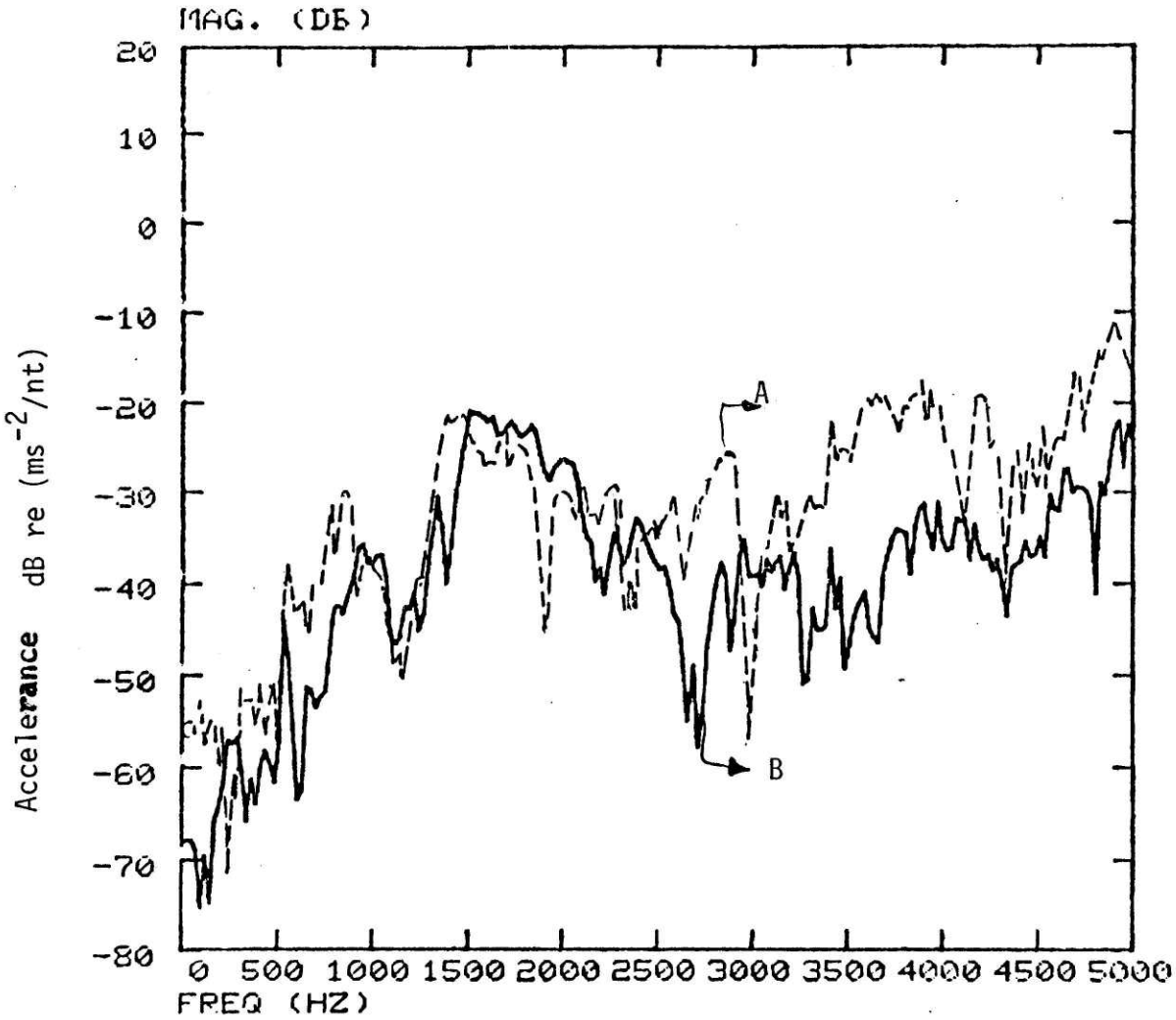

FIG.3.3A :- MAGNITUDE OF SVTF -- POINT 2A TO :

A) PISTON# 1, B) PISTON #4

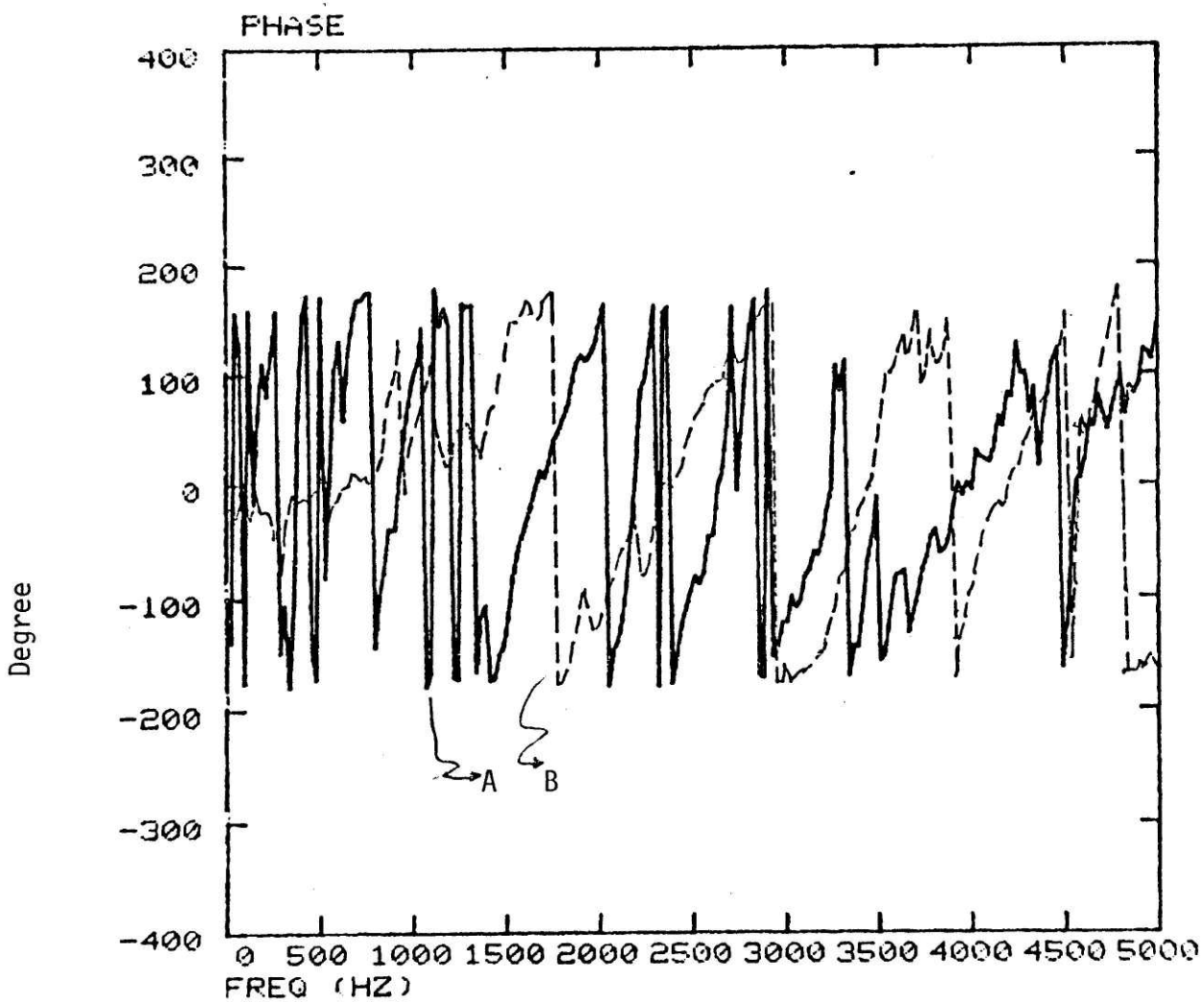

FIG. 3.3B :- PHASE OF SUTF -- POINT 2A TO :

A) PISTON #1 , B) PISTON # 4

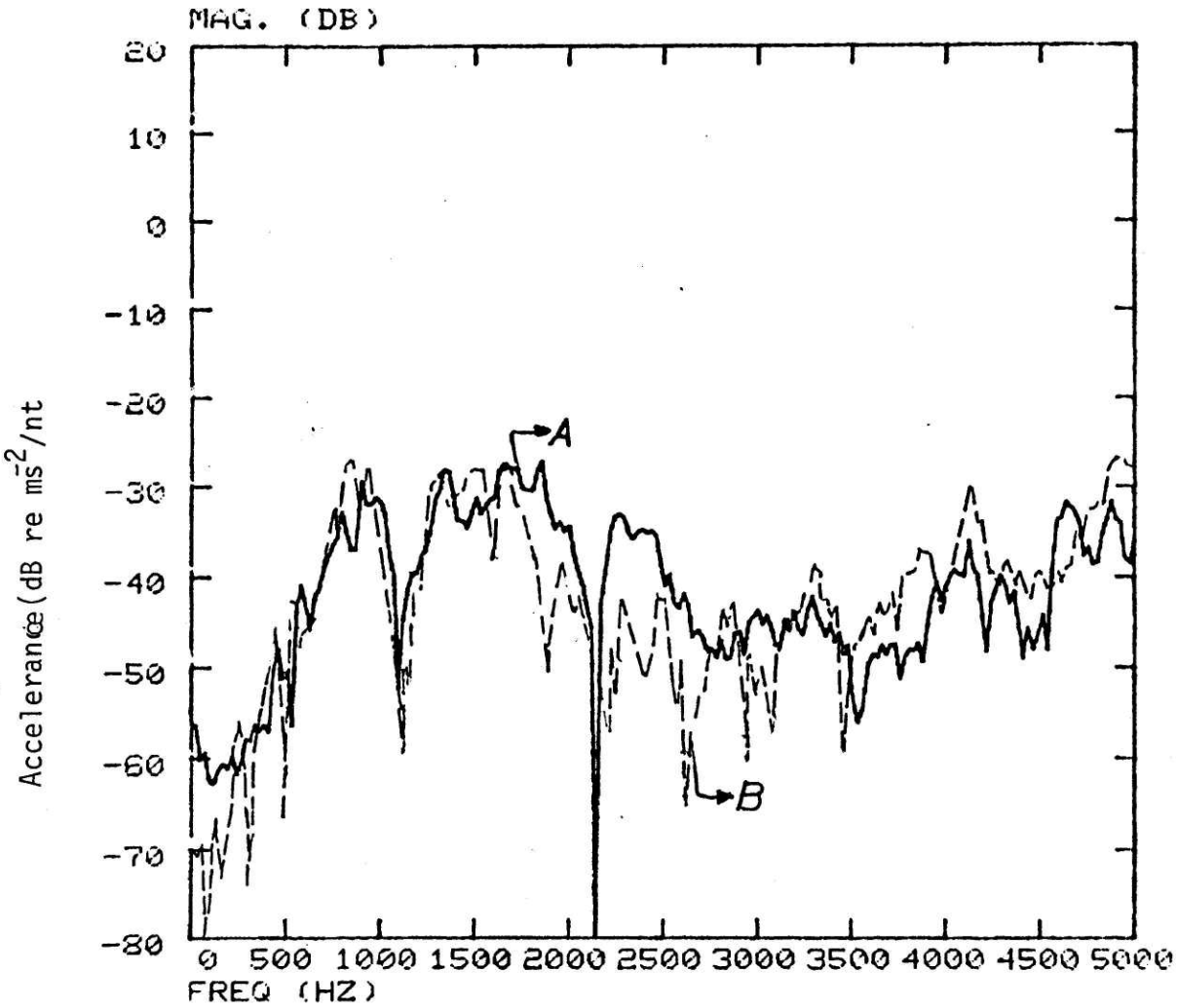

FIG.3.4A :- MAGNITUDE OF SVTF -- POINT 2B TO :

A) PISTON # 1, B) PISTON # 4

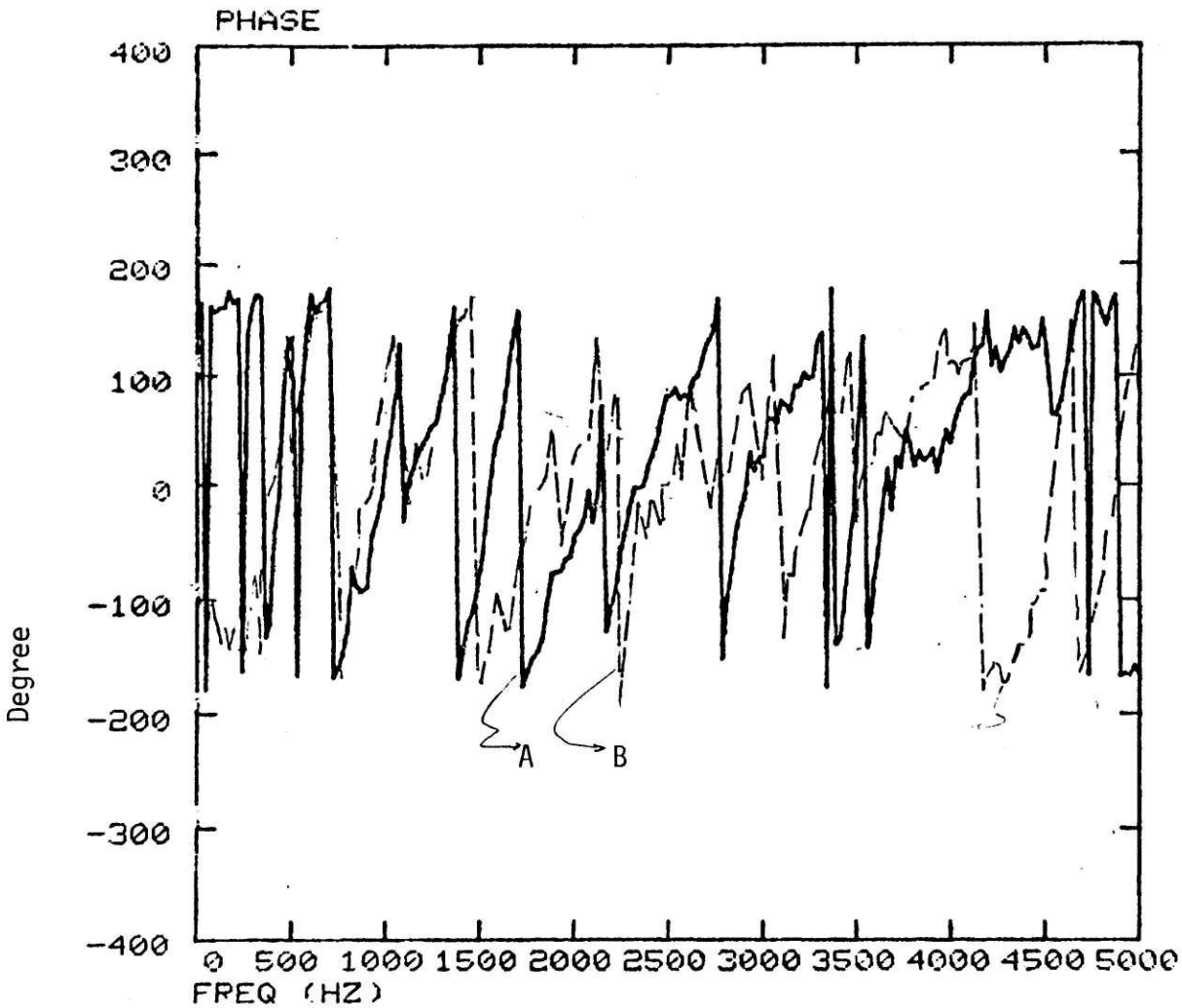

FIG.3.4B :- PHASE OF SVTF -- POINT 2B TO :

A) PISTON # 1 , B) PISTON # 4

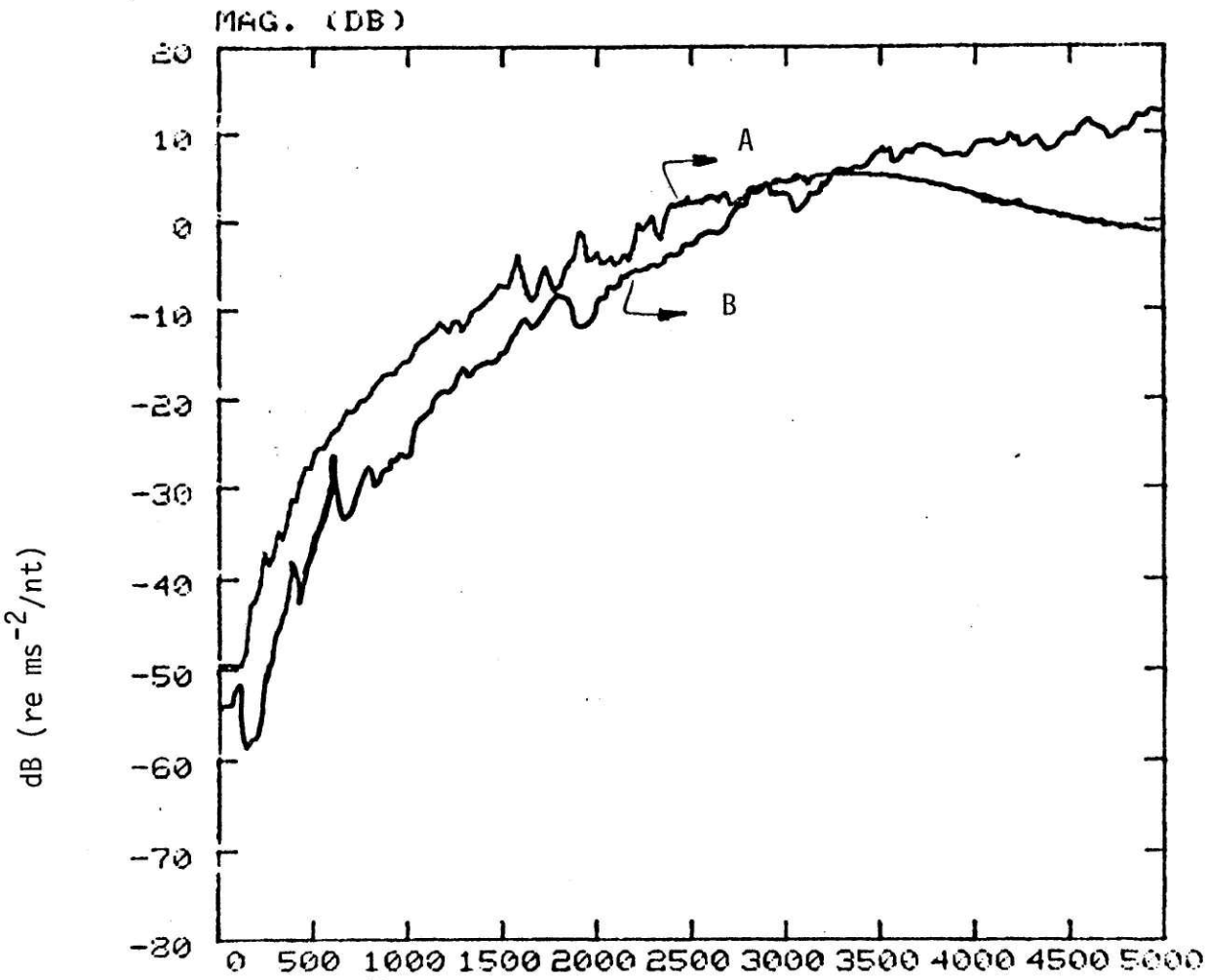

FIG. 3.5:- MAGNITUDE OF INPUT INERTANCE TO
A) PISTON , B)CYLINDER HEAD

the SVTF of the path through the head was found using reciprocity [3]; the engine block was excited at an observation point and the resultant acceleration inside the cylinder head at TDC was measured. To eliminate the vibration transfer through the piston path, the pistons were removed.

The SVTF at point 2a to cylinder 3 was measured both directly and reciprocally (Fig. 3.6). The results show that reciprocal measurement gives the equivalent SVTF. Input inertances were also measured.

Typical measured magnitude and phase of the SVTFs are shown in Figure 3.7 for points 1b and 2a. The other measured SVTFs are similar to these. The estimated input inertance is similar to input inertance of the pistons. It resembles a pure stiffness at low frequencies (up to 2000 Hz) and resembles stiffness plus damping at higher frequencies. The SVTFs of the head paths also show a high pass filtering behavior. Comparison between the VTF of the two paths show that for the majority of SVTFs, the head path is dominant above 2 or 2.5 kHz.

3.1.4. The total vibration transfer path

The total SVTF was found by adding the SVTF of the two paths together. The addition was done on the computer. The total SVTF also shows the high pass filtering characteristic (Fig. 3.8).

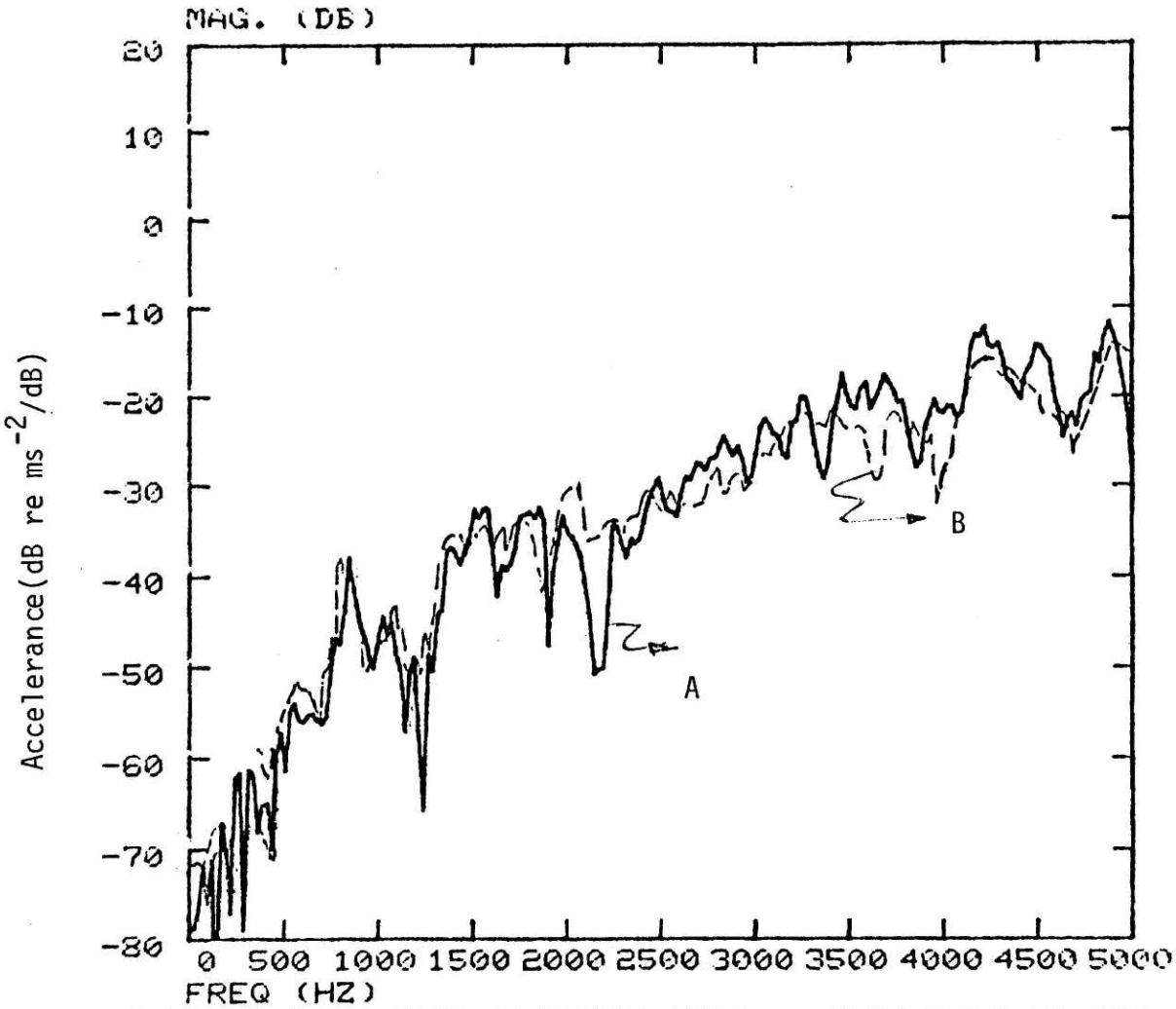

FIG. 3.6 :- SUTF THROUGH HEAD -- POINT 2A TO CYL.#3

A) USING RECIPROCITY , B) MEAS. DIRECTLY

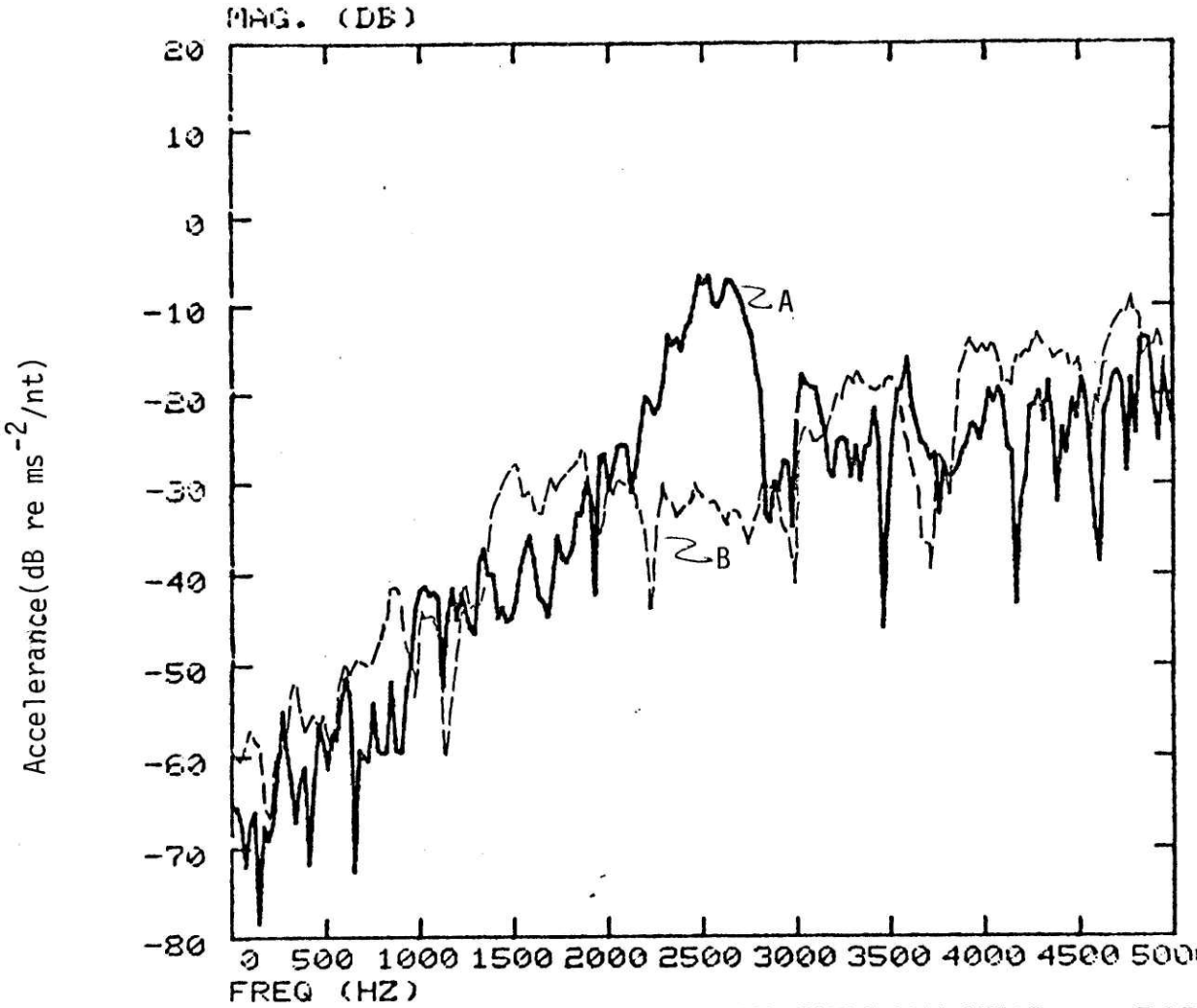

FIG.3.7 :- MAGNITUDE OF SUTF THROUGH HEAD -- POINT 2A

A) TO CYLINDER #1 , B) TO CYLINDER # 4

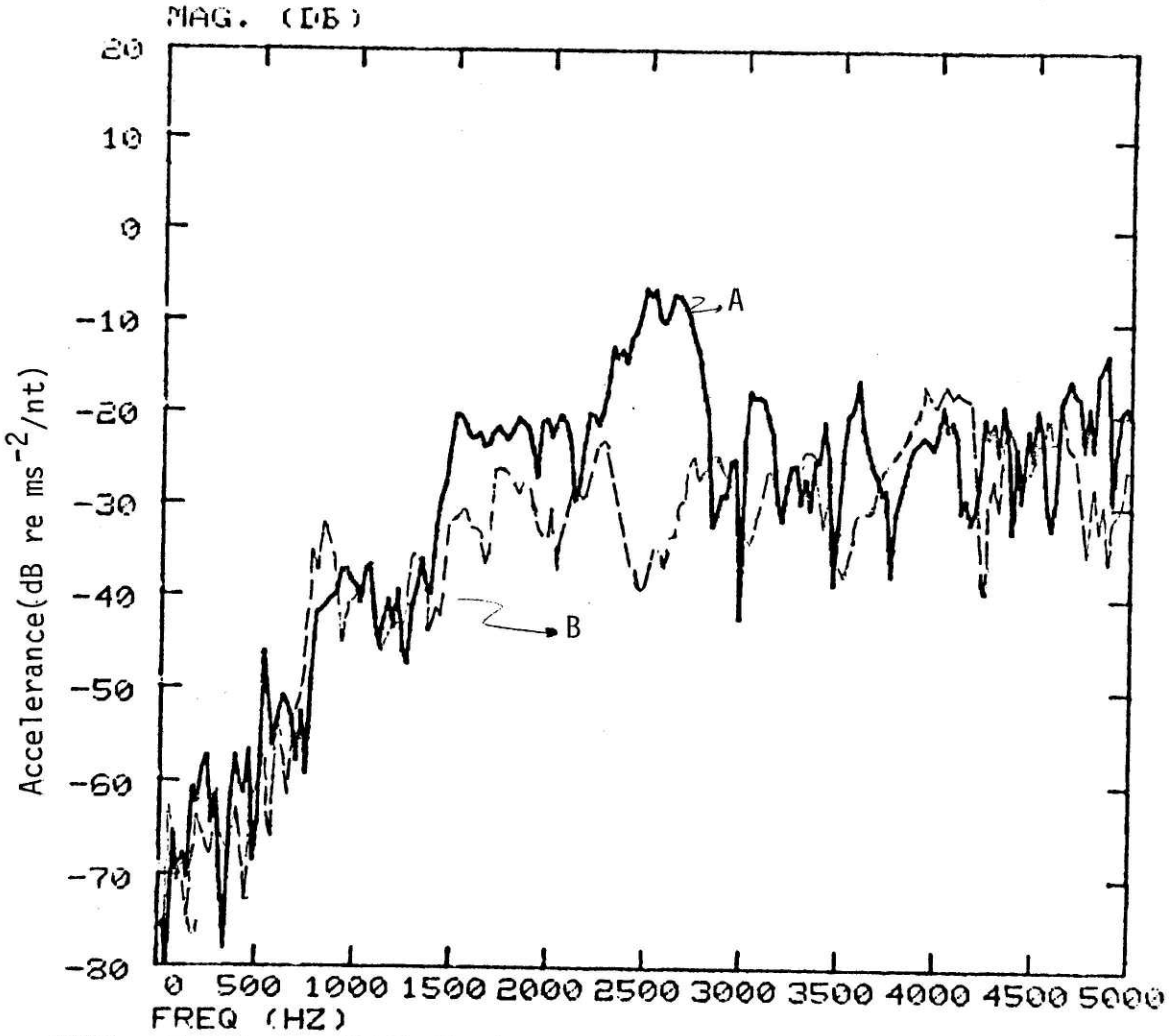

FIG. 3.8A :- MAGNITUDE OF TOTAL SVTF -- POINT 2A TO :
A) CYLINDER # 1, B) CYLINDER # 4

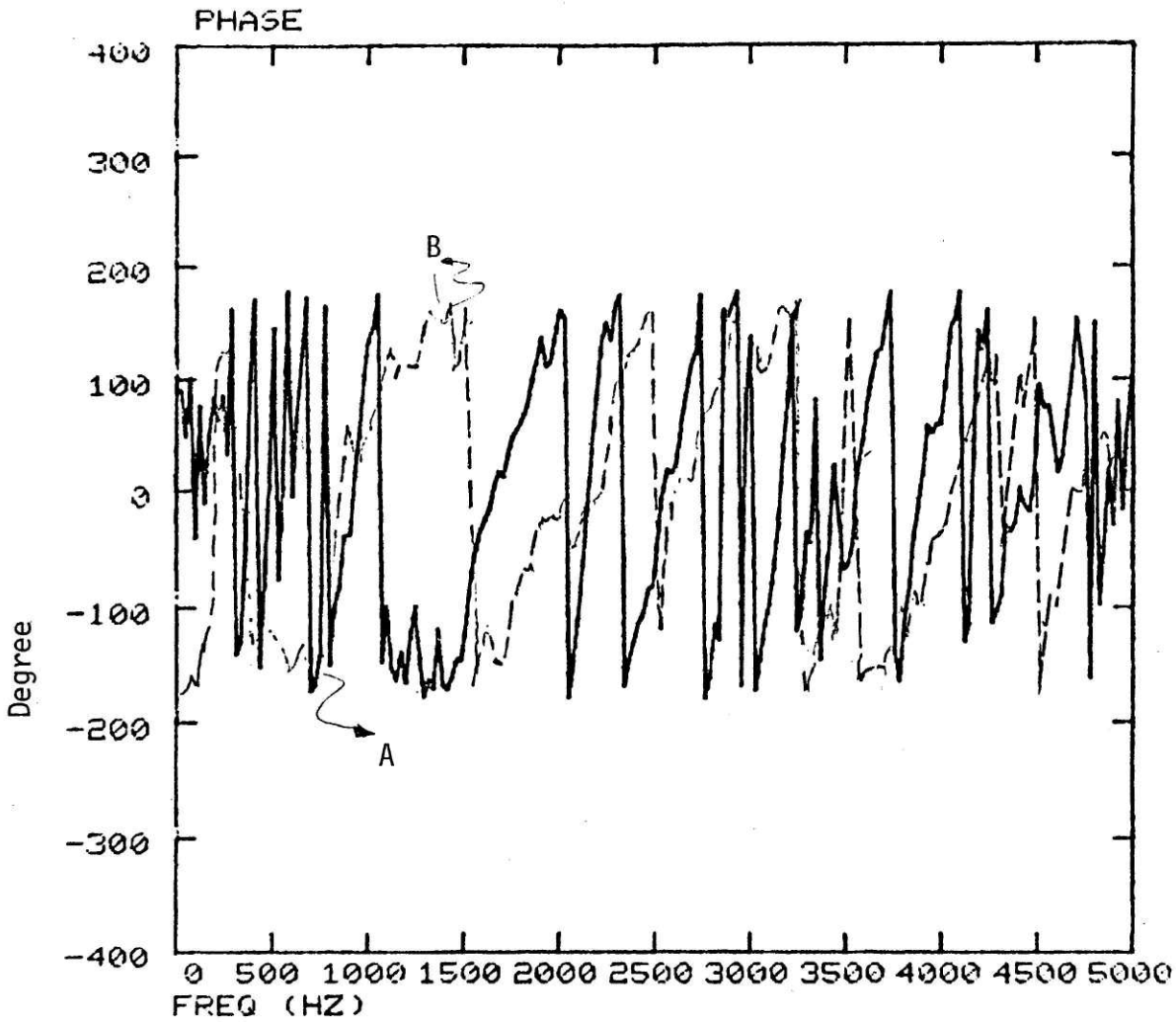

FIG. 3.8B :- PHASE OF TOTAL SUTF -- POINT 2A TO :
A) CYLINDER # 1 , B) CYLINDER # 4

3.2 Measurements on the Running Engine

In this section, measuring the cylinder pressure, engine block acceleration and their timing relative to TDC of the operating engine and defining DVTF of the engine is discussed.

The acceleration and pressure measurements were repeated for several load/speed conditions. A special valve switch was put on the injector to enable selective shut off of one or more of the cylinders [23]. The cylinder pressure and block acceleration was measured with one, two or three of the cylinders shut off.

The tests were conducted at MIT facility for engine noise studies. The load was applied by a water brake dynamometer (see Appendix A). The speed was controlled by a special throttle. Load, speed, water and oil temperature and pressure were monitored during the tests. A cooling tank provided cooling water for the engine.

The acceleration was measured by a 14 gram B&K accelerometer. The accelerometer was mounted on studs cemented to the engine block. The accelerometer had a Teflon cable to tolerate the high temperatures of the engine block. Cylinder pressure was measured by a pressure transducer mounted in the head of cylinder #4. The TDC of the piston #4/#1 was marked on the pulley of the engine. A Fotonic sensor was used to pick up and record the mark.

The experimental set up is shown in Fig. 3.9. The accelerometer was calibrated before each test with a 100 Hz, 1 g rms input. The calibration signal was also recorded to enable the adjustment of levels in playback.

The normal operating speed of the engine was 1500 rpm (the maximum torque). The top speed was 2500 rpm. For the tests, the engine was operated at speeds of 1500 rpm and 2500 rpms. At 1500 rpm, three different loads were applied: (1) no load, (2) 60% (24 HP) of the full load and (3) full load, (36 HP). At 2500 rpm, the engine was operated under no load and with 50% load (15 HP). The engine ran stable under all of the conditions. No excessive temperature increase or other abnormal behavior was observed. Some measurements were taken with one, two or three of the cylinders shut off. For this set of measurements, the engine was initially operated at 1500 rpm and no load. When one or more cylinders were shut off, the speed decreased and the load on the operating cylinders increased.

Four sets of simultaneous measurements were taken at each operating condition -- load and speed:

(a) Acceleration and cylinder pressure

(b) Cylinder pressure and timing mark

(c) Acceleration and timing mark

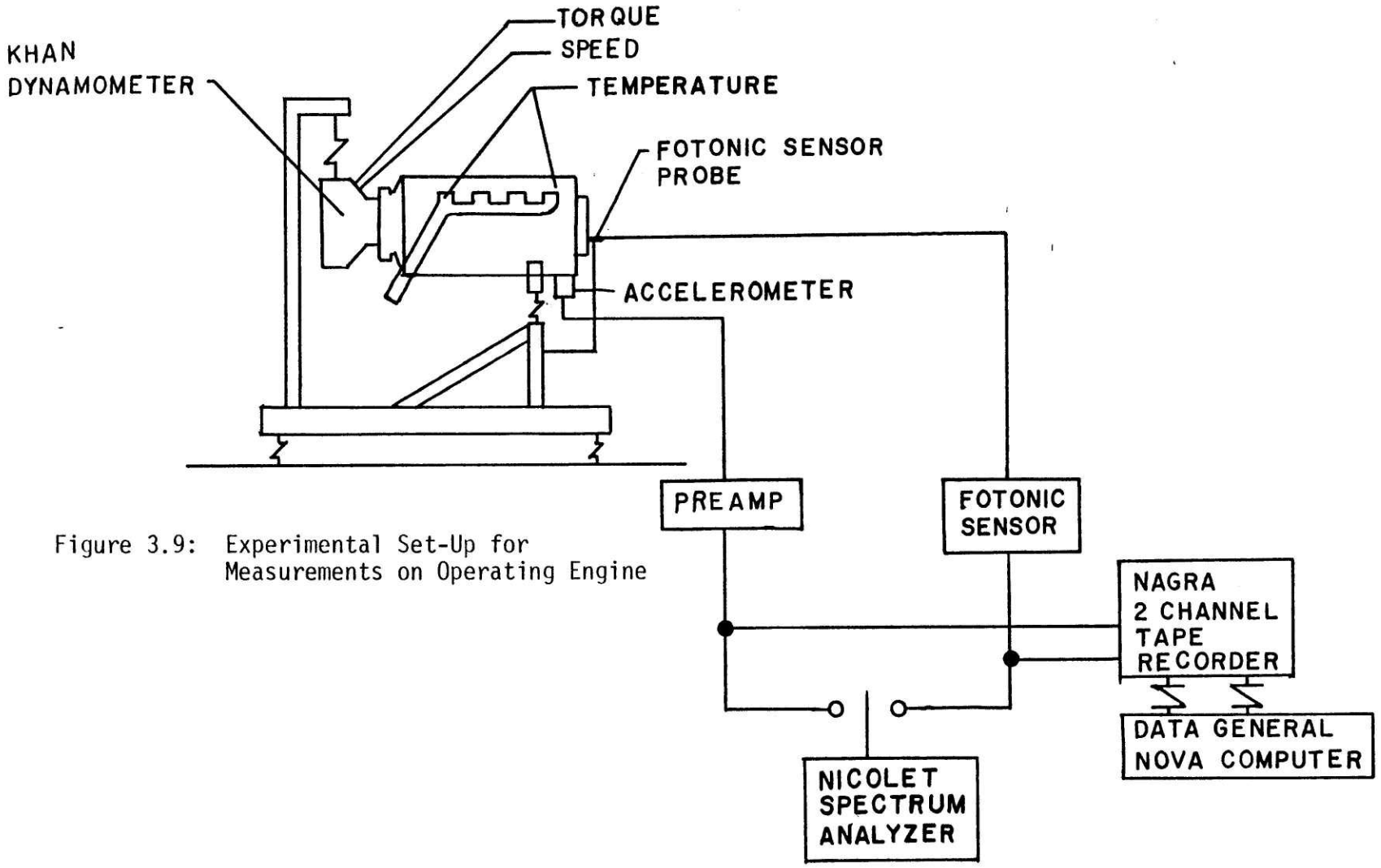

Figure 3.9: Experimental Set-Up for Measurements on Operating Engine

(d) Acceleration at a pair of points (a and b).

Tests a, b, and d were repeated for all of the observation points.

3.2.1 The cylinder pressure

The power spectrum of the cylinder pressure at 1500 rpm under different load conditions (Fig. 3.10) showed that most of the energy is in the 25 to 2.5 kHz frequency range. The energy dropped at the rate of approximately 12 dB/octave in the 25 to 500 Hz frequency bands regardless of the load. The rate of drop in the spectrum above 500 Hz strongly depended upon the load. This behavior was consistent with the model developed in Chapter II. The energy in the 25 to 500 Hz frequency range depended on the compression cycle alone. The higher frequency energy; 500 to 2500 Hz was associated with the combustion process. High frequency energy associated with resonances in the cylinder cavity which has been reported [24] to occur at 3.5 to 5 kHz frequency bands was not observed.

The pressure trace is a better indication of the operation under different load conditions (Fig. 3.11). The timing mark in Fig. 3.11* shows the TDC of piston #4. Under a no load condition, pressure dropped at TDC and peak occurred after TDC. Under a high load, 60% of full load, the pressure rose sharply before TCS and peak pressure occurred *at* TDC. The pressure peak was broader at higher loads.

---

*Figure shows the recorded pressure trace. The DC component is removed and the signal was tapered with a cosine window on the first and last 10% of the record during processing.

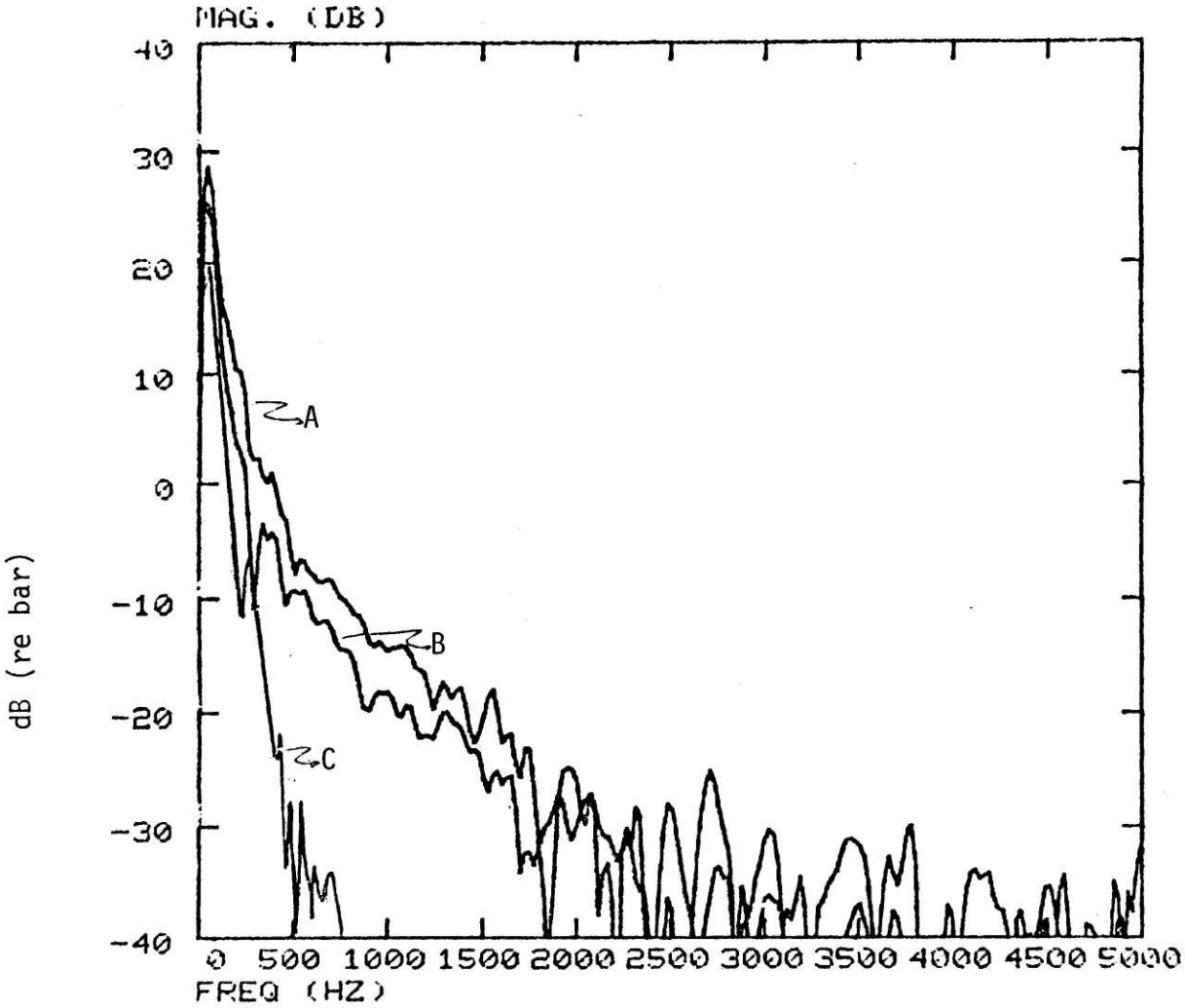

FIG. 3.10:- SPECTRUM OF CYLINDER PRESSURE AT 1500 RPM &
A) FULL LOAD , B) NO LOAD , C) INJECTOR SHUT OFF

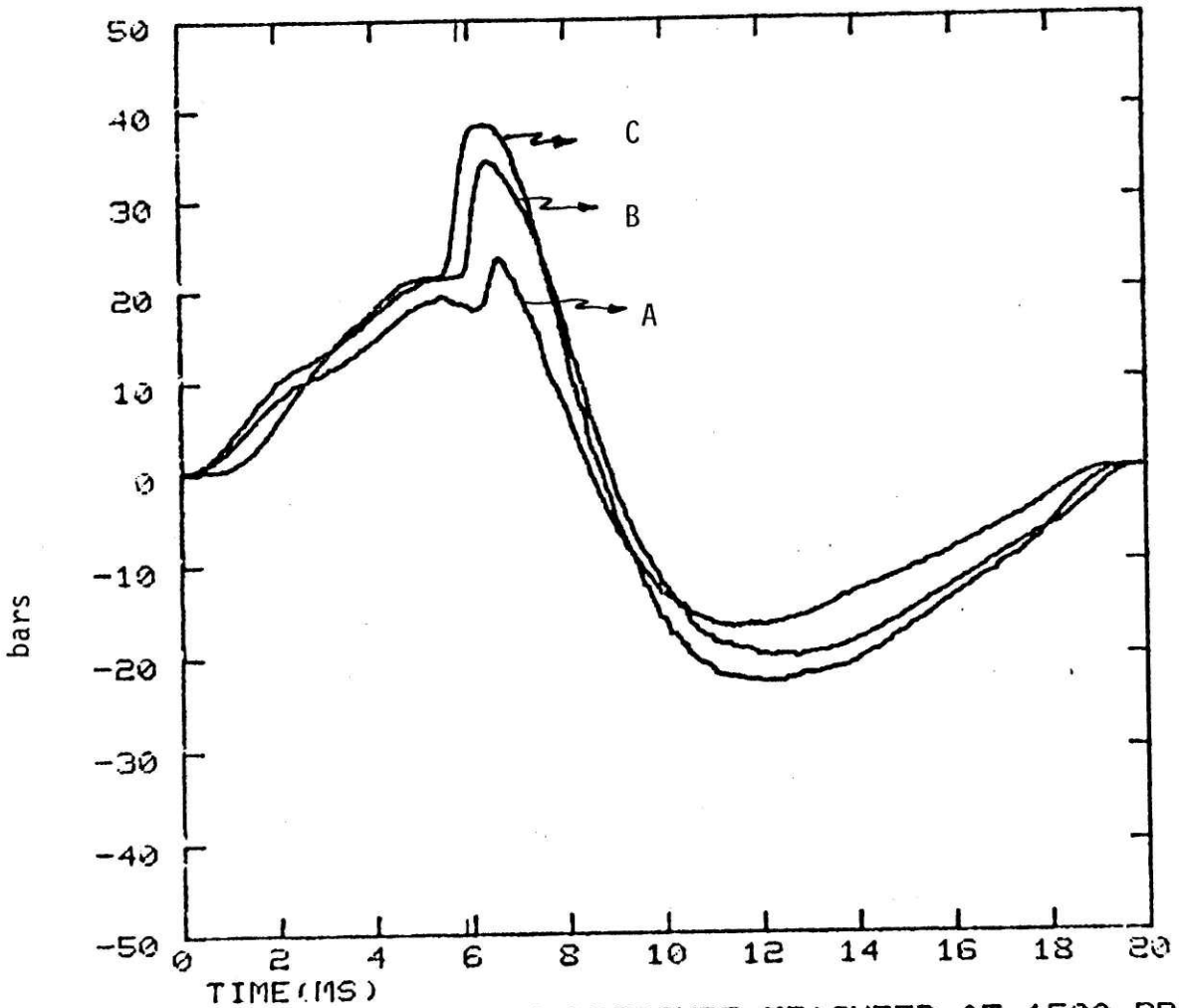

FIG. 3.11:- CYLINDER PRESSURE MEASURED AT 1500 RPM
A) NO LOAD , B) 60% OF FULL LOAD , C)FULL LOAD

Both the pressure spectrum and trace at 2500 rpm were similar to those at 1500 rpm (Fig. 3.12). The spectrum was shifted in frequency. The amount of the shift was the ratio of the two speeds, or approximately 1.6. The pressure trace at 2500 rpm and 50% load showed that peak occurred after TDC. It is consistent with the fact that the time required for combustion to start is independent of speed.

To study the statistical variation of the cylinder pressure, the ensemble average of the pressure trace record was found, i.e., averaging equivalent points of the different traces. Two methods for selecting (windowing) of the traces were employed: (1) using TDC mark as a trigger, and (2) constant time gating.

In the first case, each record (pressure trace sample) started 4 ms before TDC. This method eliminated the effect of speed variation in averaging. The second method averaged records taken two revolutions (T_r = 60/rpm seconds) apart regardless of where the TDC mark occurred in the record. In both cases the record length was 180° crank angle.

The two averages of 20 records each and their respective spectra were compared with a typical pressure trace and its spectrum. All of the pressures were measured under the same operating condition. The results are summarized as follows:

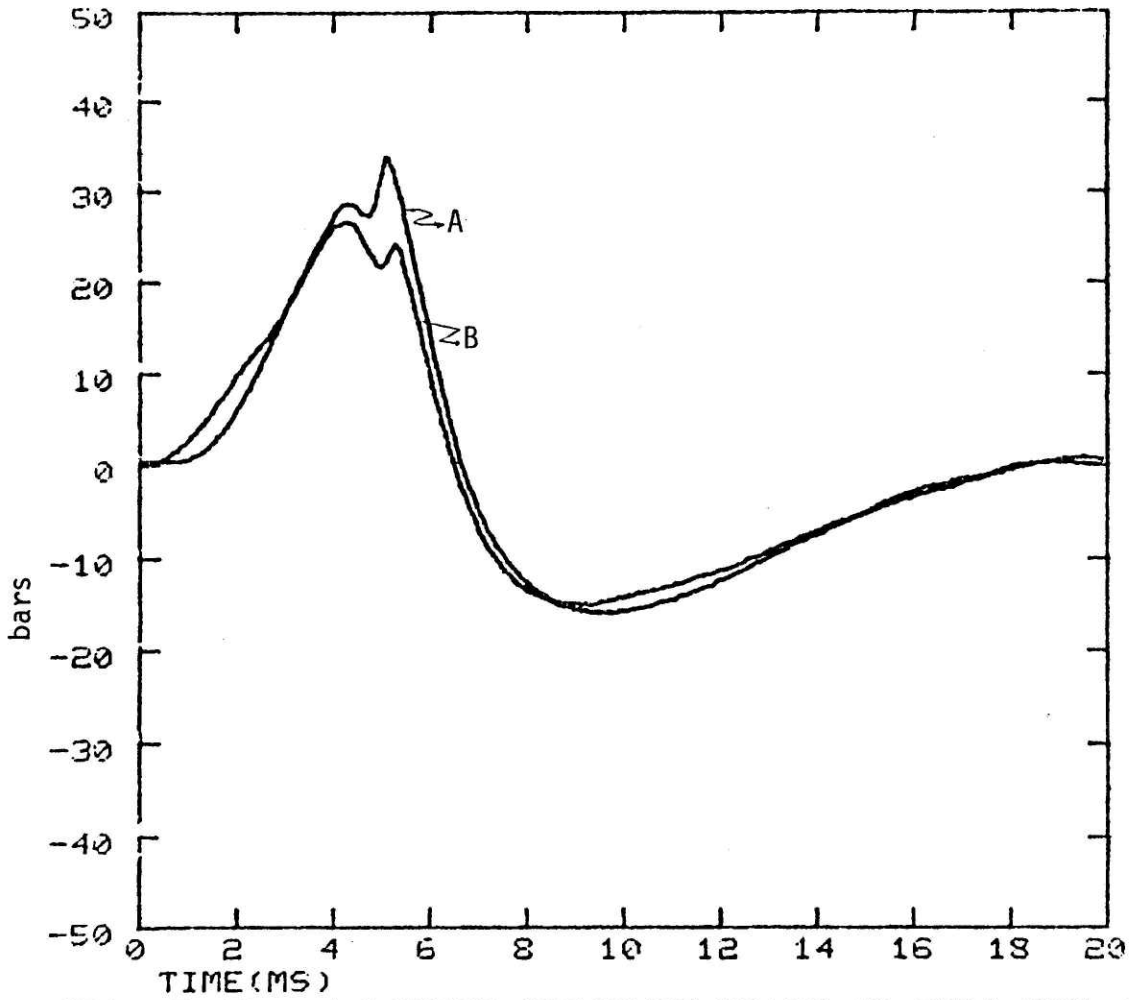

FIG. 3.12:- CYLINDER PRESSURE TRACE AT 2500 RPM AND
A) 50% OF FULL LOAD , B) NO LOAD

(a) The average of the records triggered by the TDC mark was very similar to a typical individual pressure trace. The rapid pressure rise was preserved. The frequency content of the average trace was comparable to the single pressure trace.

(b) In the average taken by the second method, the sharp pressure rise indicating combustion process disappeared. The energy frequencies of 1000 to 2500 Hz diminished.

The two averages of the 20 records of pressure traces of the engine at 1500 rpm and 60% of the full load and their spectra is given in Figures 3.13 and 3.14. Therefore, the variation in cylinder pressure is much less than the variation in engine speed.

A quantitative measure of the variation is defined as normalized ensemble variance, S,

$$S = \left(\left(\frac{1}{N-1}\frac{1}{M-1}\sum_{m=1}^{M}\sum_{n=1}(x_m(n)-\bar{x}(n))^2\right)\frac{1}{\Sigma\hat{x}^2(n)}\right)^{1/2}$$

where n is discrete time or sample number, $x_m(n)$ is the n^{th} sample of the m^{th} record, $\bar{x}(n)$ is the average record, N is the total number of the time samples in each record and M is the total number of the records.

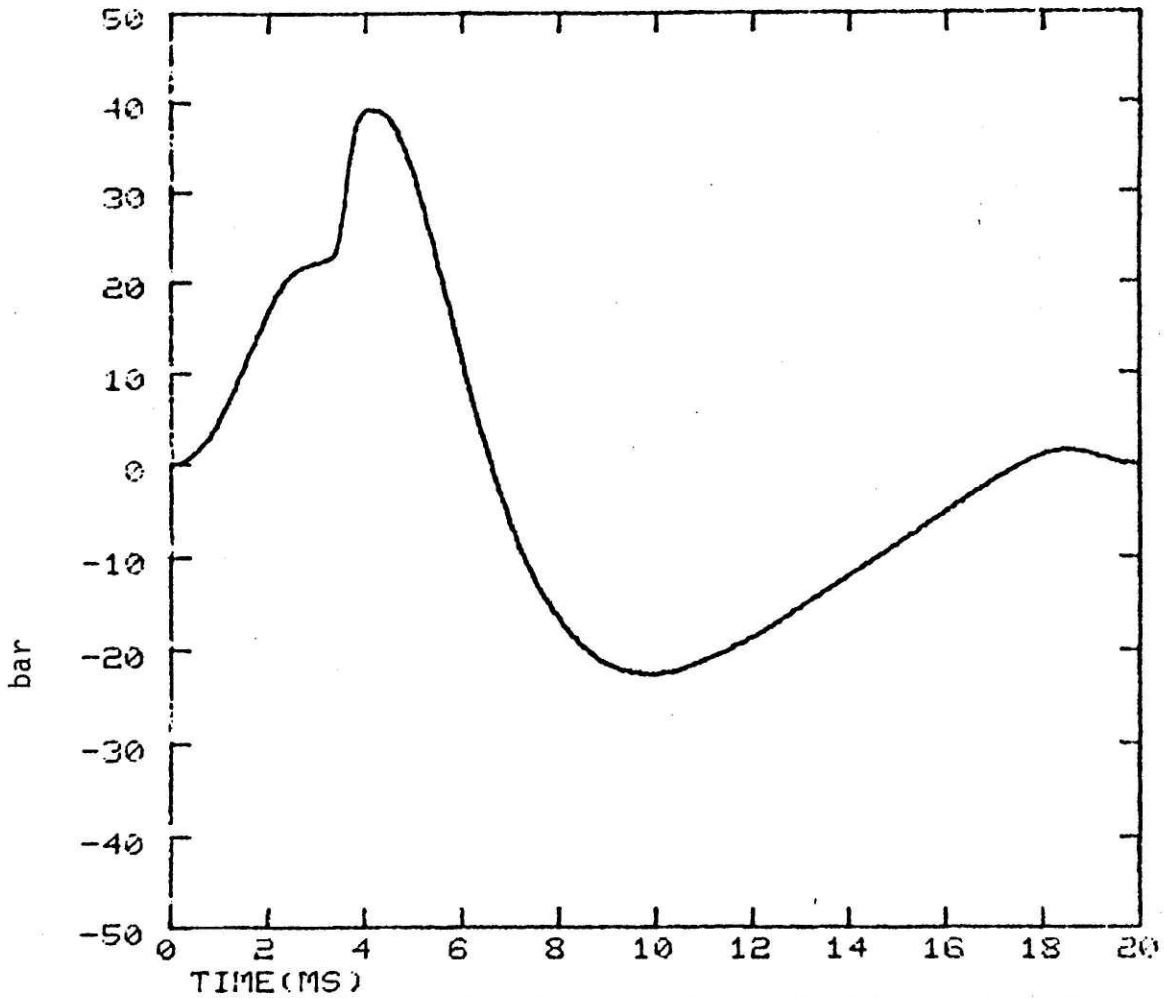

FIG. 3.13:- THE AVERAGE OF 20 CYLINDER PRESSURE TRACES; AVERAGED USING TDC MARK

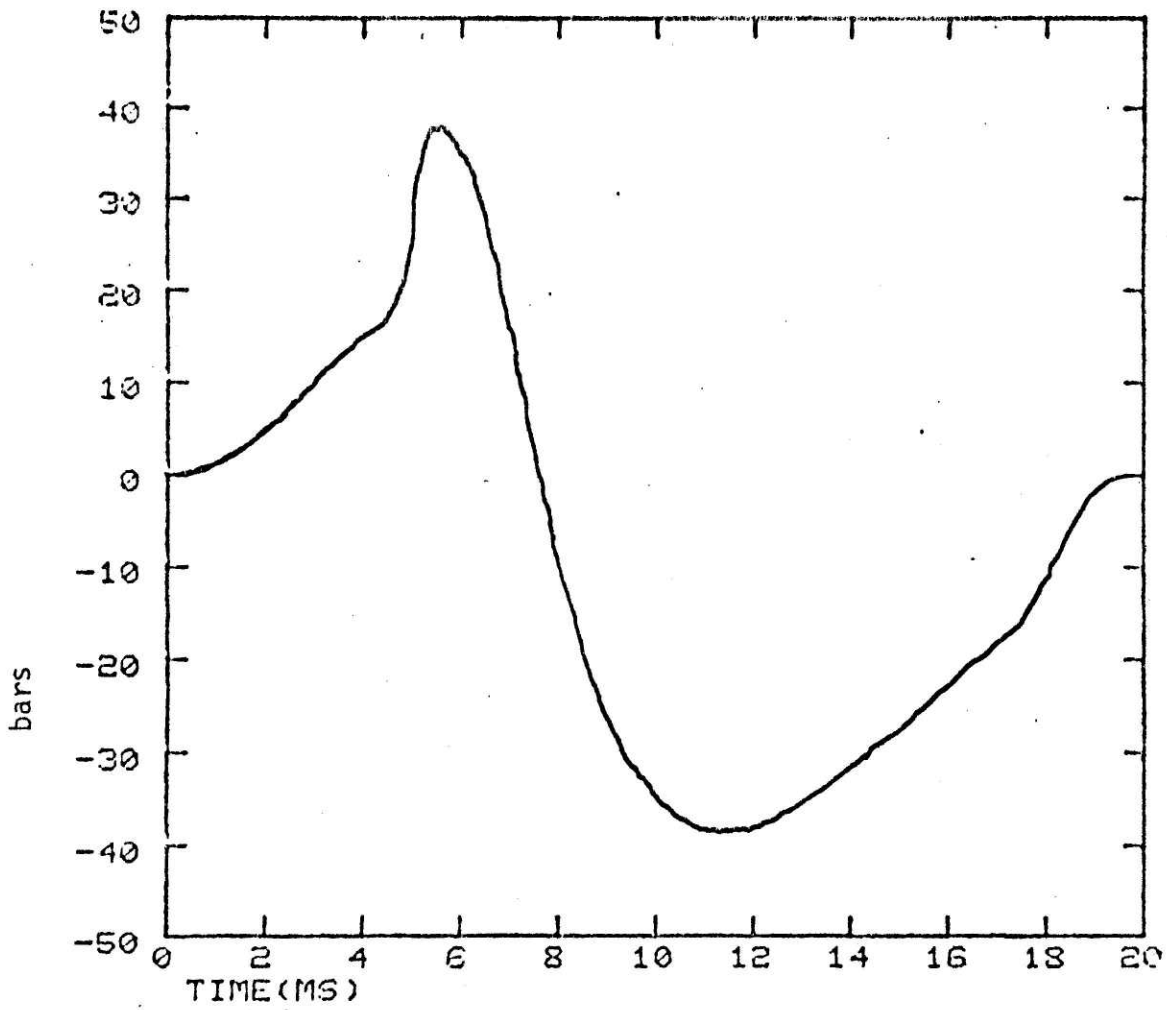

FIG. 3.14:- THE AVERAGE OF 20 CYLINDER PRESSURE TRACES AVERAGED USING CONSTANT TIME GATING

The normalized variance, S , of 20 pressure traces taken at 1500 rpm and 60% load averaged by TDC triggering method is 1.6×10^{-3}. The normalized variance of the same data by the second method is 0.12. When the effect of speed variation is eliminated, the variance is reduced by a factor of 100.

3.2.2 Acceleration of the engine block

The acceleration of the engine block was measured at all of the observation points under all of the operating conditions discussed in Section 3.2 The acceleration time trace [Fig. 3.15] showed that the acceleration caused by firing of each cylinder forms a burst of energy which attenuates before the next firing. The excitation from each cylinder produced a very distinct acceleration signature. The signature that is repeated in many engine cycles appears to be a composite signal [3.16].

However, the magnitudes of acceleration spectra [Fig. 3.17], associated with firing of different cylinders were very similar. These spectra were taken in a 180° crank angle time window. Therefore, the time occurrence of the events within the time window was important. If frequency domain analysis is desired, the relative phase of spectrum is an important factor in distinguishing the firing of different cylinders. In fact, a time signal similar to acceleration can be constructed from a spectrum with a flat magnitude and the phase of the measured acceleration [Fig. 3.18].

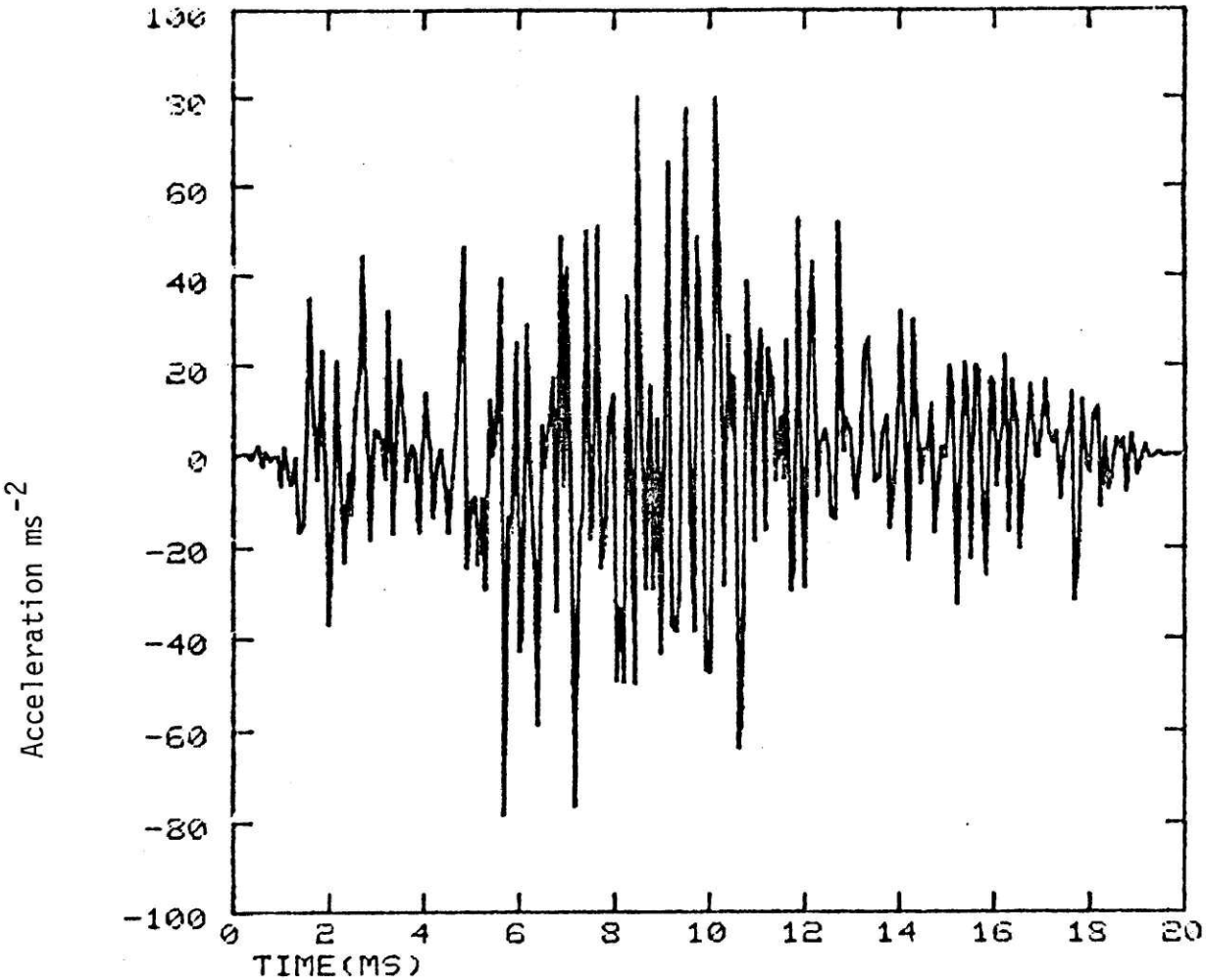

FIG. 3.15:- ACCELERATION AT POINT 2A, EXCITED BY FIRING OF CYLINDER #4, AT 1500 RPM AND 60% LOAD

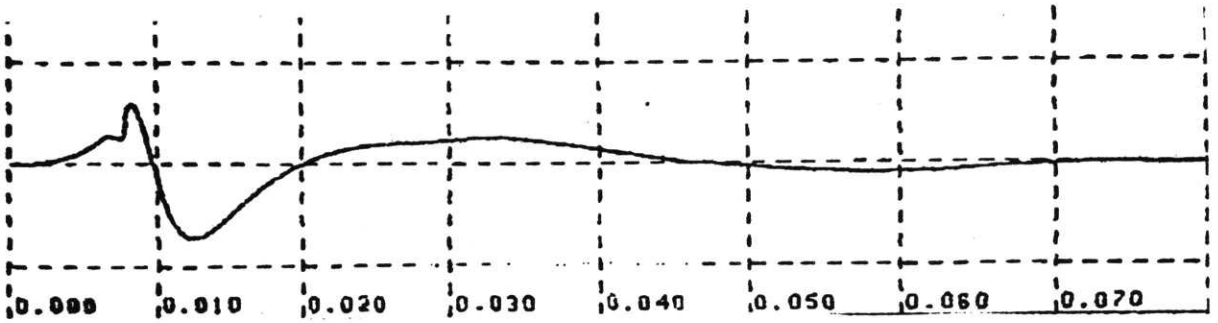

time sec
Cylinder Pressure

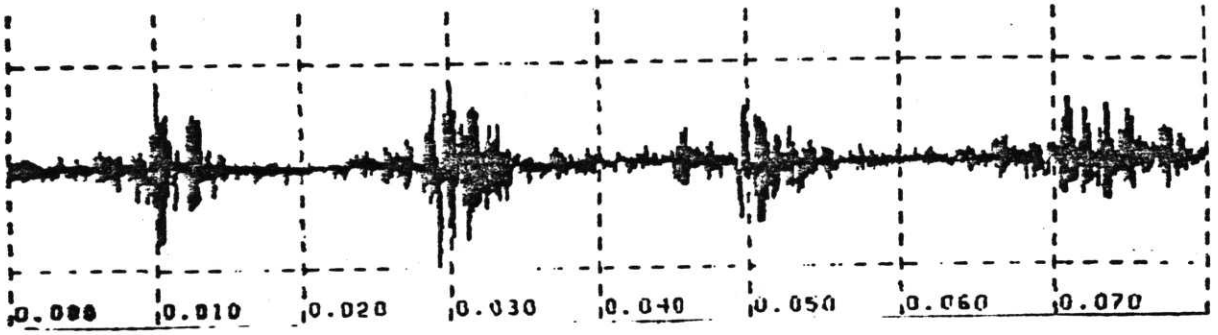

time sec
Acceleration on the Block -- Cycle 1

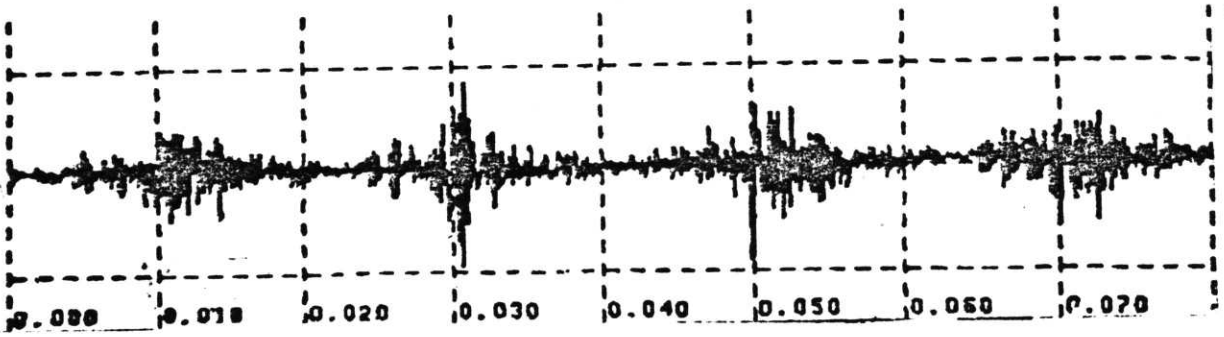

time sec
Acceleration on the Block -- Cycle 2

Figure 3.16: Measured Acceleration on Engine for Several Engine Cycles

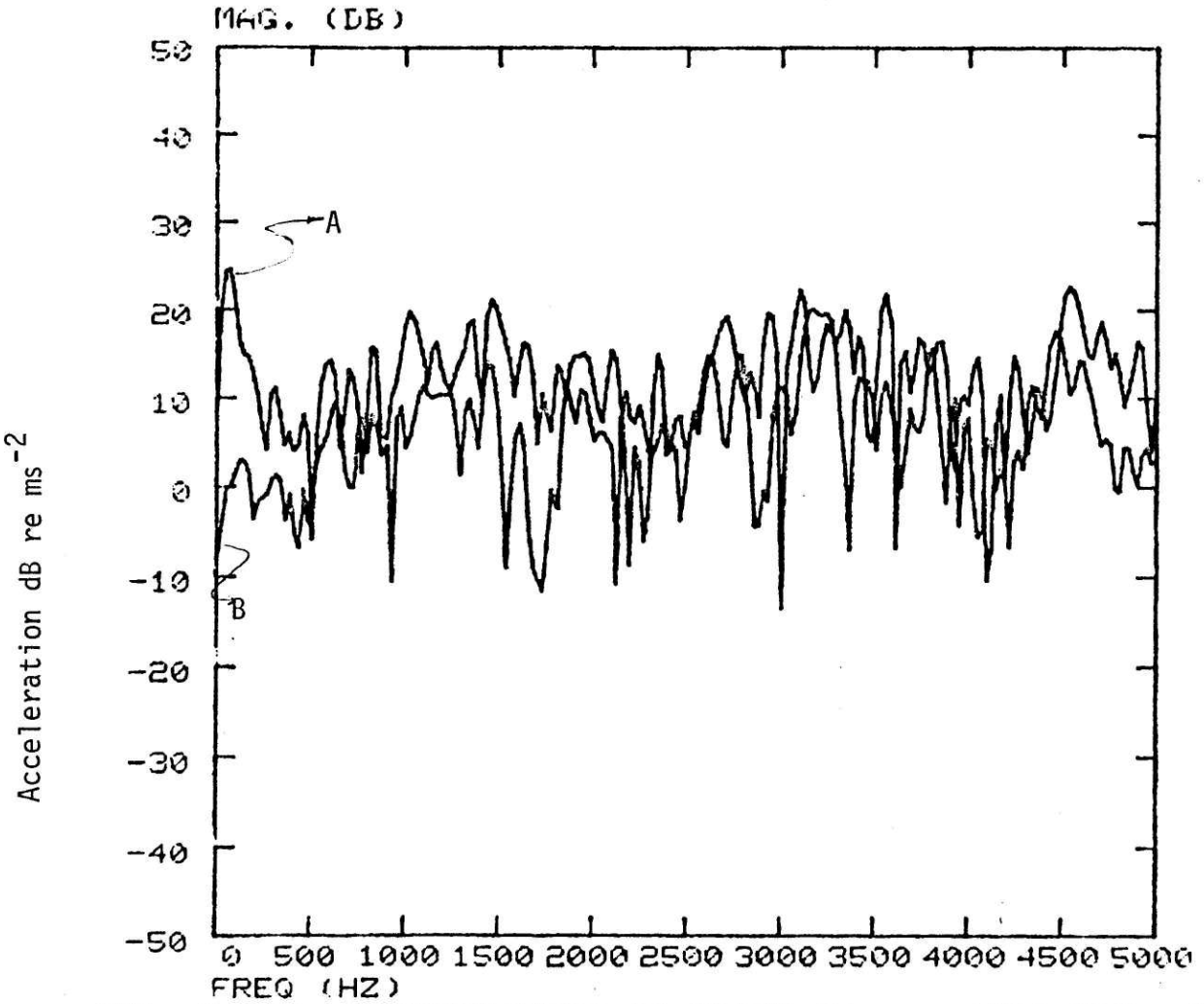

FIG. 3.17:- ACCELERATION AT POINT 2A --- 1500 RPM AND
A)FULL LOAD , B) NO LOAD

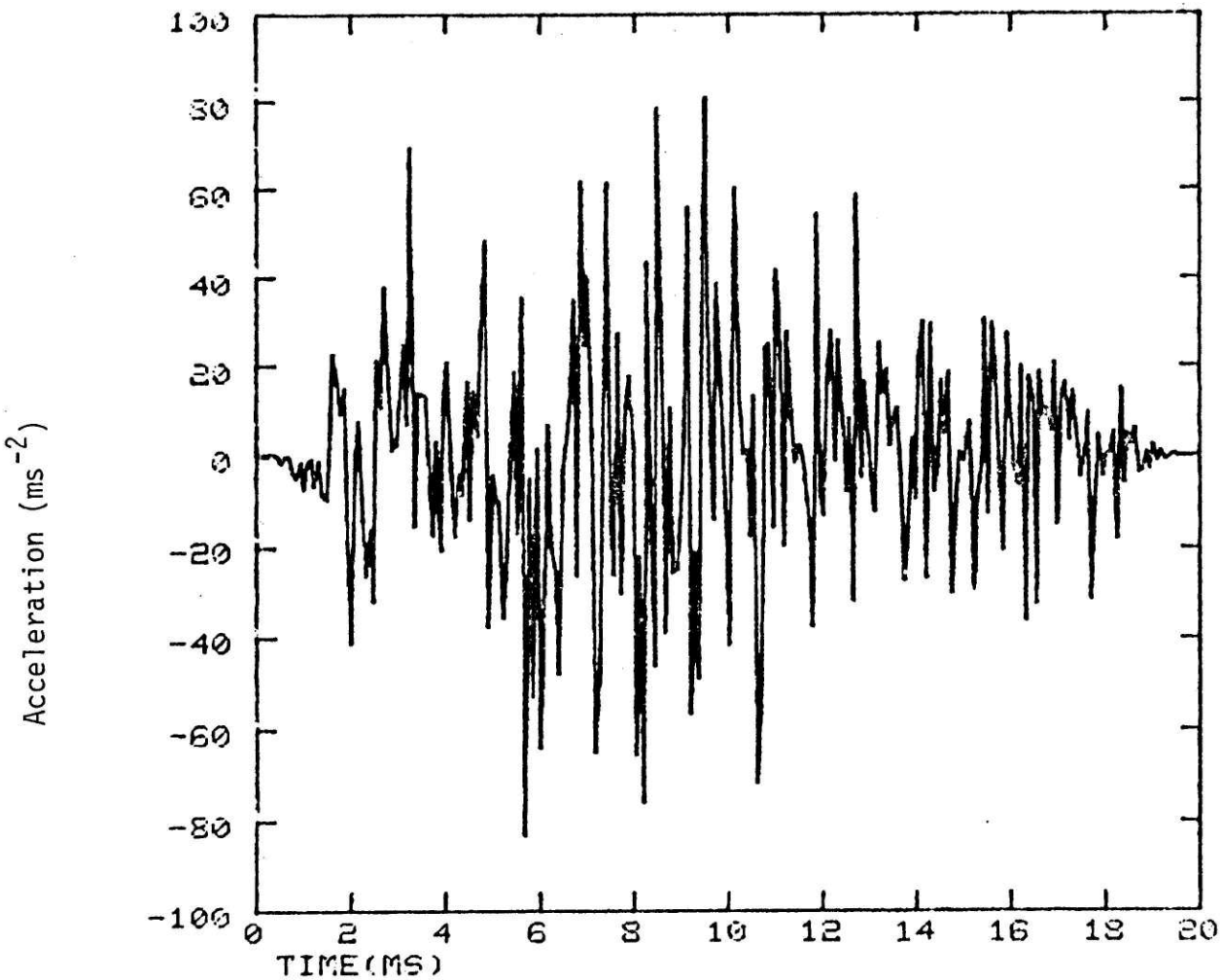

FIG. 3.18:- CONSTRUCTED ACCEL. FROM THE PHASE OF MEASURED ACCEL. AND A FLAT MAG. -- POINT 2A AT 1500 RPM, 60% LOAD

The shape of spectrum at frequencies below 1 kHz and in the range 3 to 4 kHz is load dependent. The total energy of the signal is also dependent on the load and drops significantly at no load.

However, even when a cylinder is shut off Fig. (3.19), a burst of energy associated within the excitation of the cylinder still exists. This acceleration is produced by the compression cycle as well as piston slap and valve openings. The impact that occurs approximately 1 ms after TDC when the cylinder is shut off is associated with the piston slap.

Cepstral smoothing of the acceleration would reduce the effect of multi-path transmission as well as the mechanical noises (see Chapter II). A cepstrally smoothed acceleration Fig.(3.20) shows the decomposition of frequency components in time which is characteristic of a dispersive media. The cepstral window of 2 ms long, put on low-time portion of complex cepstrum, was used to smooth this acceleration signal.

Simultaneous records of acceleration at a pair of points showed that for the points close to the cylinder head (pair #1), a measurable time lag between the two acceleration traces existed (Fig. 3.21)

The acceleration spectrum (Fig. 3.17) has a rather constant energy density over the 25 Hz to 5 kHz frequency range. This type of spectrum is expected from convolution of cylinder pressure and the engine VTF.

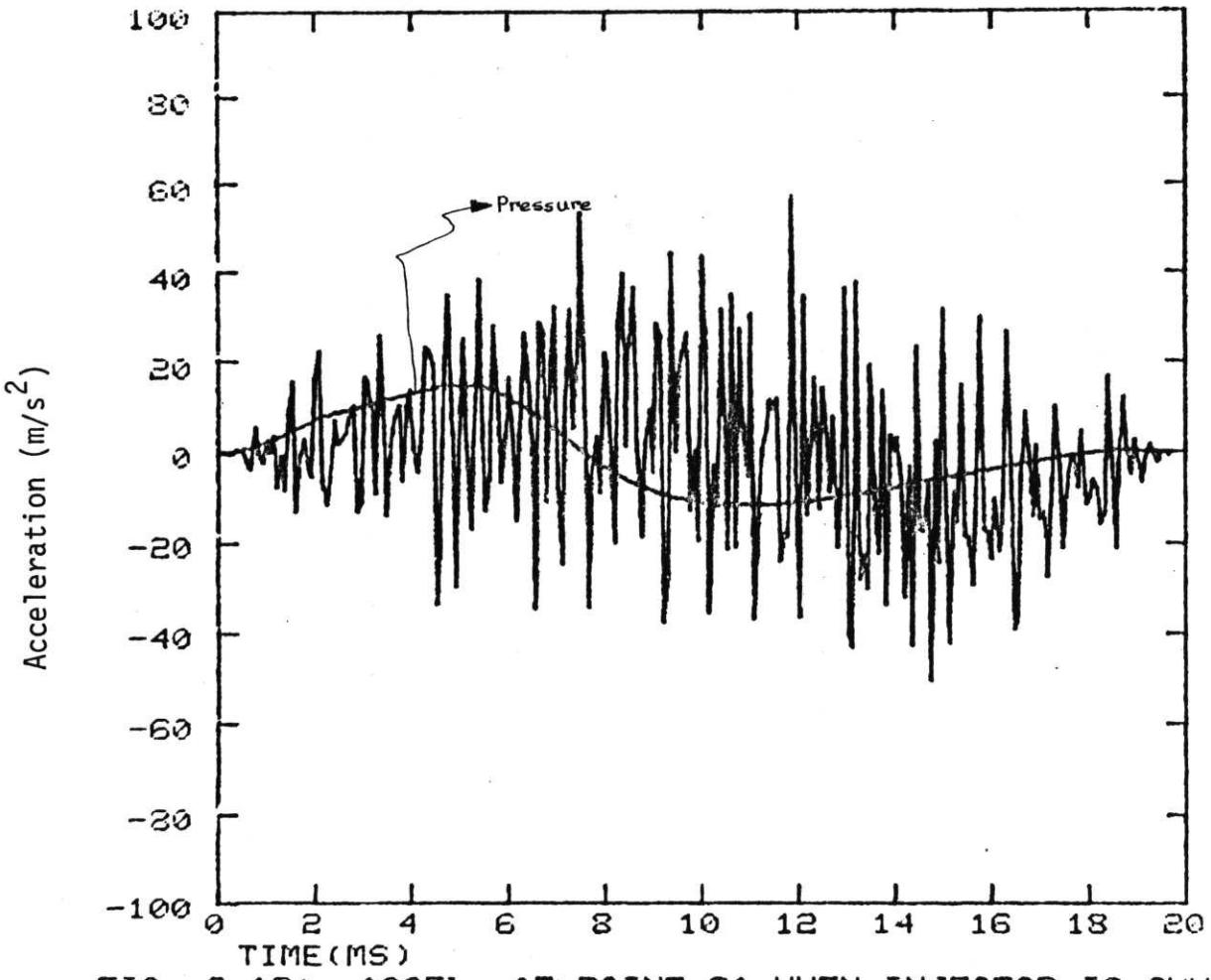

FIG. 3.19:- ACCEL. AT POINT 2A WHEN INJECTOR IS SHUT THE MEASURED CYLINDER PRESSURE IS ALSO SHOWN

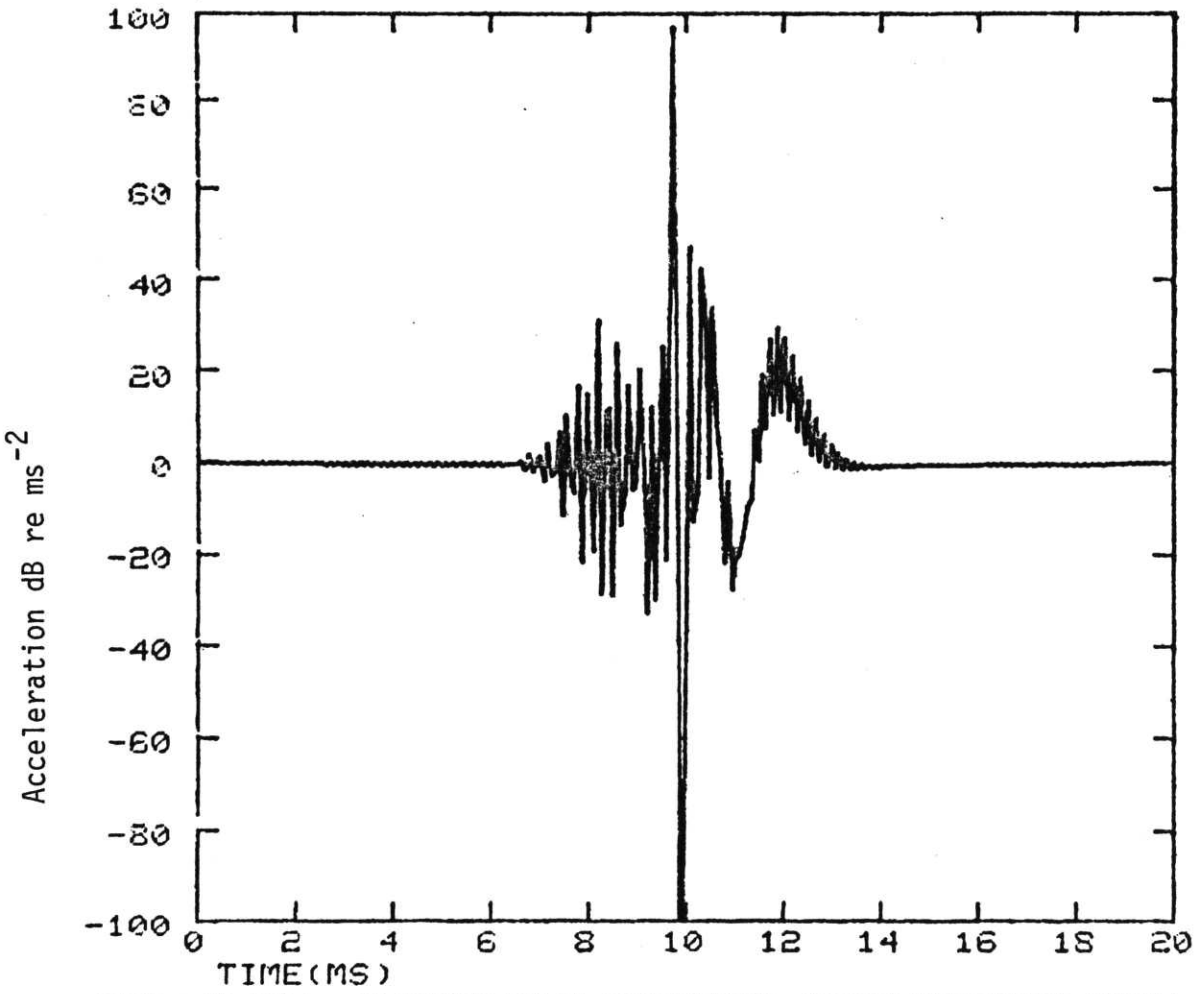

FIG. 3.20:- CEPSTRALLY SMOOTHED ACCELERATION WITH A SYMMETERIC WINDOW WITH LENGHT OF 40 SAMPLES

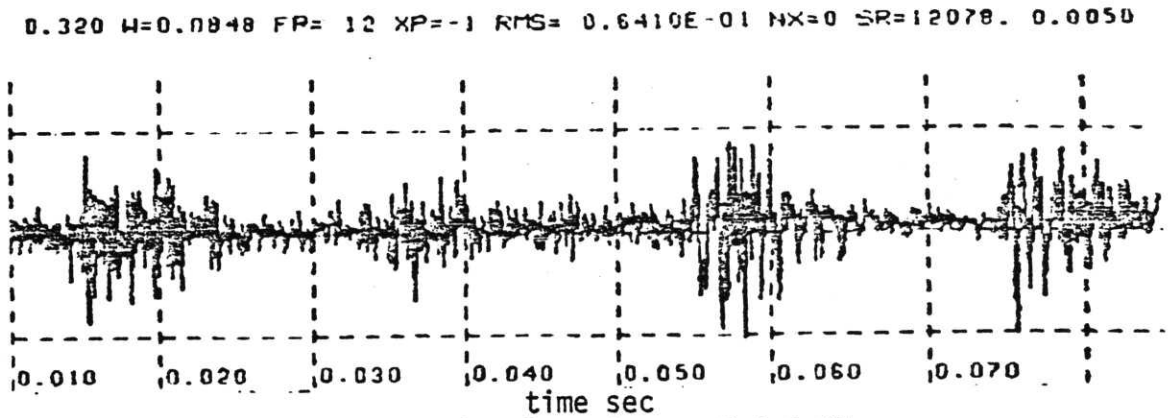

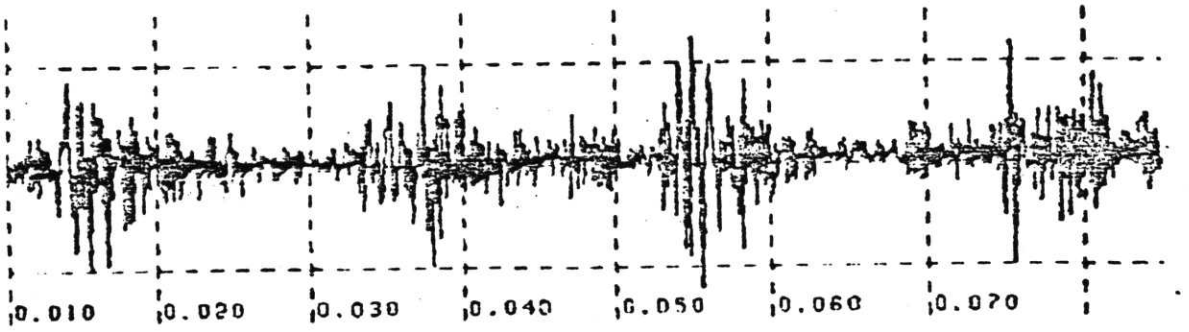

Figure 3.21: Acceleration Measured on Points 2A and 2B Simultaneously

3.3 The Vibration Transfer Function of the Operating Engine

The acceleration of the engine block on a running engine in a short-time window is given in Eq. 2.21. In frequency domain, the acceleration for k *th* set of data, $A_k(\omega)$ is:

$$A_k(\omega) = P_k(\omega)\, H_p(\omega) + S_k(\omega)\, H_s(\omega) \tag{3.5}$$

where $P_k(\omega)$,$S(\omega)$, $H_p(\omega)$ and $H_s(\omega)$ are the Fourier transforms of the cylinder pressure, piston slap and the impulsive responses of the engine to these forces, respectively. The estimated DVTF from this data, $\tilde{H}_k(\omega)$ is:

$$\tilde{H}_k(\omega) = \frac{A_k(\omega)}{P_k(\omega)} = H_p(\omega) + \frac{S_k(\omega)H_s(\omega)}{P_k(\omega)} \tag{3.6}$$

Therefore, while measuring the VTF on an operating engine eliminates some of the problems introduced by measuring VTF on non-running engine, DVTF1 is also contaminated by the effect of secondary vibration sources, especially piston slap. The error introduced by these forces. The estimate error $\varepsilon_k(\omega)$ is defined as

$$\varepsilon_k(\omega) = \frac{\tilde{H}_k(\omega) - H_p(\omega)}{H_p(\omega)}$$

From Eq. 3.6:

or

$$\tilde{H}_k(\omega) = H_p(\omega) \left[1 + \frac{S_k(\omega)}{P_k(\omega)} \cdot \frac{H_S(\omega)}{H_p(\omega)}\right] \qquad (3.7)$$

$$\tilde{H}_k(\omega) = H_p(\omega) \left[1 + \beta_k(\omega) \quad \alpha(\omega)\right]$$

where $\alpha(\omega)$ is $H_s(\omega)/H_p(\omega)$ and $\beta(\omega)$ is $S_k(\omega)/P_k(\omega)$. Therefore,

$$\varepsilon k(\omega) = \beta_k(\omega) \ \alpha(\omega). \qquad (3.8)$$

The ratio of the two transfer functions $\alpha(\omega)$ is independent of the operating condition. It is assumed that because of the similarities between transfer paths for combustion and piston slap, the magnitude of $\alpha(\omega)$ is close to unity. The phase of $\alpha(\omega)$ depends on the details of the transfer paths.

The ratio of two forces, $\beta(\omega)$, depends on the load and speed. Because of the statistical variation of both combustion and piston slap, $\beta(\omega)$ is also a random variable. The magnitude of $\beta(\omega)$ depends on the energy of two forces and *decreases* as the load increases because $P(\omega)$ increases with load more rapidly than $S(\omega)$. The magnitude of $\beta(\omega)$ is small for the frequencies below 2 kHz. The phase of $\beta(\omega)$ depends on the time delay between the combustion force and piston slap. The estimation error $\varepsilon(\omega)$ should decrease as the load increases. Therefore, DVTF measured on high loads is more accurate.

Piston slap contamination effects the phase of VTF more significantly than its magnitude. A phase error, ε_ϕ, may be defined as:

$$\varepsilon_\phi = \bar{\phi}_p - \bar{\phi}_{p,r} \tag{3.9}$$

where ϕ_p is the phase of VTF and $\phi_{p,r}$ is the estimated phase of it. Experiments showed that ε_ϕ has a pure time shift component of 1 to 2 msec or 9° to 18° crank angle, which is similar to the time delay between piston and combustion forces.

The DVTF1 was estimated by short time deconvolution of the cylinder pressure from the acceleration signal. The time window for acceleration signal was half of one revolution. At each observation point, the DVTF between the point and all four cylinders were estimated for different operating conditions.

The DVTF was found for the engine operating at 1500 rpm and under no load, 60% and 90% of the full load. The cylinder pressure in cylinder #4 was measured. It was assumed that under normal operating conditions, the pressure trace of all four cylinders are similar. Four different DVTFs were constructed for each operating condition. [See Table 3.1].

3.3.1 The processing technique

The two major processing techniques used to estimate DVTF and predict input forces (see Chapter IV) were the fast deconvolution method and the cepstral smoothing method. A program GTDATA, was used to take and store data records. A program "PROCES" was developed to calculate short-time fast convolution/deconvolution as well as cross and auto-correlation.

Another program "CEPSTR" was developed to calculate real and complex cepstrum, put "windows" on cepstrum and take inverse cepstrum of the windowed signal. Part of this program which unwraps the phase was used independently to study the phase of different signals.

All the programs were interactive. They were written in Fortran for a Data General Nova Computer. Listings of both programs are given in Appendix C.

The flow chart of PROCES is given in Fig. 3.22. The program does the following tasks:

(a) Reads two data records (x and y).

(b) Eliminates the DC component and tapers the signal with either cosine or hamming window, if desired.

(c) Zero pads the signals to avoid wrap around error [23].

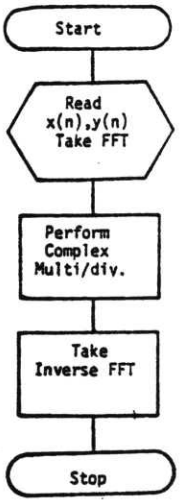

Fig. 3.22: The Flow Chart for Program "PROCESS"

(d) Takes FFT of both of the inputs, adjusts the gain, eliminates time shift.

(e) Calculates the spectrum of the output by complex multiplying/ dividing or multiplying by the complex conjugate (for auto/cross correlation) as specified.

(f) Takes inverse FFT of the output.

(g) Displays the results of either inputs, in time or frequency domain .

(h) In the user's option, saves the output data or its spectrum.

The "PROCES" is generally fast. Accuracy of the procedure is the accuracy of the FFT (see Section 3.1).

The error which frequently occurs in deconvolution using Fourier Transform technique results from division by zero in the frequency bands where the spectral energy is low. The spectrum of cylinder

pressure is very low above 2.5 kHz. This introduces large errors in finding DVTF from acceleration and pressure signals. To overcome the problem, the pressure spectrum was "thresholded"; the spectral values 60 dB less than the peak was equalized to -60 dB of the peak. The value of 60 dB was chosen because dynamic range of the system, A/D converter and tape recorder, is 60 dB. Any spectral values less than this value is the result of numerical error. To demonstrate that "thresholding" does not affect the shape of the cylinder pressure, the inverse DFT of the threshold spectrum was taken (Fig. 3.23). This reconstructed pressure is similar to the original.

The other main program used is "CEPSTR". This program was used to calculate and manipulate the cepstrum and the inverse cepstrum of the sequences. The flow chart of the program CEPSTR is given in Fig. 3.24. The program performs the following tasks:

(a) Reads the data file x(n).

(b) Takes out DC component and window tapers the data. Three different windows are available: hamming, cosine and exponential.

(c) Pads the data with zeroes, if complex cepstrum is desired, forms the signal n x(n), where n is discrete time.

(d) Takes FFT of x(n) and n x(n)..

(e) Calculates the logarithm of amplitude, calculates the phase.

(f) Unwraps the phase (adds proper 2π factors).

(g) Calculates and displays cepstrum.

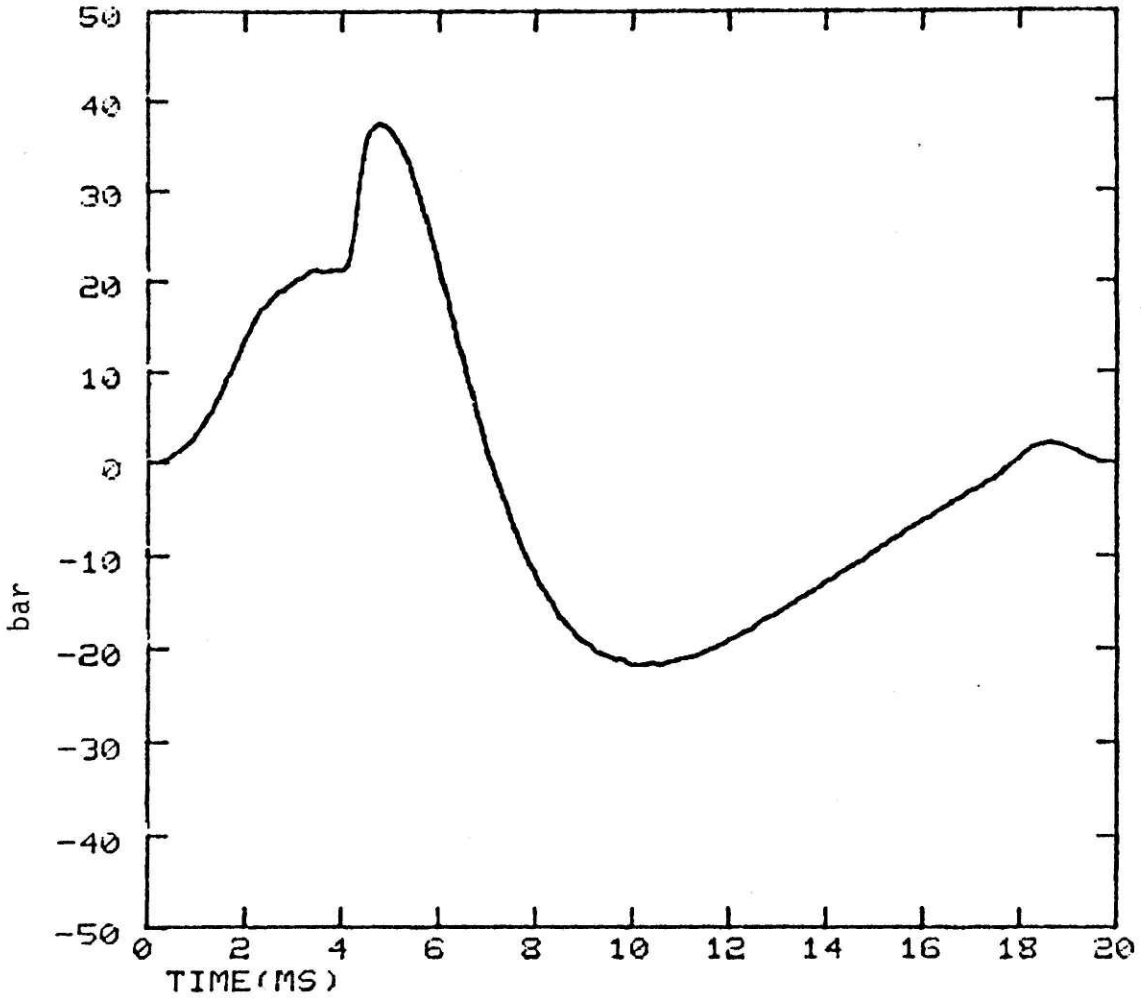

FIG. 3.22:- TRESHOLDED CYLINDER PRESSURE

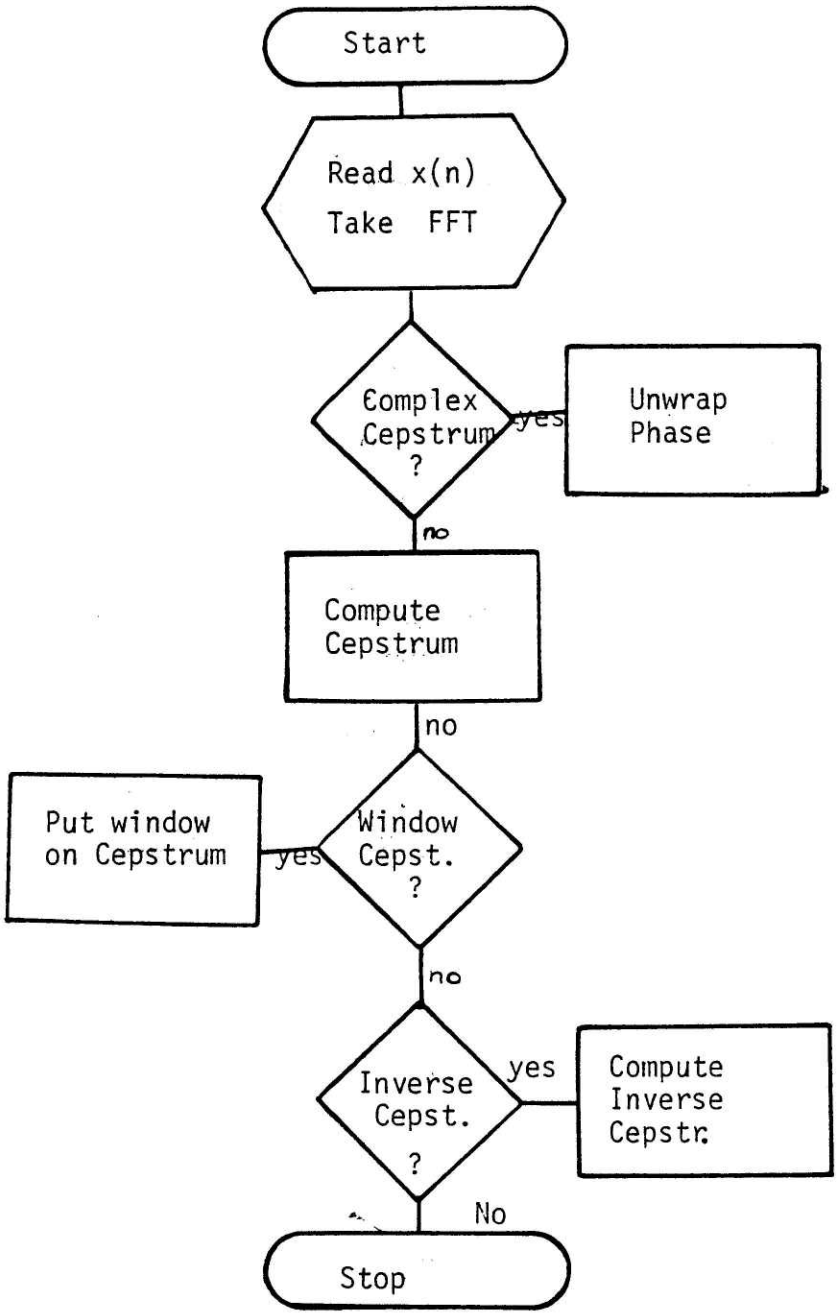

Figure 3.24: Flow Chart of Program "CEPSTR"

(h) Puts a window over the cepstrum. The length and the starting point of the window is defined by the user.

(i) Takes the inverse cepstrum and displays it.

(j) In the user's option, saves either cepstrum or inverse of the windowed cepstrum, which is the cepstrally-smoothed signal.

(k) In the user's option, goes back to h.

The phase unwrapping of spectrum is adding the integer multiple of 2π eliminated from the phase of spectrum in calculating the phase from inverse tangent routine. To calculate complex cepstrum, it is necessary to define phase as a continuous function of frequency [25].

One method to solve the ambiguity in phase is to calculate phase by integrating its derivative,

$$\left[\frac{d \arg [_{\omega}(e^{j\omega})]}{d\omega}\right. = \frac{X_R X_I' - X_I X_R'}{|X|^2} \tag{3.10}$$

where X_R and X_I are real and imaginary parts of the Fourier transform of the sequence $x(n)$, and X_I' and X_R' are their derivitive with respect to radian frequency ω. In addition,

$$X' = X_R' + j\, X_I' = -\, j\, FT\{nx(n)\} \tag{3.11}$$

and

$$\arg(X) = \int_0^{\omega} \arg'(X)\, d\omega. \tag{3.12}$$

The phase unwrapping algorithm used, was an adaptive integration technique proposed by J. Tribolet [28]. The algorithm uses the inverse tangent routine to calculate the principal values of phase, ARG(X), and adaptive integration to calculate the proper integer of 2π which should be added to the principal. If the correct phase at the frequency Ω_0 is known, then for $\Omega_1 > \Omega_0$

$$\text{ARG}(X(\Omega_1)/\Omega_0) = \int_{\Omega_0}^{\Omega_1} \text{ARG}'(X)\, d\omega \qquad (3.13)$$

Eq.3.13 is evaluated numerically. The accuracy of the integration depends on the number of summation points between Ω_1 and Ω_0; integration steps. Instead of predefining an arbitarily large number of steps, the "adaptive integration" technique doubles the number of steps until a consistent phase estimate is found. A phase estimate at frequency Ω_1 is consistent if the difference between the phase at Ω_1 and Ω_0 is less than a threshold θ_1. This threshold should be less than π. The accuracy of the phase unwrapping depends on θ_1. However, increasing the threshold makes the program slow and unstable in the presence of spectral zeroes. The value of θ_1 was chosen to be 1.5.

Phase unwrapping is unsuccessful when spectrum of signal has sharp zeroes. The program, in general, is slow unless special hardware devices are used to calculate cepstrum.

3.3.2 Vibration transfer function

The magnitude of DVTF (Fig. 3.25) is comparable to the magnitude of SVTF. The unwrapped phase $\phi(\omega)$, of the measured DVTF may be modeled as (Fig. 3.26).

$$\phi(\omega) = a\omega^{1/2} + b\omega \tag{3.14}$$

where a depends on the phase speed in the medium and the distance between force input and measuring point and b is related to the time delay. The phase is consistent with the propagation model for transfer function.

For DVTF of point 2b, (Fig. 3.27) the time delay is 2 msec. The distance assuming phase speed of bending wave in 3/16 inch steel is around 1.2 meter for DVTF from cylinder 1 and .5 m for cylinder 4. The distance is the average length of many paths. Part of the time delay, about 1 ms may be acounted for as the effect of piston slap (see Chapter II). The remainder is associated with phase unwrapping errors at spectrum zeroes as well as changes in DVTF because of engine rotation. This DVTF was measured for the engine operating at 1500 rpm and 60% of full load.

The unwrapped phase of DVTF, taken for the other operating conditions shows comparable distance dependence and time shift. Similarly the time shift of 1.6 to 2.5 ms observed for these DVTFs are more than what may be accounted for by the effect of piston slap.

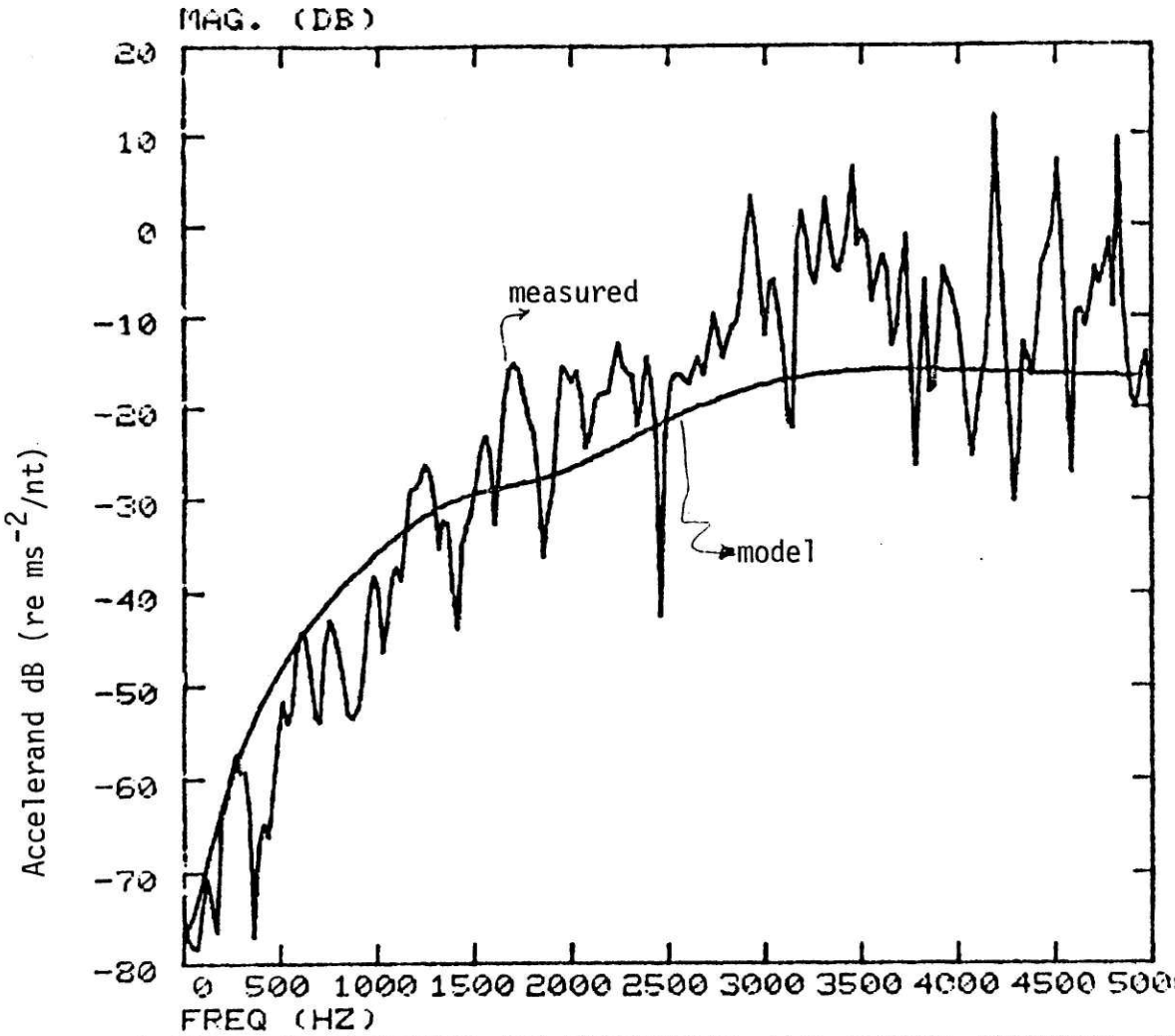

FIG. 3.25:- MAGNITUDE OF MEASURED AND MODEL VIBRAT. TRANS. FUNCTION OF THE OPERATING ENGINE -- 1500 RPM,60% LOAD

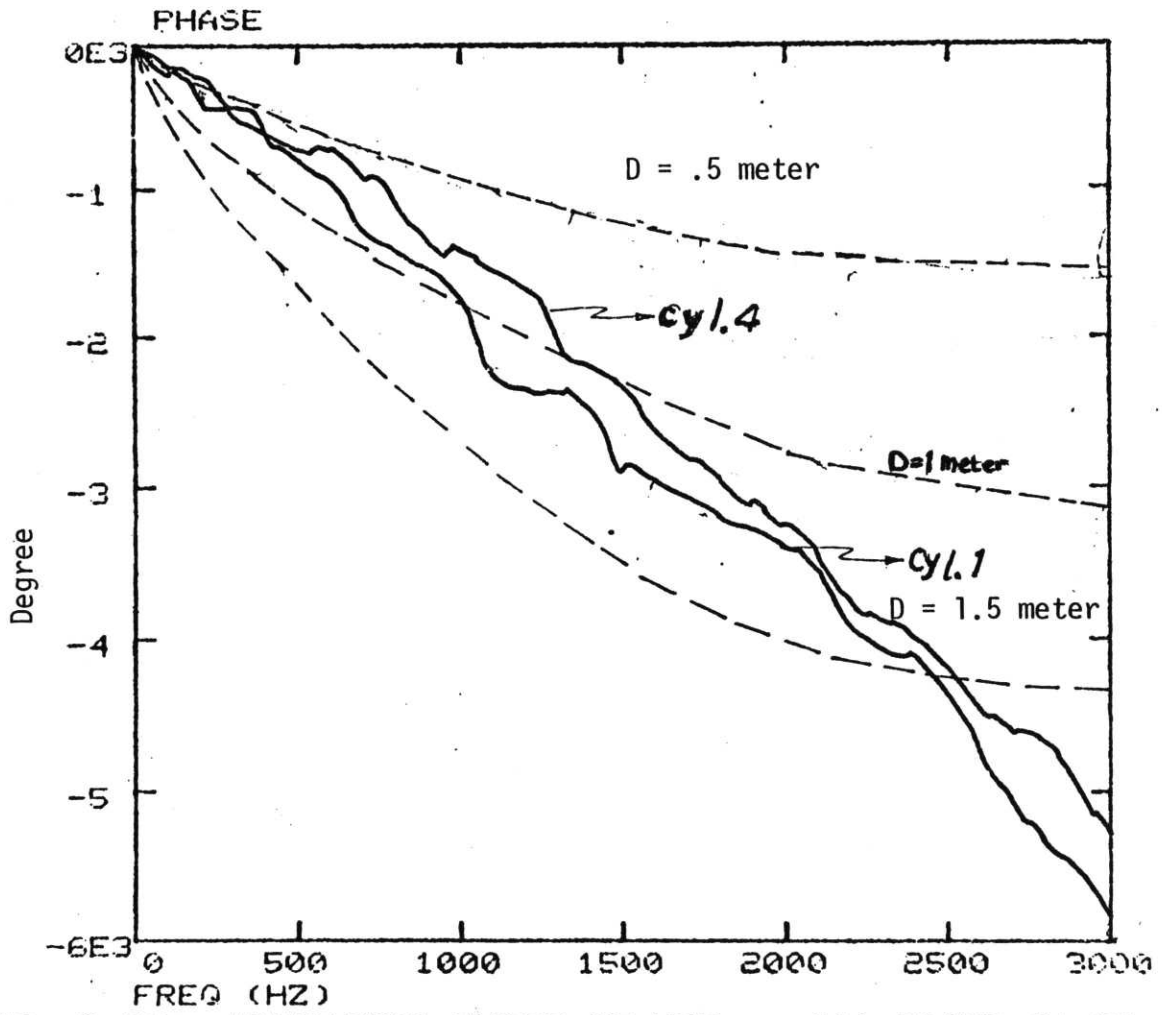

FIG. 3.26:- UNWRAPPED PHASE OF VTF -- (A) POINT 2A TO CYLS. 1 AND 4, (B) 3/16 INCH THICK STEEL PLATE, AT DISTANCE D

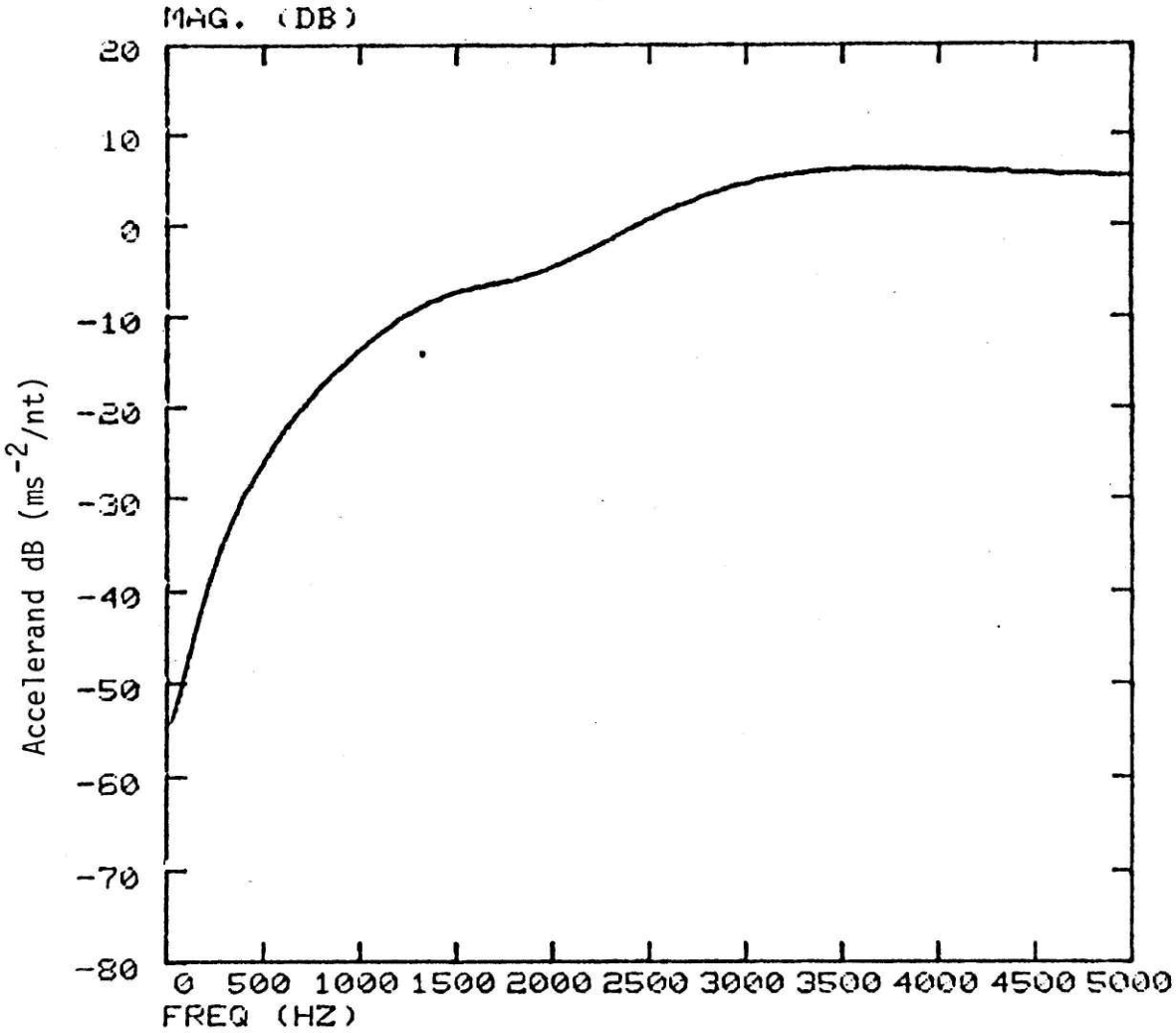

FIG. 3.27:- MODEL INPUT INERTANCE

To study the relative importance and comparison with different VTF models developed in Chapter II, four different DVTF were estimated/ reconstructed for each operating condition. The DVTF1 was found by deconvolving the cylinder pressure from acceleration. The other DVTFs were reconstructed by modifying or smoothing the phase, magnitude or both of the DVTF1.

The four DVTFs all have the same input inertance $I(\omega)$. The experiment (see Section 3.1) showed that this $I(\omega)$ may be modeled as a stiffness (zero at zero frequency) and two damped resonances. A 3 degree of freedom model (Fig. 3.27) represents the engine $I(\omega)$. This model has a zero at zero frequency and two poles at 1500 Hz and 2500 Hz. The poles are very damped (σ = .12).

The VT part of DVTF1 is the result of short time deconvolution of acceleration and cylinder pressure when the $I(\omega)$ is factored out. The magnitude of spectrum of $I(\omega)$ of DVTF2 is flat, its phase is similar to that of DVTF1. DVTF3 is the cepstrally smoothed DVTF1 with a 3 ms cepstral window on low time portion. DVTF3 is comparable to propagation in a single path. The magnitude of spectrum of $I(\omega)$ part of DVTF3 is similar to that of DVTF2.

The magnitude of DVTF4 is the same as DVTF1 and its phase

is the Hilbert transform of the magnitude.

DVTF2, is comparable to the propagation model and DVTF4 to the resonance model for the vibration transfer in the engine developed in Chapter II. The performance of these four DVTF in predicting input cylinder pressure from the acceleration under different operating conditions is discussed in Chapter IV.

CHAPTER IV: ESTIMATION OF EXCITING FORCES FROM ACCELERATION

Estimating the combustion force from engine block acceleration is an inverse filtering problem, i.e., the input signal to a system with a known transfer function and known output is to be determined. In general, the basic issues involved are that of the stability and causality of the inverse filter. In engines, there are additional complications: such as defining a proper vibration transfer function, VTF; determining the time window for data records and taking into account the effect of vibration sources other than combustion.

The VTF for an engine operating under all conditions should be definable if the exact mechanism and path(s) of vibration transfer were known. The VTF models developed in Chapter II and measured or constructed in Chapter III, represent some of the possible transfer functions. The performance of a VTF in recovering the cylinder pressure from the acceleration is a criterion for accepting or rejecting the VTF as proper for diagnosis of faults. Studying the performance of different VTF in recovery of the cylinder pressure from acceleration signals also gives insight into the vibration transfer of the engine.

The estimated cylinder pressure is considered "good" when such important features as the magnitude of compression cycle, the shape and magnitude of the combustion and the onset of rapid

pressure rise is preserved.

The degree of resemblance between the estimated and measured cylinder pressures may be quantified by several performance indices. These indices are also a measure of acceptability of the VTF used in finding the cylinder pressure for fault diagnosis under different operating engine conditions.

Another criterion for testing performance of a VTF in fault detection is its ability to distinguish the firing of different cylinders; especially the alternating ones, such as cylinders #1 and #4 in the John Deere engine studied. The estimated cylinder pressure should resemble the measured pressure only when the acceleration resulting from firing of a cylinder is deconvolved from the VTF between the observation point and the same cylinder.

In this chapter the cylinder pressure is found by deconvolving the engine block acceleration and the VTFs obtained in Chapter III. The estimated cylinder pressure was compared with the measured pressure at several engine operating conditions. The estimated pressure is subjectively judged for its resemblance to the measured signal. In addition, a series of performance indices for quantitative comparison of the estimated and measured pressure signals are developed.

The acceleration was measured on the engine operating at 1500 rpm and no load, 25%, 60% and 90% of the full load. The data was taken from several engine runs on different dates including one

set of data taken prior to disassembly of the engine for vibration transfer measurements. The acceleration was measured at Point 2a. The duration of each acceleration data record for processing was one-half of a revolution or 180° crank angle. Each data record started 4 ms before TDC of the piston to include all the pressure cycle information.

The combustion force in cylinders #1 and #4 are studied in this chapter. These cylinders were fired alternately in the engine studied. Each acceleration signal record was deconvolved with the two VTF between Point 2a and cylinders #1 and #4 to test the ability of VTF in discriminating between the firing of each cylinder.

The error, $\varepsilon_{P,k}(\omega)$, introduced by estimating the pressure of a data set ℓ using the estimated DVTF from the kth set of data, is defined as:

$$\varepsilon_{P,k}(\omega) = \left| \frac{\tilde{P}_e(\omega) - P_e(\omega)}{P_e(\omega)} \right| \tag{4.1}$$

where $\tilde{P}_e(\omega)$ is the spectrum of the estimated pressure. The spectrum $\tilde{P}_e(\omega)$ is equal to $A_e(\omega)/H_R(\omega)$ where $A_e(\omega)$ is the acceleration of lth set of data. $A(\omega)$ in frequency domain is derived from Eq. 3.7

$$A_\ell(\omega) = P_\ell(\omega)\, H_p(\omega) + S_\ell(\omega)\, H_s(\omega) \quad . \tag{4.2}$$

Therefore,

$$\tilde{P}_{\ell}(\omega) = P_{\ell}(\omega) \left[\frac{1 + \alpha\beta_{\ell}}{1 + \alpha\beta_{k}}\right] \tag{4.3}$$

and the error in pressure estimation is:

$$\varepsilon_{P,k}(\omega) = \alpha \frac{(\beta_{\ell} - \beta_{k})}{1 - \alpha\beta_{k}} . \tag{4.4}$$

Eq. 4.4 shows that if the statistical variation of β is small, the error in estimating cylinder pressure is small when both sets of data k and ℓ used to estimate DVTF and cylinder pressure were taken under the same operating conditions of the engine. The experiments (see Chapter IV) support the conclusion and shows that the statistical variation of β is small compared with its variation with load.

4.1 Performance Indices

Performance indices provide a quantitative means for comparing the estimated cylinder pressure, $\tilde{p}(n)$ with the measured pressure $p(n)$. These indices should emphasize those features in the pressure signal that might be important in detection of faults in an engine. These features (parameters) are discussed in Chapter II. All of the signal characteristics cannot be represented by a single index. Therefore, several performance indices are defined,

each emphasizing particular characteristics of the cylinder pressure.

The indices defined in this section represent the general characteristics of the signal rather than any particular feature/parameter. For any specific application where detection or definition of one or more of the parameters is desired, a performance index emphasizing that particular feature should be defined.

Five different performance indices are defined in this section. These indices are concerned with the ratio of rms of the estimated and measured signals, correlation between them and the variation in the estimated signal with respect to the measured pressure signal. The five indices are labelled PI1, PI2, PI3, PI4 and PI5.

In this study the PIs were used to evaluate the performance of the VTFs, however, these are likely to be useful in on-line fault detection and in monitoring the operation of an engine. Therefore, the ease and speed of the calculation are important factors. At the present time, calculating the parameters of Eq. 2.5 for pressure signal is a very slow process. Further study in developing faster algorithms are necessary before this type of calculation can be successfully employed.

The indices defined are concerned with several features of the pressure signal: index PI1, is the ratio of the total rms

energies of the two signals. Another index, PI2 is a function of the value and the lag of the peak of the cross correlation of the two signals. The three other indices, PI3, PI4, PI5 define the variation between the estimated and measured cylinder pressure. They differ in the functions used to weight them.

PI1 is the ratio of the rms of the estimated and measured pressure signals:

$$PI1 = \underline{\tilde{p}}/\underline{p} \tag{4.5}$$

where the bar under the signal denotes its rms value:

$$\underline{p} = \left(\frac{1}{N} \sum_{n=0}^{N-1} p^2(n) \right)^{1/2} \tag{4.6}$$

where N is the total number of samples in the time window.

When the two signals resemble each other, the cross correlation of the two approaches the autocorrelation for each of them. The value and origin of the peak of the cross correlation and the lag of the peak are indications of the resemblance of the two signals and their relative time shift.

The cross correlation of $p(n)$ and $\tilde{p}(n)$, $R_{p,\tilde{p}}(k)$ is:

$$R_{p,\tilde{p}}(k) = \sum_{j=0}^{n-1} p(j)\, \tilde{p}(k-j) \tag{4.7}$$

where k is the lag.

The cross correlation can be normalized by the rms of the two signals to result in correlation coefficient, $\rho_{p,\tilde{p}}(n)$:

$$\rho_{p\cdot\tilde{p}}(k) = \frac{R_{p\cdot\tilde{p}}}{\underline{pp}} \tag{4.8}$$

Auto correlation coefficient (normalized auto correlation) of the measured cylinder pressure is shown in Figure 4.1. The correlation coefficients of this measured pressure with two pressure curves constructed from acceleration data -- one subjectively considered "good" and the other "bad" -- are also shown in the same figure. The peak value of the good estimate is .95 and that of the bad is .68. The difference between the two numbers .95 and .68 is signficantly large for categorizing the two estimates e.g., in a pattern recognition scheme.

The lag of the peak can affect its value if the correlation coefficients are weighted with a proper weighting function such as a triangular function

$$\rho_{m,p\tilde{p}}(n) = \rho_{p\tilde{p}}(n)w(n) \tag{4.9}$$

where $\rho_{m,p\tilde{p}}$ is the weighted coefficient and $w(n)$ is the weighting function. For a triangular weighting, $w(n)$ is:

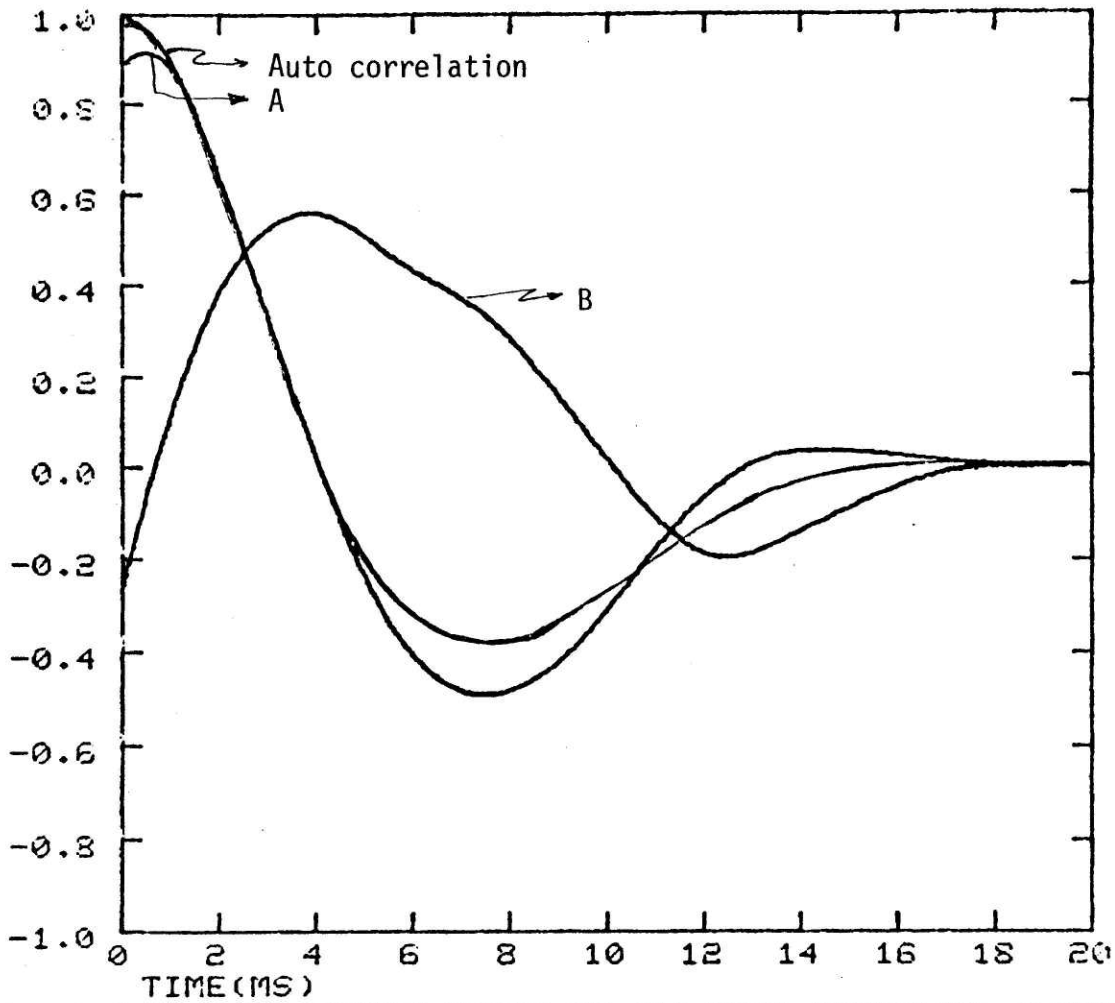

FIG. 4.1:- AUTO CORRELATION OF CYLIDER PRESSURE ALONG WITH TWO ESTIMATES OF IT -- A)USING COR.VTF , B)USING WRONG VTF

$$w(n) = \frac{N-n-1}{N-1} \qquad n = 0, \quad N - 1 \tag{4.10}$$

where N is the total number of signal samples in the time window. Triangular windowing of the cross correlation of two signals causes the value of the peak of cross correlation to be reduced if the two signals are shifted relative to each other in time. The index PI2 is defined as

$$PI2 = |Max(\rho_{m,p\tilde{p}}(n))| \tag{4.11}$$

where $\rho_{m,p\tilde{p}}$ is triangulary weighted cross correlation coefficient of p(n) and $\tilde{p}(n)$. PI2 has a value between 0 and +1. It is not sensitive to the shape of combustion cycle because of the large energy in the compression cycle compared with combustion; e.g., the presence of the sharp rise in pressure signal associated with onset of combustion is not reflected in PI2. Low pass filtering of the estimated and measured pressure signals (Figure 4.2) reduces the low frequency energy associated with compression. However, this type of filtering also distorts the shape of the pressure rise in the signal at the onset of the combustion.

Another approach for quantitative measurement of the details of the combustion is to find the variance of the estimated pressure relative to the measured pressure signal. The variance, of the two signals v(n) is defined as:

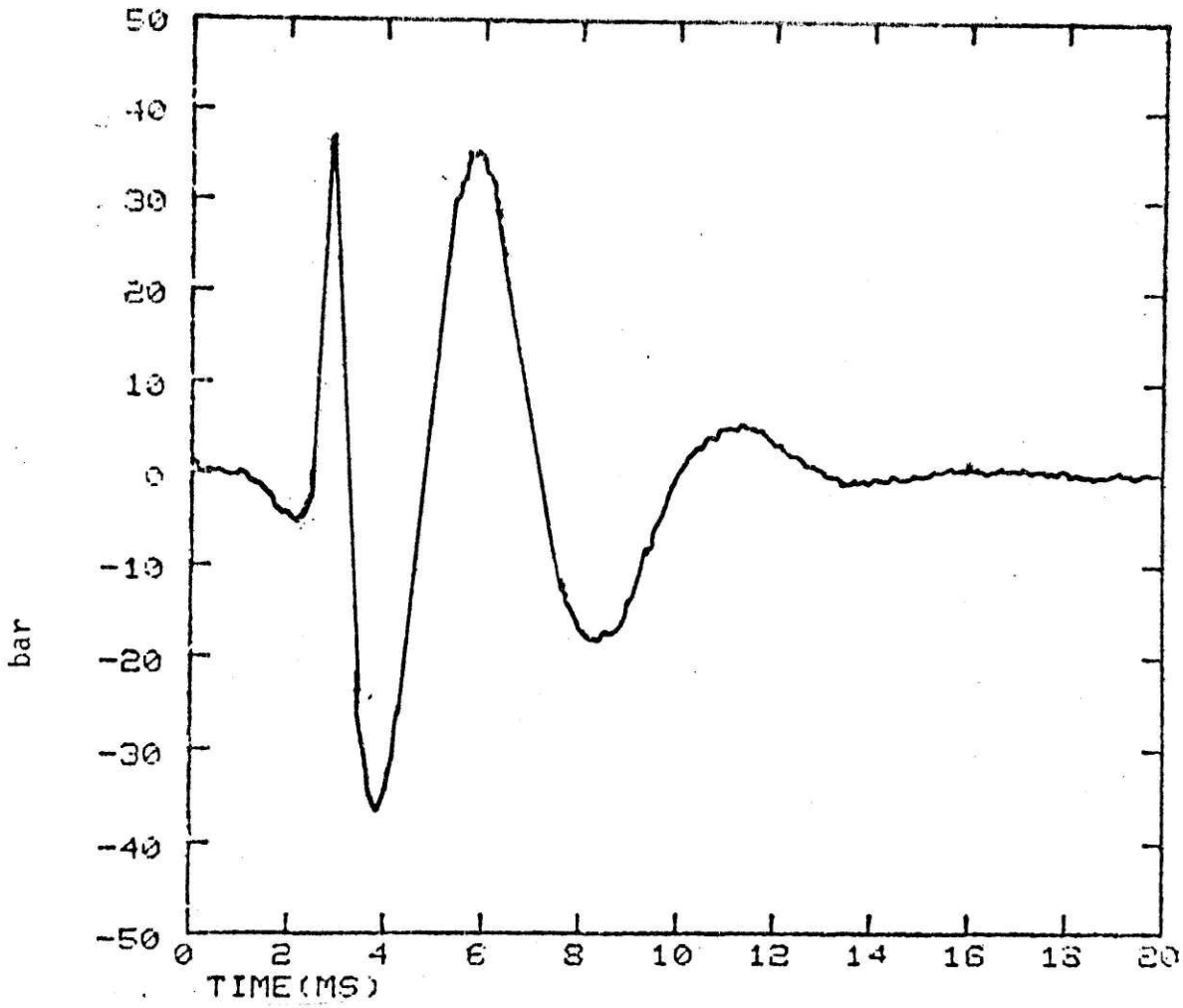

FIG. 4.2:- CYLINDER PRESSURE HIGH PASS FILTERED AT 200 HZ

$$v(n) = [\tilde{p}(n) - p(n)]^2 \qquad n = 0, N-1 \quad . \qquad (4.12)$$

To eliminate the effect of gain factors and time lags, both signals are normalized with respect to their rms values and the time shift of the two is eliminated so that the peak of the two signals occur at the same time.

$$v(n) = \left[\frac{\tilde{p}(n)}{\tilde{p}} - \frac{p(n)}{p} \right]^2 \qquad n=0, N-1 \qquad (4.13)$$

Most of the information in pressure signal is in the first half of the cycle. In fact, if the effect of low pass filtering of measuring and processing equipments are eliminated, the second half of the signal should have negligible energy. The variance in Eq. 4.13, therefore, can be weighted to emphasize the effect of the first half of the signal:

$$v\ (n) = v(n)w(n) \qquad n=0, N-1 \qquad (4.14)$$

where w(n) is the weighting function. Two appropriate weighting functions are: $w_1(n)$ and $w_2(n)$: where

$$\begin{aligned} w_1(n) &= 2 \quad 0 \leq n \leq N/2 - 1 \\ &= 1 \quad N/2 \leq n \leq N - 1 \end{aligned} \qquad (4.15)$$

TABLE IV-1

PERFORMANCE INDICES

P_I	description
PI1	$\tilde{\underline{p}}(n)/\underline{p}(n)$
PI2	$\lvert \mathrm{Max} \lvert \rho_{m,\underline{p}\tilde{\underline{p}}}(n) \rvert \rvert$
PI3	$\frac{1}{N} \sum_{n=0}^{N-1} v(n)$
PI4	$\frac{1}{N} \sum_{n=0}^{N-1} v(n)\, w_1(n)$
PI5	$\frac{1}{N} \sum_{n=0}^{N-1} v(n)\, w_2(n)$

$p(n)$ -- measured pressure, $\underline{p}(n)$ -- rms of measured pressure

$\tilde{p}(n)$ -- estimated pressure, $\tilde{\underline{p}}(n)$ -- rms of estimated pressure

$\rho_{m,p,\tilde{p}}(n)$ -- Triangularlyweighted correlation coefficient of p and $\tilde{p}$

$v(n)$ -- variance of normalized and aligned $p(n)$ and $\tilde{p}(n)$

$$v(n) = \left[\frac{p(n)}{\underline{p}} - \frac{\tilde{p}(n)}{\tilde{\underline{p}}}\right]^2$$

$w_1(n)$ -- weighting function $w_1(n) = \begin{cases} 1, & 0 \le n < N/2, \\ 2, & N/2 \le n \le N-1 \end{cases}$

$w_2(n)$ -- weighting function, $w_2(n) = \begin{cases} 1 & 0 \le n \le N/2 \\ 0 & \text{otherwise} \end{cases}$

and

$$w_2(n) = 1 \quad 0 \leq n \leq N/2 - 1$$
$$0 \quad \text{otherwise} \tag{4.16}$$

Three performance indices: PI3, PI4 and PI5 are defined as follows:

$$PI3 = \frac{1}{N} \sum_{n=0}^{N-1} v(n) \tag{4.17}$$

$$PI4 = \frac{1}{N} \sum_{n=0}^{N-1} v(n)w_1(n) \tag{4.18}$$

$$PI5 = \frac{1}{N} \sum_{n=0}^{N-1} v(n)w_2(n) \tag{4.19}$$

Prior to calculating PIs, the dC components of both measured and calculated pressure signals were eliminated and the two signals were tapered with a cosine window. The definitions for PIs are summarized in IV.1.

4.2 Inverse Filtering -- Processing Technique, Stability and Causality

Convolving the acceleration signal and the inverse of the engine impulse response results in an estimate of the cylinder pressure:

plex s plane. A minimum phase signal is stable because all of the poles of its z transform are inside the unit circle. Physically, if the signal is the impulse response of a system, the minimum phase requirement is equivalent to requiring the damping of the system to be real and positive for resonances and anti-resonances of the system. Therefore, the impulse response of a stable, passive system such as resonance response of the engine is minimum phase. A system with a minimum phase impulse response is a minimum phase system.

The above definition is useful in categorizing a signal as minimum phase when the z or Fourier transform of the system is a finite rational function of z or ω and the zeroes of the transform are distinguishable. The z and Fourier transform of the propagation impulse response of the engine, as defined by Eq. 2.15 are not rational functions. However, various studies on the transfer function of dispersive media have shown that when the medium is loss less, it is equivalent to a minimum phase system [26]. Practically when the losses in the medium is small, the medium is treated as lossless and the effect of attenuation is taken into account as a correction gain factor.

Although both propagation and resonance responses of the engine are minimum phase, the sum of the two is not necessarily minimum phase. In addition, VTFs estimated on the operating engine may not be minimum phase because of the contaminating effect of piston slap and other sources of noise.

$$\tilde{p}(n) = a(n) * h_1(n) \tag{4.20}$$

where $h_1(n)$ is the inverse of impulse response of the engine to combustion, $h_c(n)$:

$$h_1(n) * h_c(n) = \delta(n) \tag{4.21}$$

or in frequency domain

$$H_1(\omega)\, H_c(\omega) = 1 \tag{4.22}$$

In practice, the acceleration was convolved with the inverse of the VTFs developed in Chapter III. The method used was short time fast convolution technique discussed previously.

Stability and causality of $H_1(\omega)$ or IVTs are important issues in realization of $h_1(n)$ and, therefore, in convolution of $h_1(n)$ and $a(n)$. Although processing the signals by a digital computer often makes it possible to avoid or solve stability and causality problems, it is worthwhile to study the stability of IVTs.

The inverse of a stable and causal signal is stable if the signal is also minimum phase [18]. A minimum phase signal is defined as a signal in which all of the poles and zeroes of its z transform are inside the unit circle, or equivalently, all of the poles and zeroes of its Laplace transform lay in the left half of the com-

One way to solve the stability problems is by exponential weighting. A non-minimum phase signal can be converted to a minimum phase signal by exponentially weighting it:

$$h_{min}(n) = h(n) \quad e^{-\alpha n} \tag{4.23}$$

where $h_{min}(n)$ is minimum phase and α is constant. The value of α depends on the region of convergence of $h(n)$ [29]. When convolution with the inverse of a non minimum phase signal is desired, the signal should be weighted exponentially to make it minimum phase, then the inverse of this minimum phase signal can be convolved with another signal. The effect of the exponential window is then taken out of the result of convolution. This process is possible if the signal duration is finite. The method is easy to implement on a computer.

All of the VTFs used are stable in the time window considered except SVTF. Their stability is determined by forming their impulse response or taking the short time inverse Fourier transform of the inverse of the VTFs discussed previously.

The computer programs used for processing are discussed in Chapter III. To minimize the effect of windowing on the sharp pressure rise at the onset of combustion in estimated pressure, a cosine window was used to taper the acceleration signal.

4.3 Deconvolution of SVTF from the Engine Block Acceleration

The VTFs measured on non-running engine, SVTFs were the first TFs used to find the cylinder pressure from the measured acceleration signal on the engine block. The estimated pressure in cylinders #1 and #4 are discussed in this section. The pressure inside the two cylinders during combustion was estimated from the acceleration at Point 2A caused by the firing of each of the cylinders. Each acceleration record was deconvolved with both SVTF's. The resultant cylinder pressures are shown inFigures 4.3 and 4.4.

The pressure in cylinder #4 at 60% load is recovered with reasonable accuracy using SVTF between Point 2A and cylinder #4. This subjective evaluation of the comparison of the general shape of the measured and estimated pressures is enforced by the performance indices (Tables IV-2, IV-3).

The magnitude of spectrum of the pressures found for cylinder #1 at 60% of full load or higher is comparable to that of the measured cylinder pressure. However, the time trace of measured and estimated pressures are different. This observation emphasizes the importance of the phase characteristics of the transfer function.

The pressure traces estimated with the "wrong" SVTF at high loads (60% of full load and higher) is substantially worse

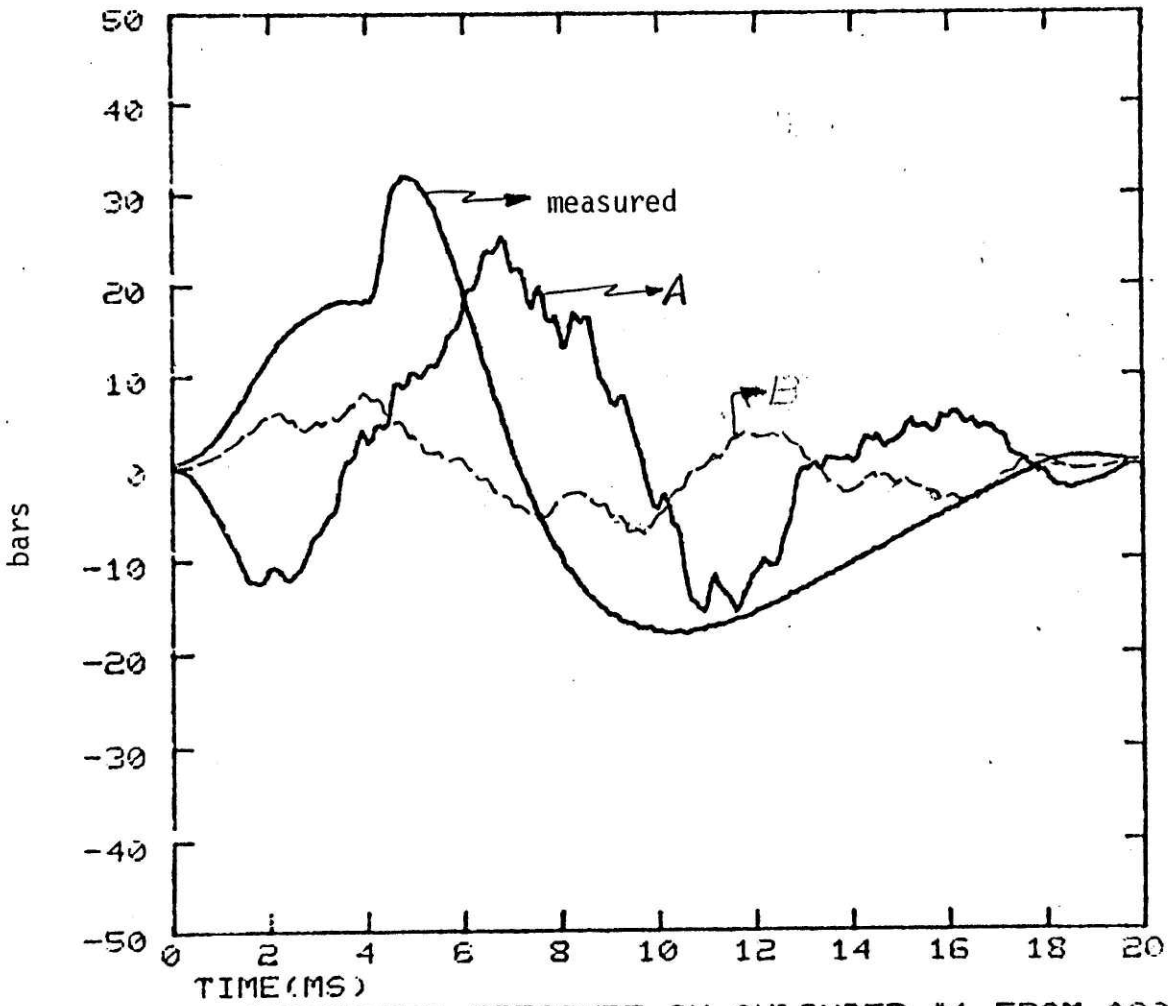

FIG. 4.3:- ESTIMATED PRESSURE IN CYLINDER #1 FROM ACCEL AT POINT 2A, USING SUTF TO A) CYL.#1, B) CYL.#4 -- 60% LOAD

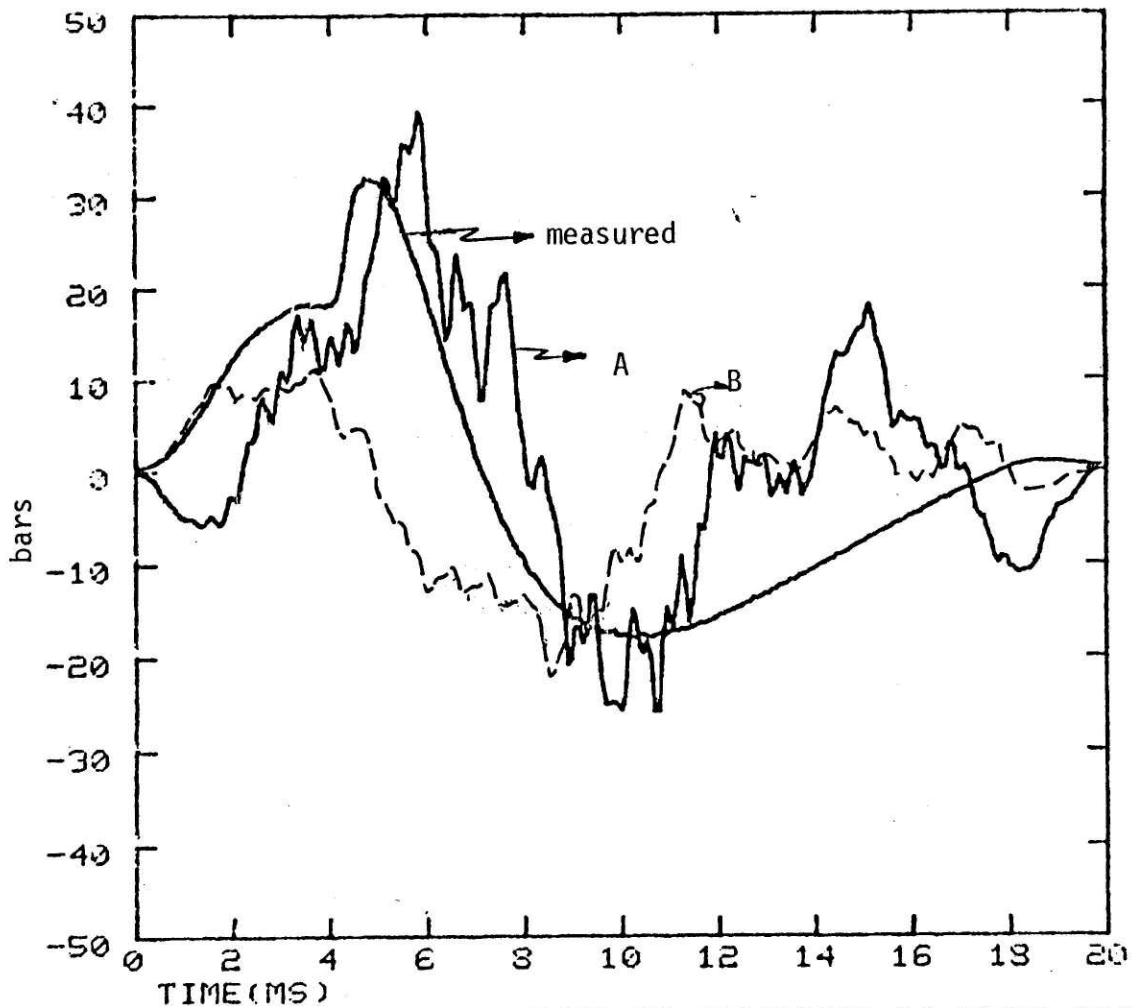

FIG. 4.4:- ESTIMATED PRESSURE IN CYLINDER #4 FROM ACCEL. AT POINT 2A, USING SUTF TO A) CYL.#4, B) CYL.#1 -- 60% LOAD

TABLE IV-2 †PERFORMANCE INDICES CALCULATED FOR CYLINDER PRESSURE ESTIMATED FOR ENGINE RUNNING AT 60% LOAD, 1500 RPM

VTF*	Cylinder#	PI1	PI2	PI3	PI4	PI5
SVTF	4	1.2	.8	.69	.94	.39
	1	1.06	.8	1.8	1.9	.95
DVTF1	4	0.843	.92	.105	.186	.12
	1	1.03	.93	.097	.156	.06
DVTF2	4	1.03	.92	.064	.098	.04
	1	1.05	.95	.056	.094	.038
	1**	1.06	.91	.08	.12	.036
DVTF3	1	1.03	.69	.63	1.08	.899
DVTF4	1	.87	0.09	1.98	3.48	1.6

†See Table IV-1

*See Table III-1

**Pressures estimated from acceleration data taken prior to re-assembly of the engine.

TABLE IV-3 †PEFORMANCE INDICES CALCULATED FOR CYLINDER PRESSURE ESTIMATED FOR ENGINE RUNNING AT FULL LOAD

VTF*	Cylinder #	PI1	PI2	PI3	PI4	PI5
SVTF	4	1.23	.85	.19	.42	.139
DVTF1	1	1.05	.95	.09	.168	.12
DVTF2	1	1.03	.98	.04	.088	.039
DVTF3	1	.93	.65	.64	.98	.57
DVTF4	1	.81	.05	1.99	3.3	1.8

†See Table IV-1

*See Table III-1

TABLE IV-4 IDENTIFICATION OF FIRING CYLINDER USING †PERFORMANCE INDICES, OF ESTIMATED PRESSURE IN CYLINDER 1, ENGINE OPERATING AT 1500 RPM, 60% LOAD

VTF	PI1	PI2	PI5
	*PIC-**PIW	PIC-PIW	PIW-PIC
SVTF	.2	.18	.23
DVTF1	.4	.25	1.7
DVTF2	.03	.4	1.85

†See Table IV-1

*PIC: PI calculated for pressure estimated using VTF measured between observation point and cylinder 1

**PIW: PI calculated for pressure estimated using VTF measured between observation point and cylinder 4

than the cylinder pressures recorded using the correct SVTF. The calculated PIs for the two traces reflects that SVTF is capable of identifying the firing cylinder (Table IV-4).

The accuracy of estimated cylinder pressures deterioriates rapidly as the load decreases. The pressure estimated at no load (Fig. 4.5) has no resemblance to a pressure trace. The PI1 for this pressure trace is comparable with PI1 obtained for band limited random noise (Table IV.4). This behavior is expected when the engine is operating under no load, since combustion is no longer the dominant force. Therefore, Eq. 2.6 does not hold and cylinder pressure cannot be obtained by simply deconvolving acceleration and SVTF.

The performance of SVTF in estimating pressure in cylinder #4 is by far better than its performance in estimating pressure in cylinder #1. One reason for this superiority is that response of the engine at Point 2a to the excitation at cylinder #4 is dominantly resonant as a result of the geometry of the engine.

4.4 Deconvoltuion of DVTF1 from Engine Block Acceleration

DVTF1 is the result of direct deconvolution of acceleration and cylinder pressure signals. The characteristics of DVTF1 and its performance in cylinder pressure estimation depends on the

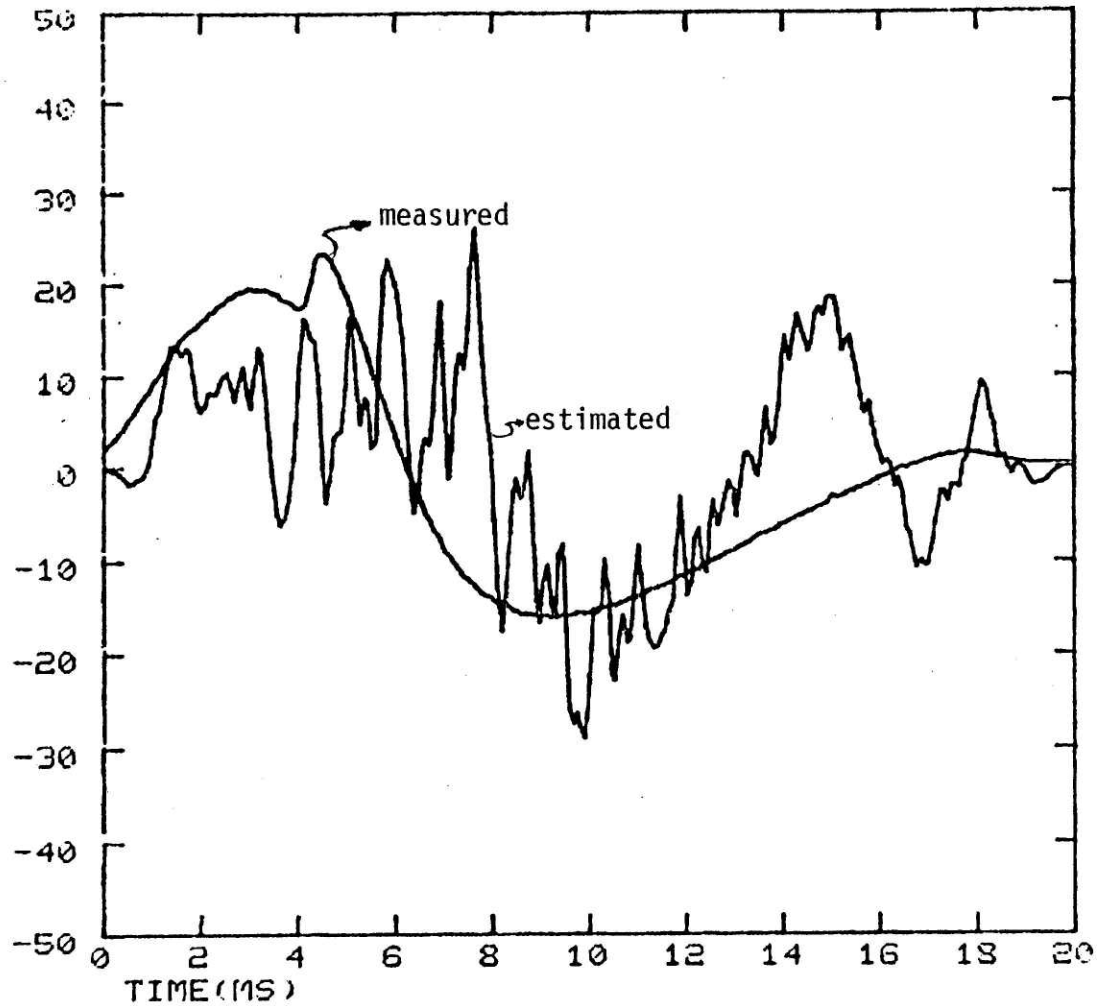

FIG. 4.5:- ESTIMATED PRESSURE IN CYLINDER #4 USING SVTF -- 1500 RPM, NO LOAD

TABLE IV-5 †PERFORMANCE INDICES CALCULATED FOR CYLINDER PRESSURE ESTIMATED FOR ENGINE RUNNING AT NO LOAD, 1500 RPM

*VTF	Cylinder #	PI1	PI2	PI3	PI4	PI5
SVTF	4	1.3	.48	1.8	2.1	.9
DVTF1	1	1.032	.86	.26	.44	.178
DVTF2	1	1.07	.9	.23	.39	.11
DVTF3	1	.7	.65	.96	1.2	.832
DVTF4	1	.18	.1	2.6	2.7	1.4

†See Table IV-1

*See Table III-1

operating condition of the engine at which DVTF1 was determined. The DVTF1 used was obtained for the engine operating under 60% load. The experiments have shown that cylinder pressure estimation is more accurate when a DVTF1 is measured at high load. The cylinder pressures was estimated from the block acceleration at engine operating at 0, 60% and full loads.

The results show a considerable improvement over the results obtained from deconvolving acceleration with SVTF. The DVTF1 recovers the pressures in cylinders #1 and #4 equally well (Fig. 4.6).

The accuracy of estimated pressures by DVTF1 also declines sharply with load; the pressure signal found at no load does not contain any of the features of a cylinder pressure (Fig. 4.7).

Comparing the cylinder pressures obtained with right and wrong DVTFs for each acceleration record, shows that distinguishing between firing of the two cylinders on the basis of the PIs as well as subjective judgement is possible. (Table IV-5, Fig. 4.8).

To study the effect of variation of DVTF1 from one engine run to another on accuracy of the estimated signal, the pressure in cylinder #1 at 60% load was found from several sets of acceleration data taken a few days apart. Each set of data was taken from the engine operating at nominally similar conditions. The results

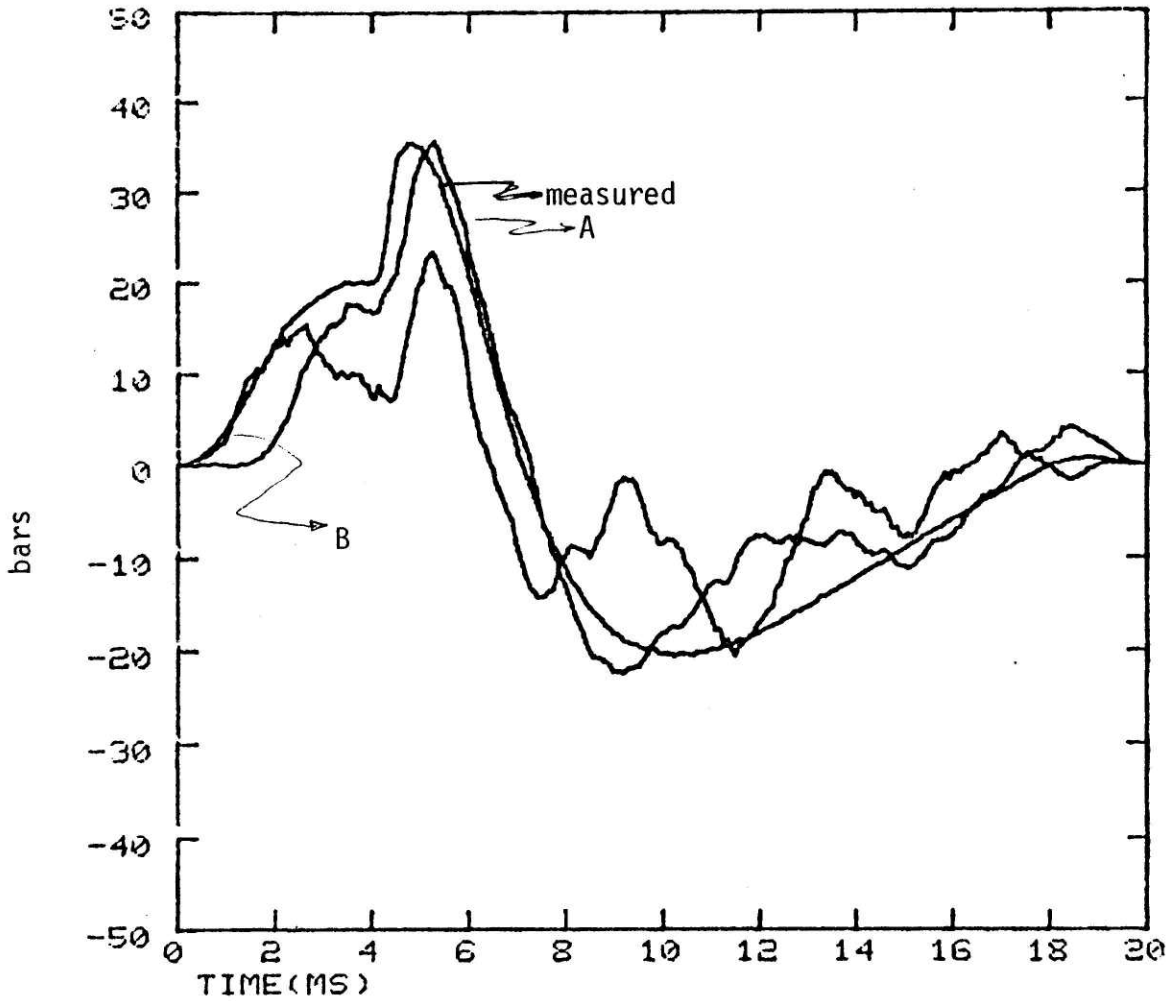

FIG. 4.6:- ESTIMATED PRESSURE USING DVTF1 AT 1500 RPM AND 60% LOAD IN -- A)CYLINDER # 1 , B)CYLINDER # 4

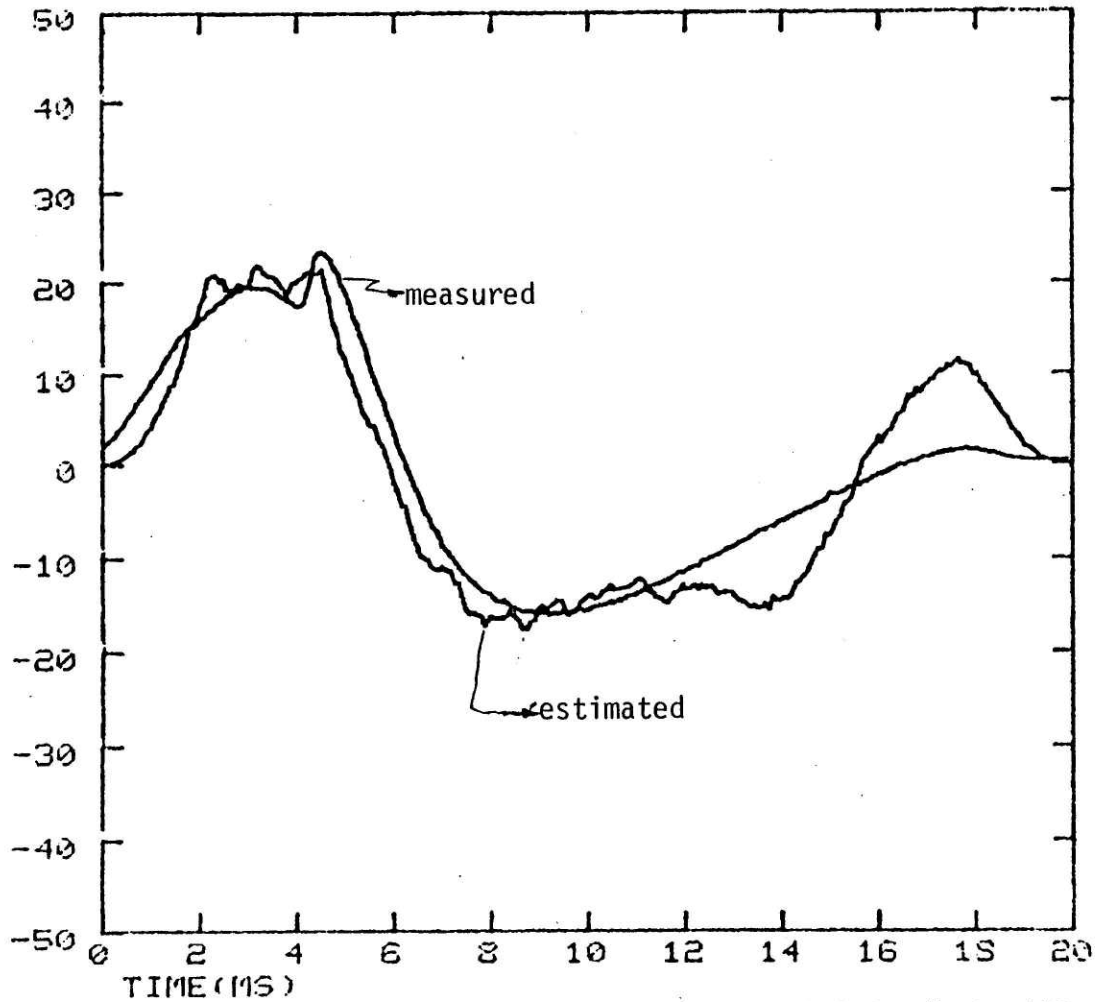

FIG. 4.7:-ESTIMATED PRESSURE IN CYLINDER # 1 USING DVTF1 -- 1500 RPM ,NO LOAD

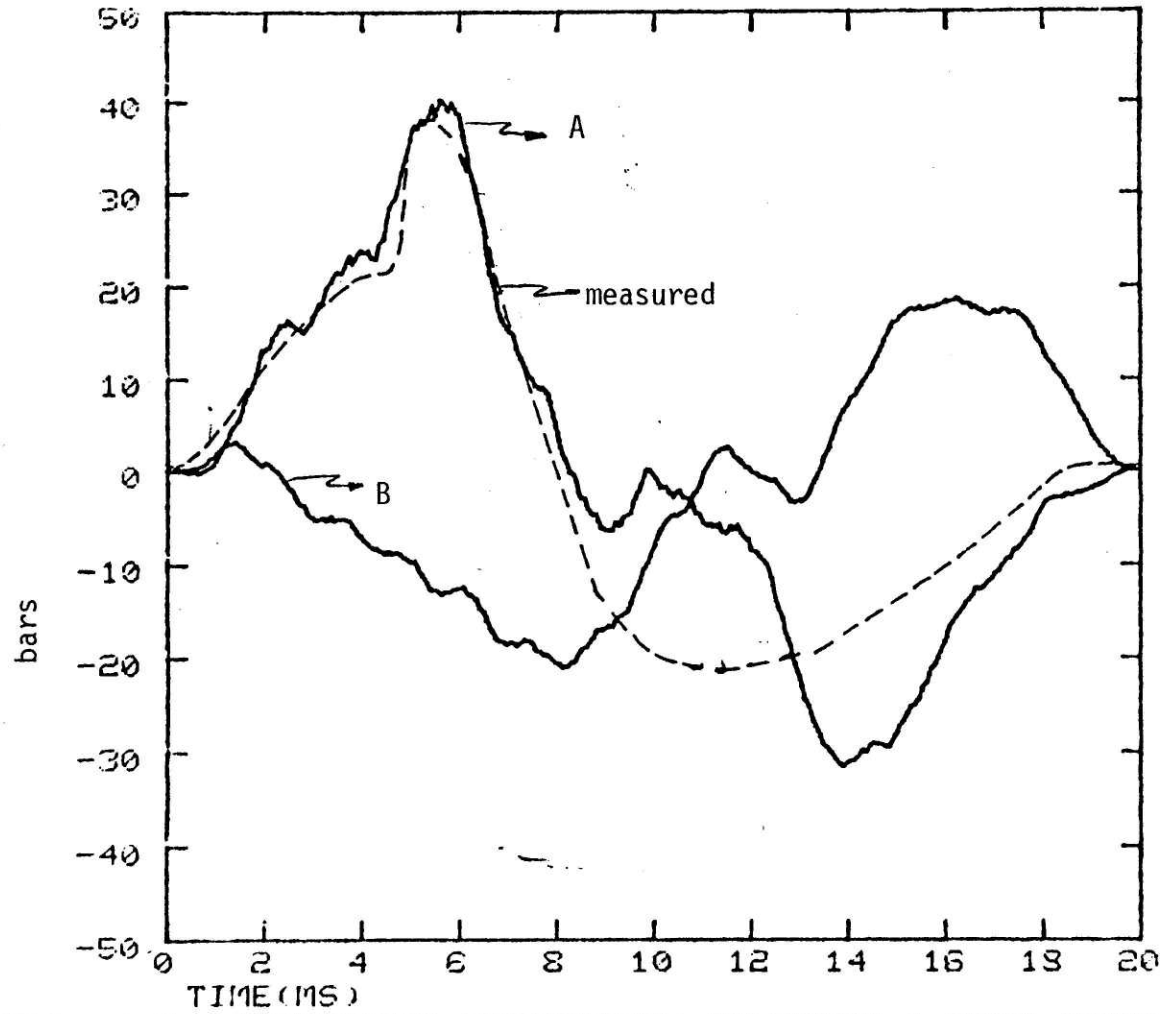

FIG. 4.8:- ESTIMATED PRESSURE IN CYLINDER 1 FROM ACCEL. AT POINT 2A, USING DVTF1 TO A) CYL.#1, B) CYL.#4 -- FULL LO

(Figure 4.9) show that DVTF1 varies slightly from one engine run to another. However, as long as operations condition of the engine remains the same, the estimated pressure is acceptable.

4.5 Deconvolution of DVTF2 from the Engine Block Acceleration

DVTF2 is found from the measured propagation VTF of the engine. The phase of DVTF2 is the same as the phase of DVTF1. The magnitude of DVTF2 is similar to the model developed for the input inertance to the engine, i.e., stiffness at low frequency and two highly damped resonances at 1500 and 2500 Hz. The observation point was Point 2A. The two DVTF2s used were constructed from the two DVTF1s discussed in Section 4.4. The cylinder pressure was estimated from the same acceleration data used in deconvolution with DVTF1 and SVTF (Section 4.4).

The measured and estimated pressures in cylinder #1 are remarkably similar for an engine operating under 60% and higher loads (Fig 4.10). Even the cylinder pressure estimated for the engine operating at no load, resembles the measured one (Figure 4.11). All important features of cylinder pressure are apparent in the estimated pressure.

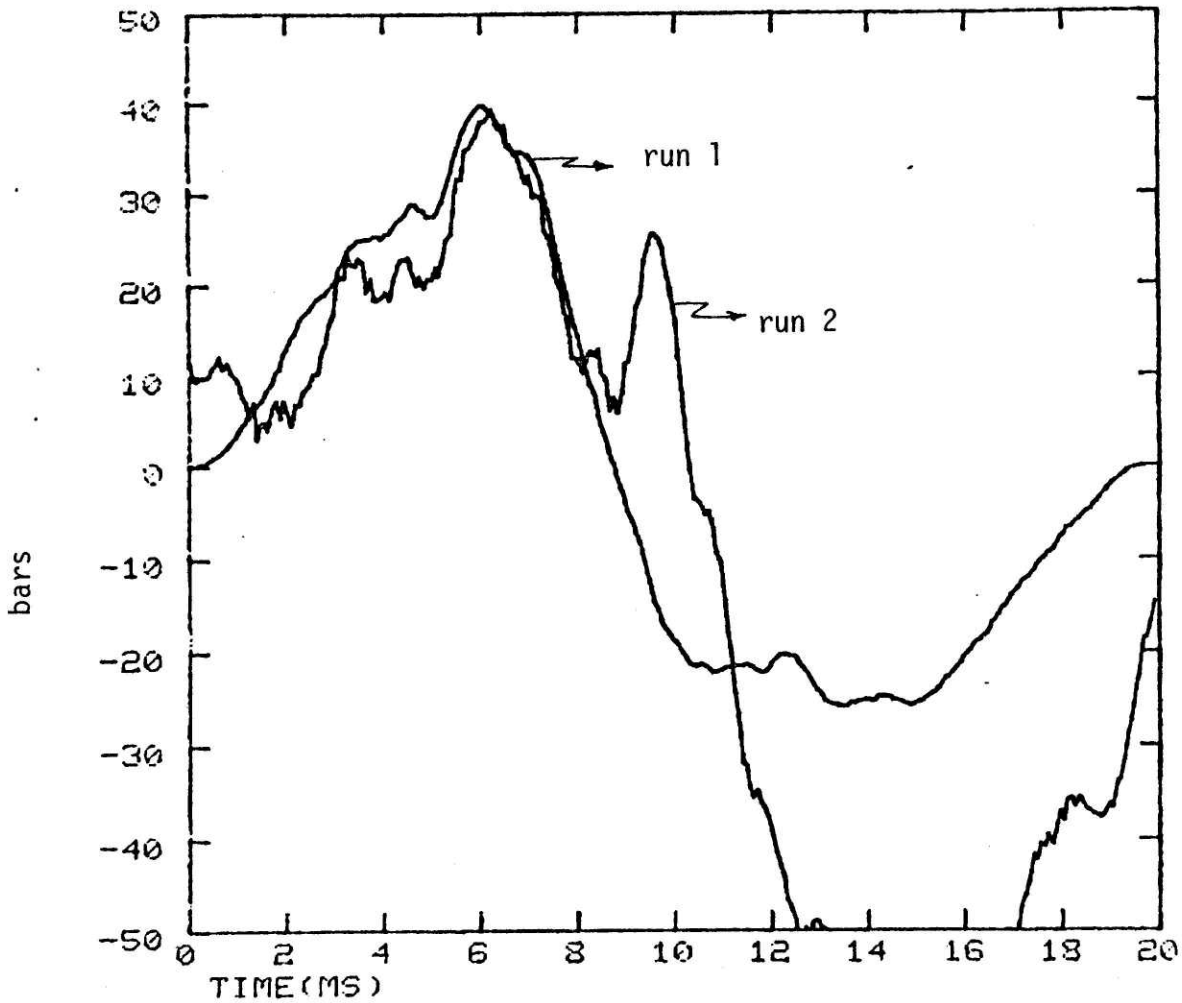

FIG. 4.9:- ESTIMATED PRESSURE IN CYLINDER 4 USING DVTF1 FOR TWO ENGINE RUNS -- 1500 RPM, 60% LOAD

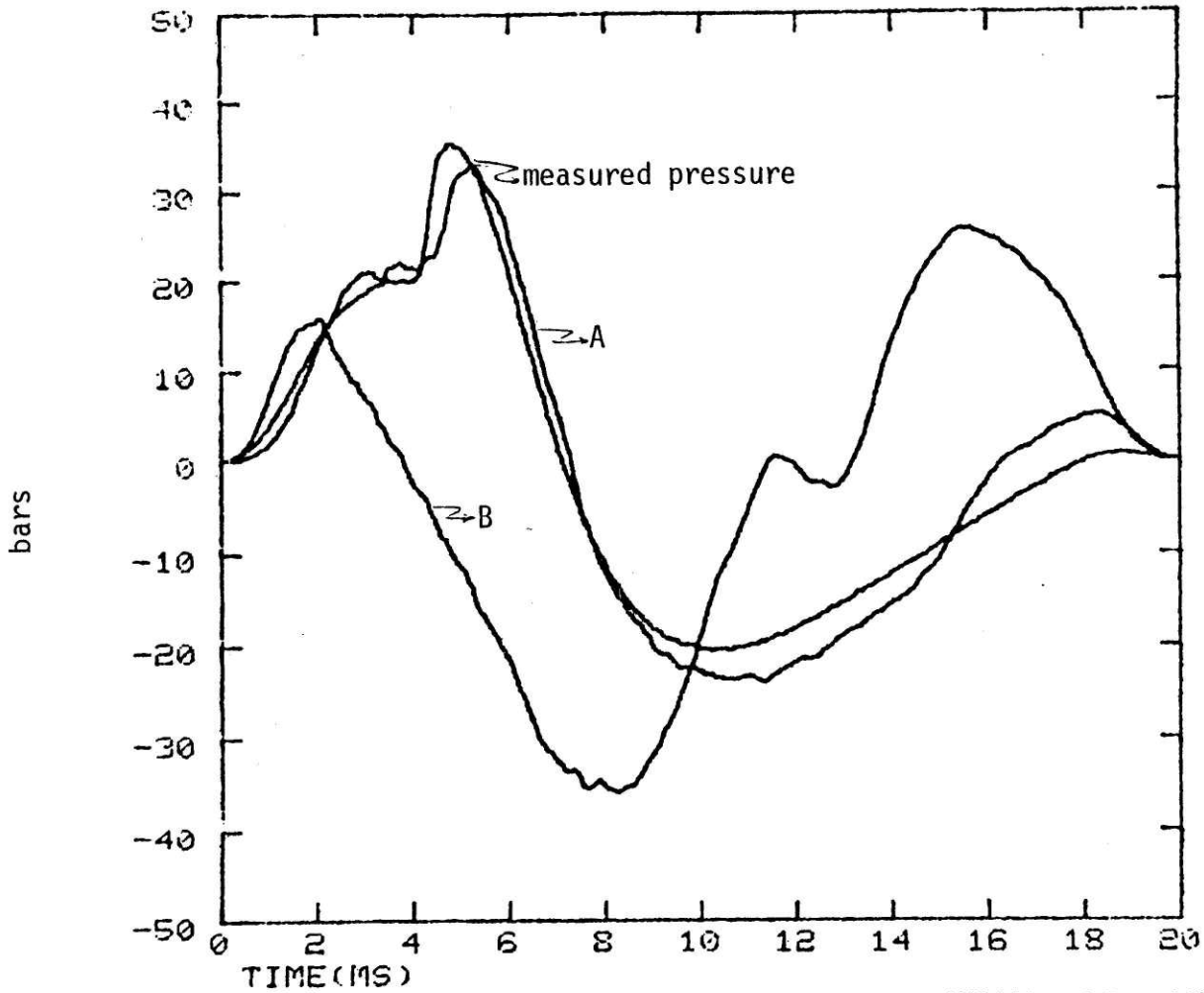

FIG. 4.10:- ESTIMATED PRESS. IN CYL. #1 ,FROM ACC. AT POINT 2A AT 60% LOAD -- A) USING CORR. VTF , B)USING WRONG VTF

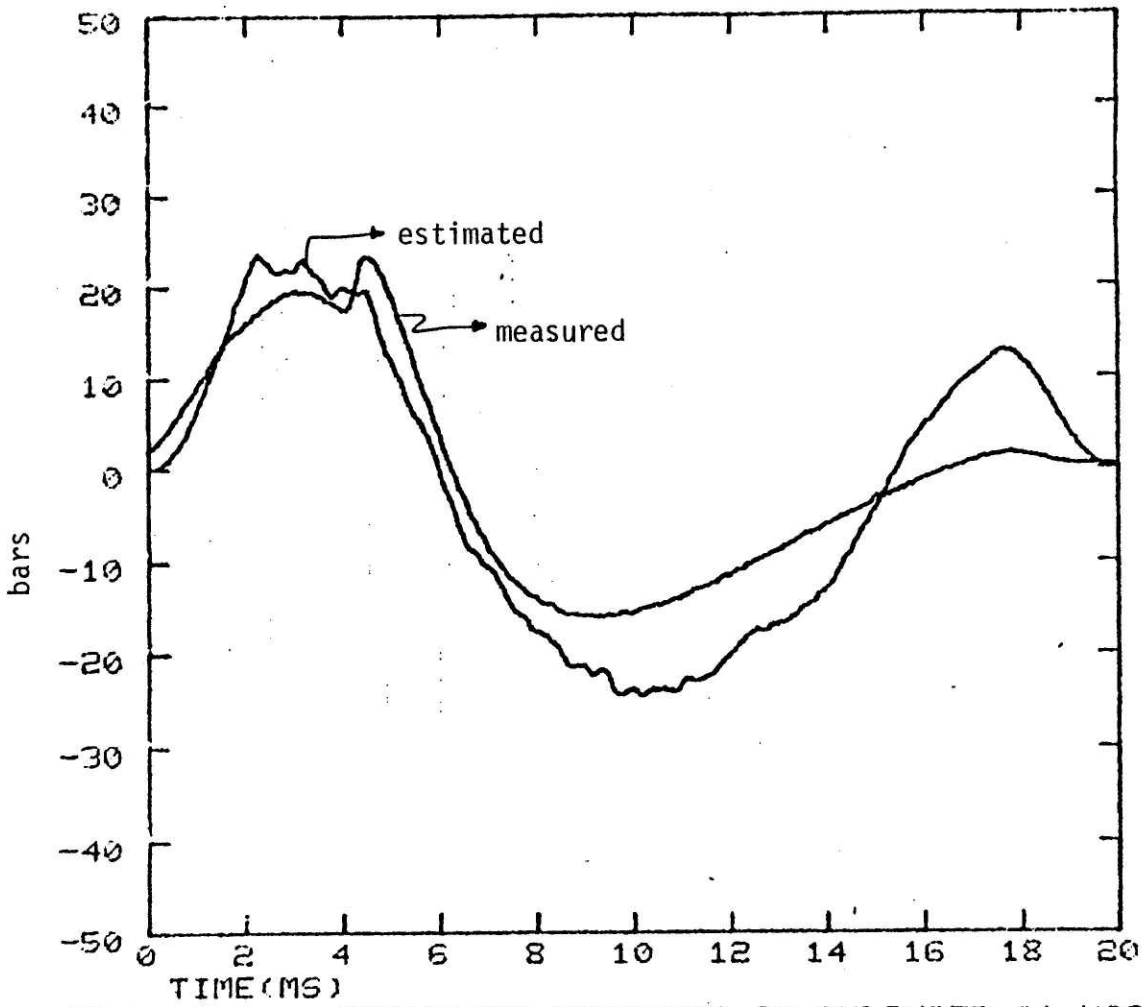

FIG. 4.11:- ESTIMATED PRESSURE IN CYLINDER #1 USING DVTF2 -- 1500 RPM, NO LOAD

The resemblance of estimated and measured pressure signals is relfected in PIs (Tables IV-2 to IV-5). All PI values are significantly better than the PI values obtained for estimated pressure using either DVTF1 or SVTF. The performance of DVTFV2 in identifying the source of the excitation is also good (Table IV-4 , Fig. 4.10).

Variation of the DVTF during the expected life of the engine as a result of nomral wear may effect the accuracy of the estimated pressure with the DVTF. To study the variation in DVTF2, acceleration data taken a year ago was deconvolved with a recently obtained DVTF2. The acceleration was measured *prior* to the disassembly of the engine, while the DVTF2 was determined *after* the engine was assembled again The pressure found for cylinder #1 (Figure 4.12) is comparable to the measured pressure signal and preserves all features of the pressure trace. This experiment shows that DVTF2 does not vary significantly from one engine run to another, and stays unchanged over a reasonable period of engine life. DVTF2 is not sensitive to practical variations of engine properties in assembly. The characteristics of DVTF2 makes it appropriate for use in fault diagnosis.

4.6 Deconvolution Using DVTF3 and DVTF4

DVTF3 has a cepstrally smoothed phase and magnitude that reflects a single path propagation. These details are

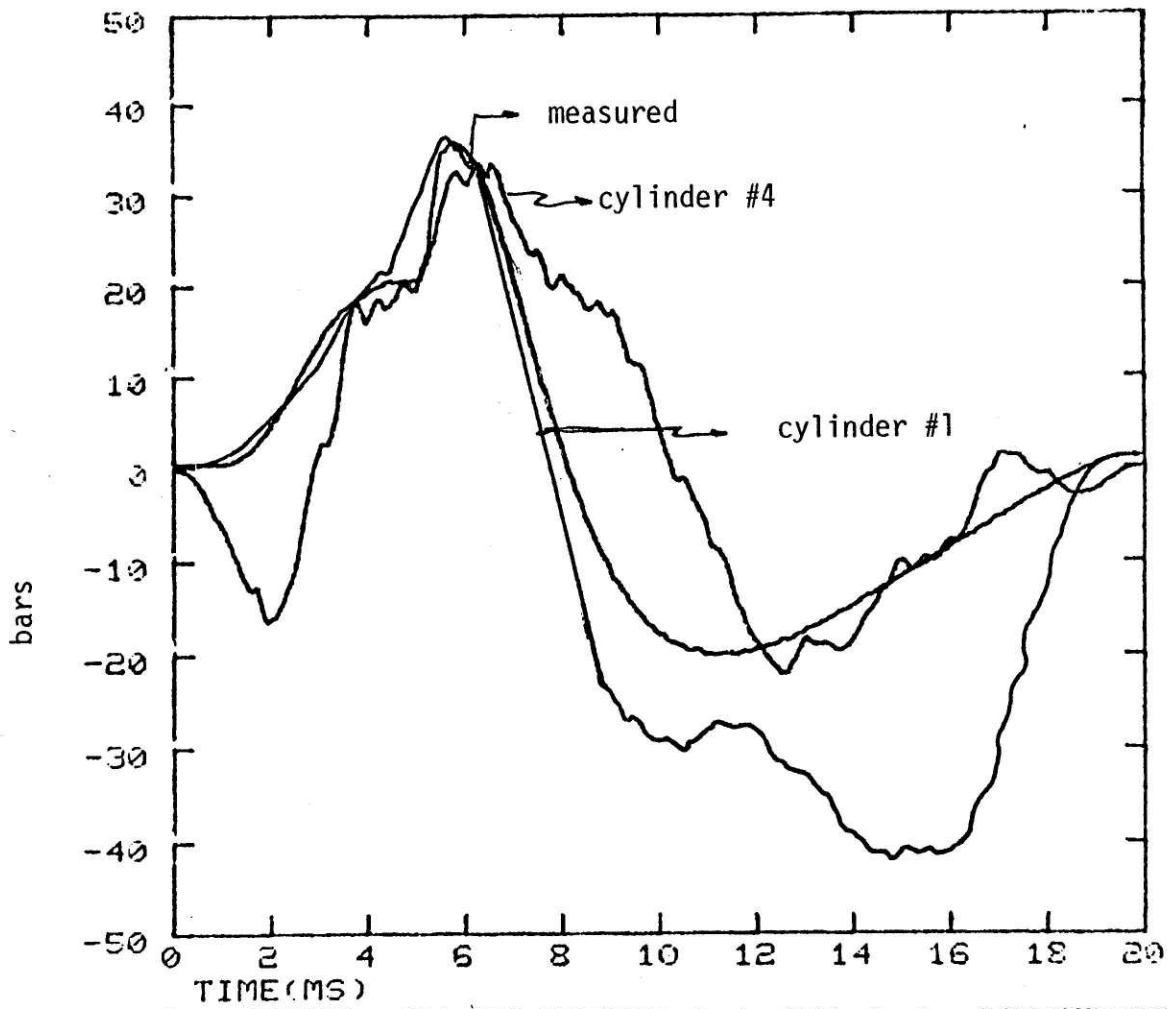

FIG 4.12:- PRESS. IN CYLINDERS # 1 AND # 4, CONSTRUCTED FROM ACCEL. MEASURED PRIOR TO REASSEMBLY OF ENGINE -- 60% LOAD

USING DVTF2

associated with complicated vibration transfer paths in the engine. The performance of DVTF3 is poor under all operating conditions (Figure 4.13, Tables IV-2, IV-3). Therefore, the details of the phase characteristic of the VTF are extremely important in recovery of cylinder pressure.

DVTF4 represents pure resonance reponse of the engine. Its magnitude is the same as DVTF1 and its phase is the Hilbert transform of the magnitude. The performance of DVTF4 constructed from DVTF1 is very poor in estimation of cylinder pressure even at high loads (Figure 4.14). This observation suggests that magnitude information alone cannot represent the characteristics of VTF on an engine.

4.7 Cepstral Analysis in Estimating Cylinder Pressure

A combination of cepstrum smoothing and deconvolution was used to find cylinder pressure from the acceleration signal; the ceptrally smoothed acceleration signal was deconvolved with the cepstrally smoothed DVTF. The cepstrum window used for both acceleration and DVTF was 4 ms long. The window was symmetric with respect to the time origin. The method is equivalent to cepstrally smoothing the estimated pressure. However, in fault diagnosis application, defining a VTF and preprocessing the acceleration signal may be preferable to processing the estimated

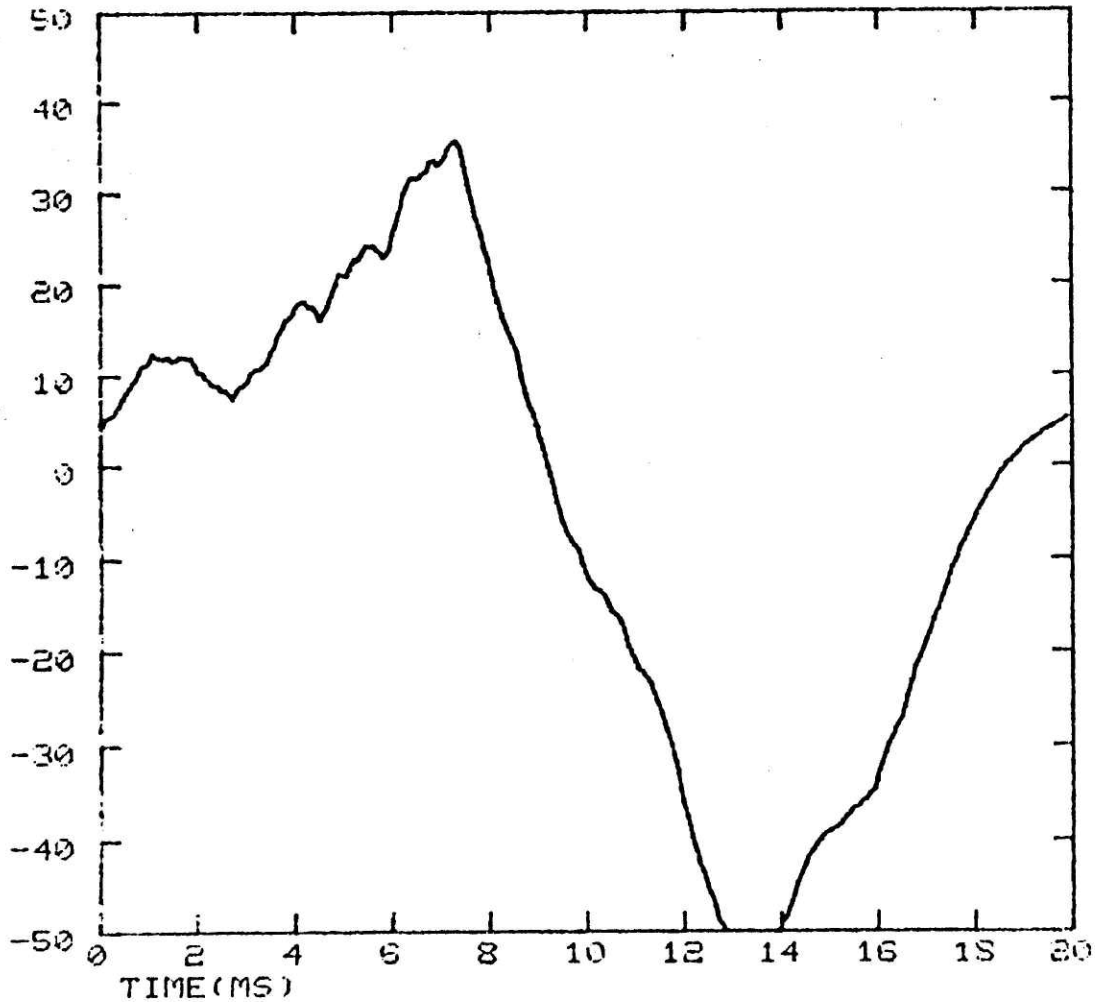

FIG. 4.13:- ESTIMATED PRESSURE IN CYLINDER 1
USING DVTF3 -- 1500 RPM, 60% LOAD

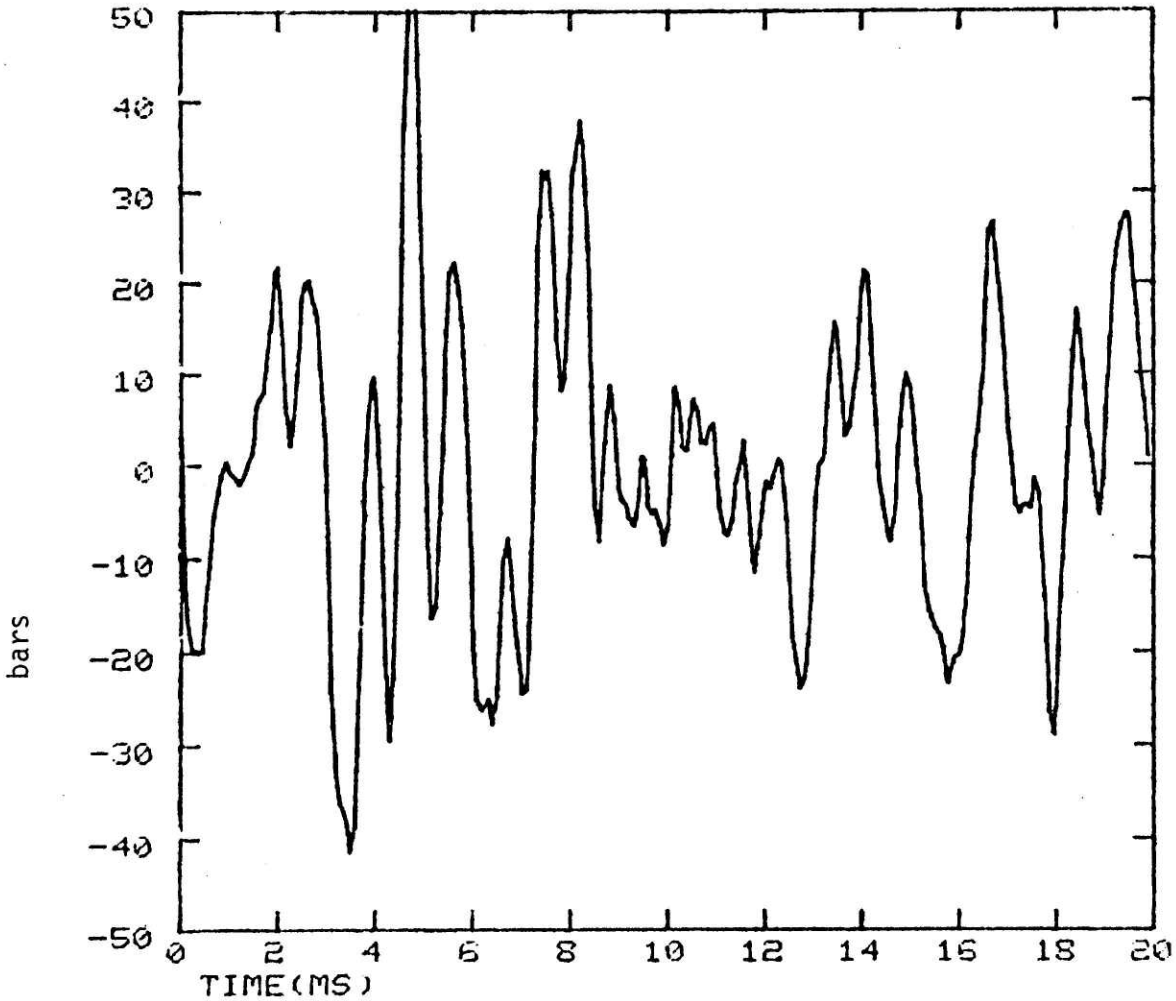

FIG. 4.14:- ESTIMATED PRESSURE IN CYLINDER 4
USING DVTF4 -- 1500 RPM, 60% LOAD

pressure. The pressure estimated with this method would then be compared with cepstrally smoothed measured in pressure signal using performance indices like those drawn in Table IV-1.

The characteristics of the pressure estimated by the combination method (Figure 4.15) are summarized as follows:

(a) The compression cycle is missing.

(b) The load on the engine is reflected on peak value of the estimated pressure.

(c) The firing of the two cylinders are not distinguishable by the shape of the estimated pressure.

However, if the same DVTF were used to process acceleration caused by combustion in cylinders #1 and #4, the estimated pressure in cylinder #1 is 3-4 dB less than that of the cylinder #4. Therefore, the firing of the two cylinders are distinguishable on the basis of the energies of the signals. The combination of cepstral analysis and deconvolution is a promising method in fault diagnosis.

At the present time, the knowledge about cylinder pressure signal and the transfer paths is not sufficient to interpret the results obtained by this method and/or to design a better cepstral domain filter for processing. In addition the processing is slow. However, the method offers many advantages over conventional deconvolution which makes further studies rewarding. Some of these ad-

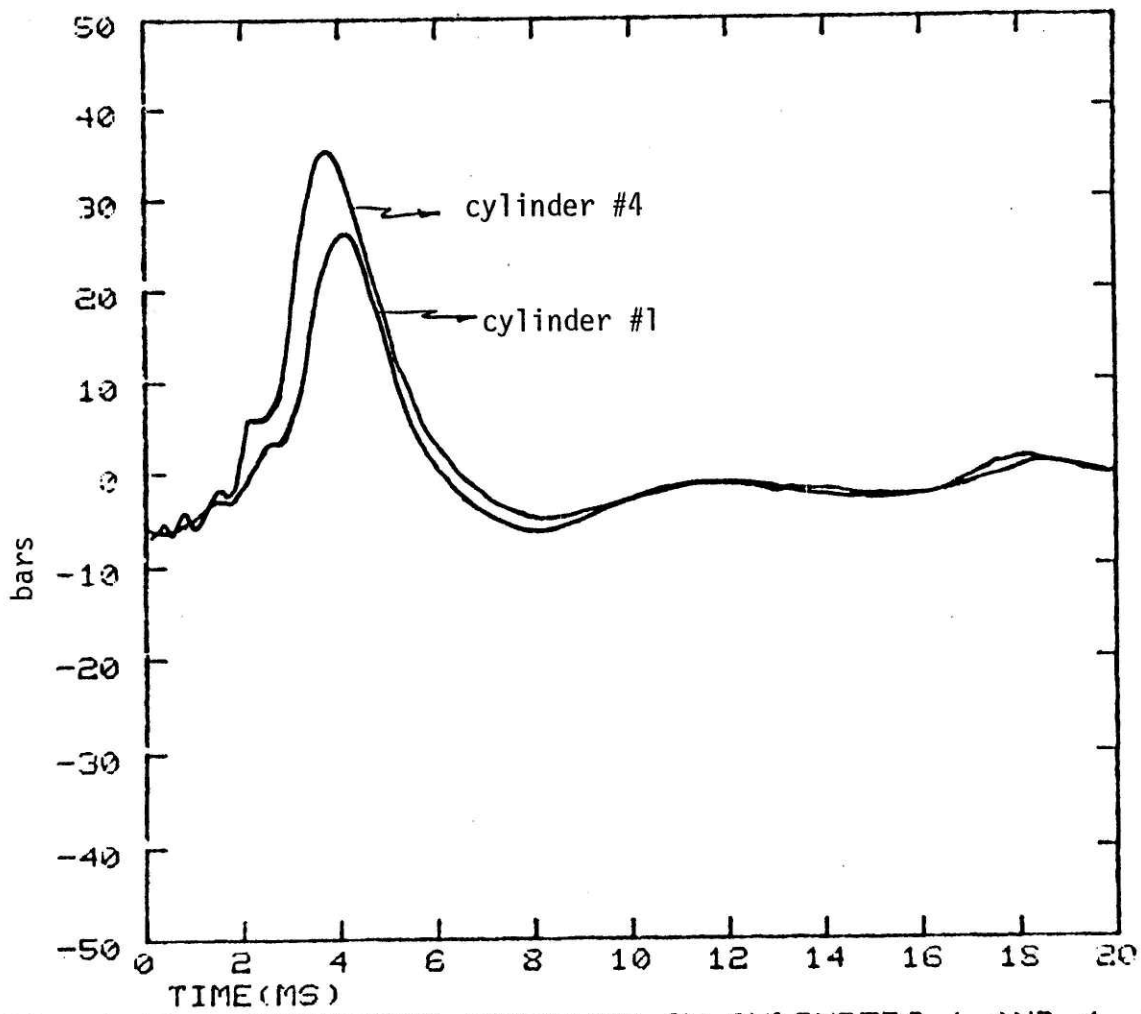

FIG. 4.15:- ESTIMATED PRESSURE IN CYLINDERS 1 AND 4, USING CEPSTRUM -- 1500 RPM, FULL LOAD

vantages are: only one VTF is needed to process the acceleration of all four cylinders; the effect of piston slap can be eliminated by proper cepstral filtering and the details in combustion cycle are not masked by the high energy of the compression cycle.

The properties of combination method are especially useful in monitoring engine operation where hardware devices can be used to speed up the processing.

4.8 Comparison of the VTFs -- Conclusion

Studying the performance of different VTFs in recovery of cylinder pressure is not only crucial in fault detection, but it is also useful in understanding the nature of vibration transfer in engines.

Although the DVTF was more successful than the SVTF in this study, further evaluation of the SVTF for other machines is encouraged. Certainly, the measurement of the SVTF has much to recommend it, and its ties to analytical modeling offers possibilities for parameter sensitivity analysis.

The magnitudes of spectra of SVTF and DVTF are similar. However, the phase of the two VTF are fundamentally different. The measuring and processing technique to obtain SVTF emphasizes the

accuracy of the magnitude and neglects the phase function which traditionally has been considered less important; especially the measured phase of SVTF at frequencies below 500 Hz, which is inaccurate. The problem with SVTF may be in the measuring technique rather than invalidity of assumption. SVTF is useful in many applications. It is worthwhile to measure SVTF using different techniques, such as exciting the engine with impulse source and then comparing it with measured DVTF. The accuracy in measuring phase should be emphasized.

The performance of DVTF2 in estimating pressure is better than that of the DVTF1 for all of the engine operating conditions considered (Tables IV-2 to IV-5). It is interesting to note that DVTF3 contains *less* information about VTF than DVTF1. Intuitively, DVTF1 should perform better than DVTF2. However, one of the principles in communication and detection theory states that *irrelevant information is noise*. If the magnitude part of DVTF is indeed irrelevant, its elimination improves the accuracy of estimation using DVTF.

The pressure signal found using DVTF4 confirms the above conclusion. DVTF4, which contains only magnitude information, performs very poorly in estimating pressure signal even at high load conditions when combustion is the dominant force.

The poor performance of DVTF3 indicates that not only the general form of the phase function, but its details are important. The details of phase function is associated with transfer paths as well as the effect of piston slap and motion of the piston during combustion process.

When two reasonably accurate estimates of a cylinder pressure are compared, PI5 is the only index which provides a quantitative measurement to indicate which of the two estimates is the "better". This is consistent with the theory that the information regarding the operation of the engine is concentrated in the first half of the cylinder pressure cycle. A PI that determines the variance of the estimated cylinder pressure with respect to the measured pressure around TDC is useful in studying the combustion on-set and process.

The conclusions of this Chapter are summarized as follows:

(a) Cylinder pressure can be recovered from block acceleration.

(b) The accuracy of the estimated pressure depends on the VTF used for deconvolving the acceleration and the operating condition of the engine. With the present processing method, in most cases, the cylinder pressure cannot be found *accurately* when the engine is operating under no loads.

(c) The phase of vibration transfer function constains *most* of the information necessary to recover the exciting force from acceleration signal. This phase information plus input inertance defines the VTF of the engine.

(d) The details of the phase of DVTF are function of transfer paths, time variation of the VTF as well as piston slap. Accuracy of the estimated pressure depends strongly to these details.

(e) The characteristics of the phase of DVTF is consistent and does not vary from one engine run to another. These characteristics are insensitive to practical variation in the engine assembly and normal wear during the life of the engine. The magnitude of DVTF varies from one engine cycle to another.

(f) Eliminating magnitude information in VTF improves the accuracy of the estimated cylinder pressure.

(g) The useful data regarding engine operation is concentrated in the first half of the cylinder pressure.

CHAPTER V: VIBRATION ANALYSIS IN FAULT DIAGNOSIS

The results obtained in Chapter IV showed that accurate reconstruction of cylinder pressure from block acceleration is possible. The changes in cylinder pressure as a result of malfunction are observed in the estimated pressure signal, and, therefore, are potentially usable to detect faults in the engine. The location of the fault is also identifiable by vibration analysis as previously discussed. Unfortunately, the effect of many engine malfunctions on cylinder pressure are only qualitatively known. Further studies on modeling the combustion process and the effect of various faults of engine on cylinder pressure will make the vibration analysis method very useful in fault diagnosis.

The effect of some types of engine malfunctions such as leaks in the injector, on cylinder pressure are known or are easy to simulate. To increase the accuracy of fault detection, the estimated pressure in each cylinder should be compared with the estimated pressure of other cylinders. A significant difference between the estimated pressure of traces for any of the cylinders signals a malfunction. Using several observation points also increases the accuracy and helps to localize and pinpoint the problem.

is an indication of a drastic change in the path. Several on-going studies are concerned with finding changes in VTF as a result of abnormalities in the path [27]. In order to distinguish between changes in combustion force and variation of VTF, from estimated cylinder pressure, at least two observation points are needed. The transfer paths between all cylinders and the two points should be different.

In the first section of this chapter, detection of faults in the engine is discussed. Changes in measured and estimated pressures as a result of injector leaks is studied by simulating the leak. A predictive method to separate the combustion force and piston slap is proposed. The generalization of vibration analyses method for fault detection in machinery is studied. The practical considerations such as using several observation points, speed and ease of computation and possibility of using micro-processors in on-line application, is the subject of the final section of this Chapter.

5.I Fault Diagnosis in Engine

Some of the engine malfunctions that are known to change cylinder pressures are injector leak or orifice problems, deposits inside the cylinder, and low quality fuel.

To study the effect of injector problems, especially leaks, the fault was simulated on the engine operating at 1500 rpm with approximately 60% load. For a small leak, the combustion cycle becomes less pronounced. In this case the power loss is negligible while the imbalance of cylinder pressure is significant which might damage the engine. When the leak becomes large, (more than 60%) the combustion cycle disappears and the cylinder pressure resembles the total shut off of the cylinder (Fig. 5.1). The power output of the engine drops drastically. The firing of the cylinders in both cases become irregular. The combination of these these two symptoms; irregular firing and imbalance of combustion in different cylinders, identifies the injector problem.

The procedure to detect simulated pressure leak from block acceleration is to compare the pressure estimatd for two cylinders: cylinder #1 (normal) and #4 (faulty) (Figs. 5.2 and 5.3, Table V-1).The change in combustion in faulty cylinders are as expected for small and large leaks. Both cylinder pressures were found using DVTF2.

Presence of deposits inside cylinder are associated with the decline in compression ratio and, therefore, general loss of power. The pressure signal of the faulty cylinder in this case is smaller than the others and has different combustion-to-compression cycle ratio. Low quality of the fuel causes extra delay in on-set of combustion cycle and changes the shape of this part of cylinder

TABLE V-1: COMPARISON OF ESTIMATED PRESSURES IN A NORMAL CYLINDER AND A CYLINDER WITH A LEAK IN THE INJECTOR

Leak	+PI	PI2	PI3	PI4	PI5
*Small	.67	.78	.51	.84	.325
*Substantial	.3	.65	1.8	2.75	1.7

+PIs are calculated for the malfunctioning cylinder with respect to the normally operating one.

*Power loss negligible. Imbalance of cylinders are main concern.

**Total power loss of the cylinder and substantial power loss of the engine.

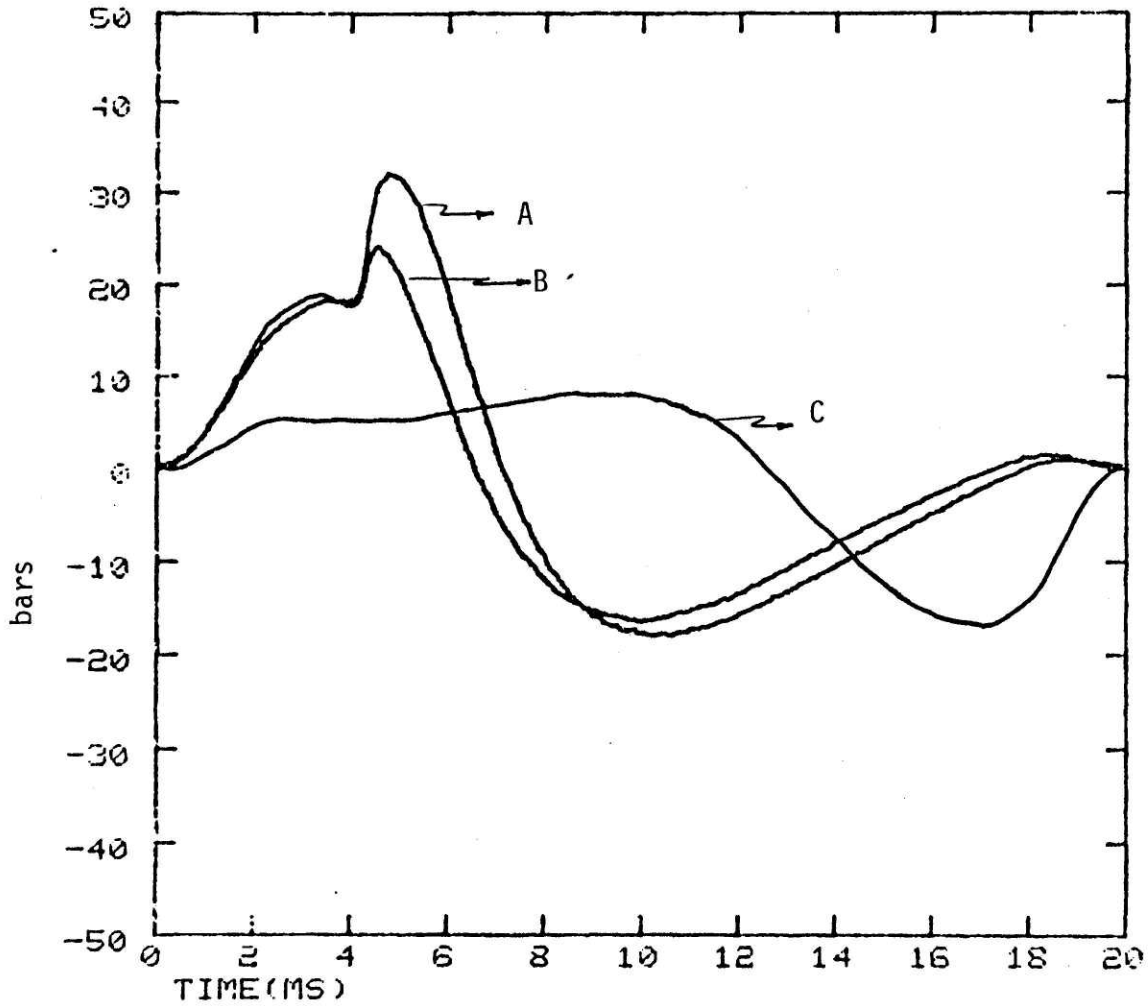

FIG. 5.1:- THE EFFECT OF INJECTOR LEAK ON CYLINDER PRESS.
A) NORM. CYL., B) SMALL LEAK, C) LARGE LEAK -- 60% INIT.LOAD

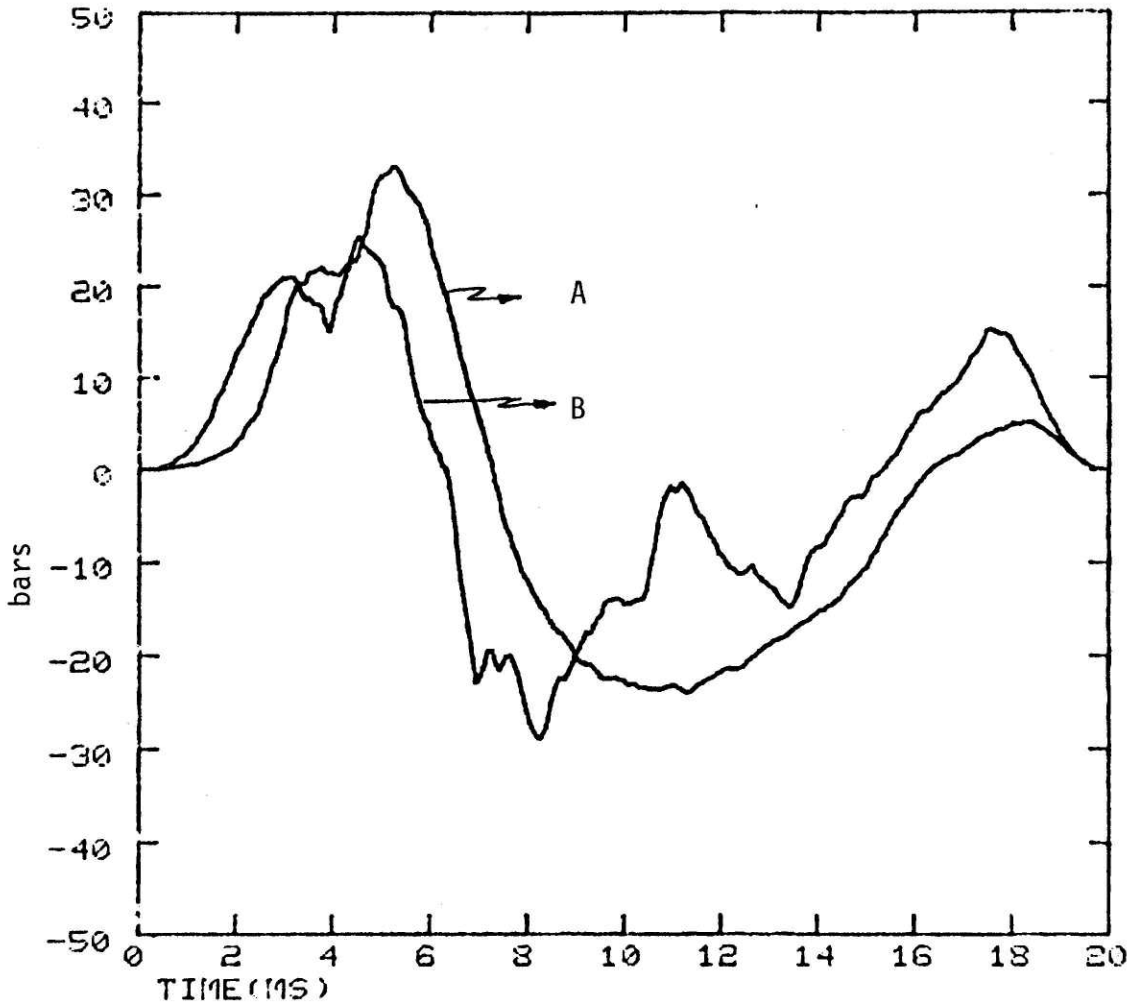

FIG. 5.2:- ESTIMATED CYLINDER PRESSURE AT 1500 RPM AND 60% LOAD, A) NORMAL CYL., B) CYL. WITH INJECTOR LEAK

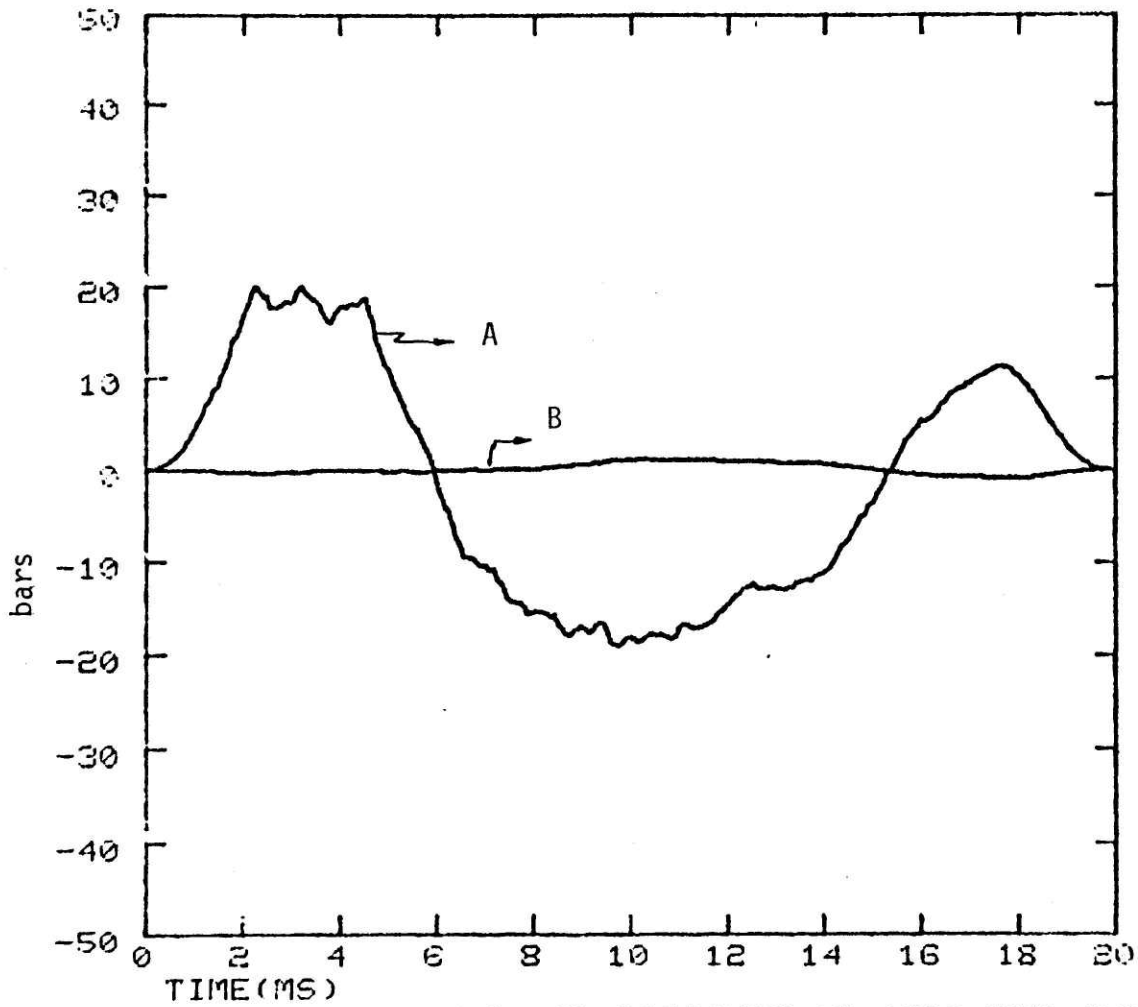

FIG. 5.3:-ESTIMATED CYLINDER PRESSURE AT 1500 RPM AND NO LOAD, A)NORMAL CYLINDER, B) CYL. WITH INJECTOR LEAK

pressure.

5.2 A Technique to Eliminate the Effect of Piston Slap

The relative time shift between combustion force and piston slap can be used to separate the effect of the two exciting forces. The technique proposed here is based on dividing the 180° crank angle time window into several frames; in this case, two, and analyzing the data in each frame by a preditive technique. Each frame contains only one source of excitation. The acceleration data in each frame except the first one contains the residue of acceleration from the previous frames. The effect of these residue acceleration can be eliminated.

The procedure can be summarized as follows:

(a) Define a VTF for each frame.

(b) Deconvolve acceleration at each frame with the frame VTF to find cylinder pressure.

(c) *Predict* the residue acceleration caused by the combustion force in the second frame by *convolving* the estimated pressure and VTF. Deduct this residue acceleration from the acceleration data of the second frame to get the acceleration caused only by piston slap.

The accuracy of the above-mentioned method depends on the time frames chosen and the technique used for convoltuion/deconvolution in the time frames. Fast convolution is not accurate for processing a short data. Calculation errors in the method may result in an unstable inverse for the VTF. Predictive methods, such as linear prediction, give good results in spectrum analysis and signal modeling of short time data. [28].

Predictive techniques are based on defining a model for the signal and finding the model parameters by minimizing the error between the hypothesized and real signal:

$$E = \sum_{n=0}^{M-1} (x(n)-\tilde{x}(n))^2 \quad n=0,\ldots,M-1 \tag{5.1}$$

$$\frac{\partial E}{\partial a_i} = 0$$

where $x(n)$ is the signal, $\tilde{x}(n)$ is the predicted signal using the model, M, is the number of data samples in the time frame and a_i is a model parameter. When the signal is impulse response of an all pole system, the set of simultaneous equations resulting from minimizing the errors are linear (linear prediction). Coefficients of this set of equations form a Toeplitz matrix [28]. There are powerful and efficient algorithms to solve a Toeplitz matrix.

The limiting factor in accurate estimation of cylinder pressure is the contaminating effect of secondary vibration sources, especially piston slap. Piston slap itself may be useful for detection of faults such as cylinder ring failure. Separation of combustion force and piston slap is the best solution to the limitation problem. Piston slap occurs 10° to 20° crank angle after TDC. This is when the cylinder pressure has started to fall and does not contain more useful information. This relative time shift suggests windowing the data before piston slap occurs.

The major problem with a short time record is that because of the slow phase speed of the medium at low frequencies, part of the vibration caused by combustion may remain outside of the window. Another problem is the computational errors caused by deconvolution of a very short data record. An appropriate solution is to use a shorter window of only 90° crank angle, and process the data by a predictive method similar to linear prediction [28]. Predictive methods give accurate results in spectrum analysis and modeling short data lengths. Such a technique adapted to the TF model of the engine is useful in this case.

Some engine problems are reflected in VTF, such as presence of cracks in a part of vibration transfer path. Detection of these types of faults is more difficult than problems reflected in combustion and piston slap. A notable change in VTF usually

Propagation impulse response of the engine has the form of equation 2.16. To find parameters of this model, the error as defined by Eq. 5.1 should be minimized:

$$\frac{\partial E}{\partial C_i} = 0, \qquad \frac{\partial E}{\partial x_i} = 0 \tag{5.2}$$

where x_i is the path length and C_i is the phase speed of the path. The set of simultaneous equations resulting from Eq. 5.2 is nonlinear. If C_i is assumed to be constant, the equations can be approximately solved by iterative optimization algorithms such as Fletcher-Powell [29]. The resultant impulse response is then used for deconvolving the acceleration signal. Deconvolution can also be done by a preditive method -- by hypothesizing a model for the cylinder pressure. The accuracy of the predictive technique depends on the model chosen for the signal, number of model parameters and a good initial guess for these parameters. Many of these factors are determined by trial and error.

The results of preliminary tests of the method with two time frames of 90° crank angle each, assuming 4 xi's with phase speed for 3/16 inch thick steel, is shown in Figure 5.4. The estimated pressure is not as accurate as the estimated pressure

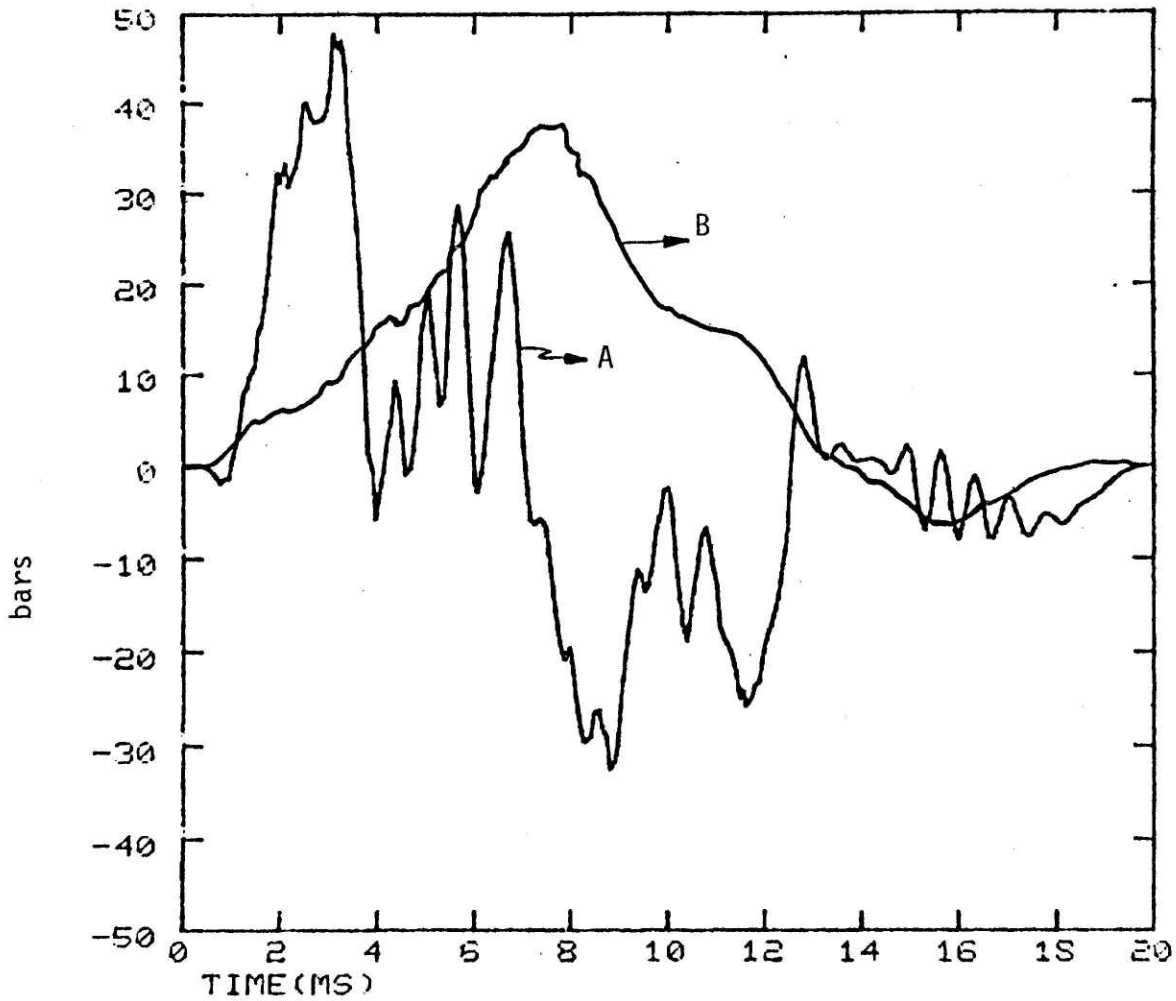

FIG. 5.4:-ESTIMATED CYLINDER PRESS. BY PREDICTIVE METHOD USING (A) MODEL VTF, (B) CEPST. SMOOTHED VTF -- 60% LOAD

using DVTF2 or DVTV1. One reason is inaccuracy of the model and its parameters. The results can be improved significantly by using a better VTF, e.g., a cepstrally smoothed VTF which represents a few propagation paths. The estimated pressure using a smoothed VTF with a 3 ms long symmetrical cepstral window is shown in Fig. 5.4. This method is promising in separating the effect of different sources on engine. The major problem at the present time is processing techniques and nonlinearity of simultaneous equations.

5.3 Fault Diagnosis in Machine Structure -- Generalization

The aim of this study is to define a method that is applicable to a variety of machines and/or systems from airplanes to sewing machines to the human body and not to focus on solving the particular problem of fault diagnosis in diesel engines. All these machines/systems share the same problem of defining a VTF that relates to the vibration measured at the periphy or surface of the system to the output signal of the vibration source inside the machine.

Vibration transfer function, VTF, of different machines are a combination of propagation and resonance. In practice one of the two VTF is dominant. Therefore, the stability of inverse filter can be guaranteed (See Chapter IV). As was shown, determining the correct form of VTF is critical in the ability to recover the excitation forces. The procedure followed in this study

seems to be appropriate in a variety of situations. The procedures are summarized as follows:

(1) Identify the important source(s) and study their characteristics.

(2) Study VTF, develop possible models.

(3) Measure VTF, modify if necessary to construct the modeled VTFs, giving special attention to the phase of VTF.

(4) Define a series of PIs based on the features in exciting signal which are essential for fault diagnosis.

(5) Test the peformance of each measured/constructed VTF by comparing the estimated input using the VTF with the measured or expected input.

(6) Choose the VTF with best performance, find the limitation and develop necessary processing techniques to overcome these limitations.

Once the proper VTF is chosen, it is possible to predict the changes in output vibration as a result of a change in excitation signal. In many cases similar to engine, the output acceleration signal is composite and the effect of faults are better seen and evaluated when the input signal is estimated from acceleration.

Characteristics of exciting source(s) affect the mode of vibration transfer in the machine. When the source(s) is impulsive and has a short duration, it is likely that there is substantial propagation in the machines. These characteristics also effect the processing technique and duration of data time window. Presence of secondary force(s) complicate the fault diagnosis, but as was shown even in the presence of these forces, recovery of exciting signal of a particular source may be possible.

5.4 Practical Consideration

A fault diagnosis scheme is designed to be used in industrial environment and for on-line monitoring. The practical considerations in successful implementation of the system are, processing time, computation ease, reliability of the method, number and location of the sensors and cost effectiveness.

The fast convolution technique that has been used extensively in this study is fast and sufficiently accurate. This type of processing requires computation of two Fourier Transforms (one forward and one inverse) and complex multiplication/division of two arrays. Both types of arithmetic can be done by commerically available hardware devices [30]. These hardware devices decrease the computation time for each FFT to 3ms [31]. Therefore, the whole process including data access time and preprocessing takes about 7 to 8 ms. This is fast enough for on-line monitoring. A number

of commercially available microprocessor can be easily programmed to do the processing, including calculation of PIs . Using techniques other than fast convolution for deconvolution such as J. Allen's method would increase the accuracy of the processing at the cost of the speed [32]. Depending on the application, one might be willing to sacrifice the speed or develop special hardware to perform the computation.

Choosing the number and location of sensors is another important practical consideration. Using several observation points will increase the confidence in the results. However, it would also increase the processing time and requires larger computer/ processor memory size to store necessary VTFs, as well as intermediate results of processing. An optimum number of sensors should be selected. Choice of the location of sensors is crucial. One requirement is the easy access, another is the expected signal to noise of the data measured at the point. In this study 8 observation points were chosen initially. Later the number of these points were reduced by 2, by trial and error. The basis of location choice was a guess rather than any optimization procedure. A thorough theoretical study on response of the surface of the machine is at least a good initial step in finding an optimum location of the sensors.

Reliability is another practical consideration. It has been shown that VTF of the engine does not change from one engine run to another and remains accurate for fault detection during a moderate period of engine operation under normal wear. However, sensitivity of VTF to small changes in sensor location is an issue that should be addressed. Variation of VTF from one engine to another engine of the same brand and design to the other engines with slightly different designs, play an important role in industrial application.

CHAPTER VI: CONCLUSION

Monitoring and diagnosis of faults in a complicated machine without interrupting its operation is essential in many industrial and research applications of machines. An analytical approach to vibration analysis in machines for detection of faults has many advantages over the data base method; such as increase in speed of computation, eliminating the need to collect and store a large amount of data and the ability to detect faults even when a similar problem has never before occurred. The method has been considered impractical because of the difficulties in obtaining a sufficiently accurate VTF for machine structures with complicated geometry.

The aim of this study was to demonstrate the feasibility of the analytical approach to fault detection using vibration signal on the surface of the machine. The goal was achieved by accurate reconstruction of cylinder pressure trace of a diesel engine from measured acceleration on the engine block. Vibration transfer mechanisms in the engine is made up of traveling wave propagation and multiple echoes from system boundaries of resonance vibration. The VTF of both modes of vibration transfer, propagation and resonance was modeled. The VTF was measured on non-running engine as well as operating engine. The VTF measured on operating engine,

DVTF1, was modified to construct three other VTFs, one representing multipath wave propagation DVTF2, one single path wave propagation DVTF3, and one pure resonance DVTF4.

The cylinder pressure under several operating conditions of the engine was estimated by deconvolving the measured acceleration from the five VTFs. The accuracy of estimation was determined by comparing estimated and measured pressure signals. Several performance indices, PIs, was defined for quantitative evaluation of the estimated pressures using different VTFs. The results using SVTF were acceptable when the engine was under 60% or more load. The accuracy of estimated pressure was improved substantially by using DVTF1. But the most accurate estimate of cylinder pressure under all engine operating conditions was obtained using the DVTF2 which represents the multipath propagation. The accuracy of pressure estimate declines with engine load and becomes unacceptable for loads less than 10%. DVTF2 was found to remain unchanged during a reasonable period of engine life. It is insensitive to practical variation in engine assembly.

The vibration analysis was used to detect simulated injector leaks. The malfunction and the location of the faulty cylinder was detected using DVTF2. A technique to separate the excitation of combustion force from that of the secondary vibration sources such as piston slap was proposed. The analysis method was generalized

for fault detection on other machines. Practical considerations such as usage of several observation points, ease and speed of processing and the possibility of using microprocessors were determined.

The conclusions of this study are as follows:

(1) Accurate reconstruction of exciting force(s) in a machine and identifying the location of the source is feasible. The key is to find the dominant mode of vibration transfer in the particular machine and at the observation point. For the diesel engine studied, the vibration transfer mode is propagation rather than resonance.

(2) At the present time, detection of faults in excitation source of a machine which has more than one source is limited to cases where the source under study is dominant, there is a known time delay between excitation of sources or the sources are separated spatially and VTF to all of the sources are known. The limit is the engine load which has to be high enough for combustion to become the dominant force. In many cases, part of this limitation can be overcome by using more sophisticated processing techniques and special properties of the VTFs.

(3) Preserving details of transfer paths is necessary.

(4) A general and rather simple and fast processing method such as fast convolution can give satisfactory results.

The above conclusions, obtained for a diesel engine, are generalized for a variety of machines.

The vibration analysis method studied in this work is a powerful tool in diagnosis of fault and monitoring the status of a machine whenever access to the source and/or interruption of the operation of the machine is impractical or impossible. The procedure is simple and straightforward. By using special hardware, processing devices and microprocessors, the method can be simplified further for industrial use. If the processing speed is increased, the reconstructed output signal of a part of a system can be used in a feed back loop.

The method is useful in quality control on assembly lines. Measuring acceleration on the block of an engine is much easier than mounting a pressure transducer *inside* the cylinders of an engine. The operation of various parts of a machine can be checked accurately at any point on the assembly line.

In acoustics, vibration analysis method is useful in source identification, when VTF of the structure for different sources

are known. The effect of modification in source and/or path of a machine on surface vibration can also be studied by this method.

This study has achieved its goal of demonstrating the feasibility of analytical approach to vibration signature analysis as well as discovering some of the advantages, potentials and limitations of the method. In a sense this is a pilot study. Further development of the method requires more study in the field. Some of the research areas in the vibration analysis field are as follows:

(a) Observation point(s) -- an optimum number and location(s) of sensors is an important factor in application of vibration signature analysis. Theoretical and experimental studies on VTF and mechanics of the system is required for determining the optimum location of sensor(s) to detect particular faults. Increasing the number of observation points increase the processing time and total cost of implementing the procedure. Therefore, optimizing number of sensors is necessary.

(b) VTF -- to generalize the results obtained on a machine to similar structures the exact relationship between VTF and physical properties of the machine structure and statistical variation of VTF with these properties

should be determined. Experimental and theoretical study on variation of VTF from one machine to another and from one design or brand to the others is also necessary. Sensitivity of VTF to small variation in location of sensor(s) is another topic for research.

(c) Measuring and processing techniques -- development of parametric (Predictive) processing techniques such as the one proposed in Chapter V and usage of cepstrum analysis reduces the limitation of the analysis method. Developing both types of processing techniques requires careful study of the signals involved. An alternate measuring technique for determining SVTF is required to increase the accuracy of the VTF phase.

(d) Specific fault(s) -- Effect of specific faults in the source signal should be determined theoretically and/or experimentally. Study on the physical nature of the process that produces the signal, e.g., combustion enables the prediction of effect of faults/modification on the output signal of the source.

(e) Multiple faults -- contaminating effect of multiple faults on diagnosis and a procedure to separate these faults is another research topic.

(f) Automatic pattern recognition -- the analysis method ultimately is used for automatic diagnosis of faults

and monitoring. Developing a pattern recognition scheme and determining the criteria for detection of faults by computing performance indices such as the one discussed in this study is the subject of research in automatic pattern recognition.

REFERENCES

1. Challen, B. "The Effect of Combustion System on Engine Noise", SAE Paper, 750798, Society of Automotive Eng., 1975.

2. Willsky, A. S., "A Survey of Design Methods for Failure Detection in Dynamic Systems", Automation, Vol. 12, pp. 601-611.

3. DeJong, R. G., "Vibration Energy Transfer in a Diesel Engine", ScD Thesis, Dept. of Mech. Eng., August 1976.

4. Baxter, R. L., et al., "Vibration Tolerances for Industry", ASME Publication #67-PEM-14, Feb. 2, 1967.

5. Report Published in *Journal of Mechanical Engineering*, Jan. 1980.

6. Saxe, R. F. et. al, "Acoustic Noise Measurements in the Fuel Failure Mock Up Facility, L and C Annual Progress Report, OAK Ridge National Lab., Sept. 1974.

7. Galotto, C. P., et. al., "The Use of a Logic Electronic Device for Detection and Evaluation of Mechanical Defects of Vehicle Gearboxes in the Inspectrion Room, ASME Publication #740951, Oct. 1974.

8. Randal, B., "Cepstrum Analysis and Gearbox Fault Diagnosis", B&K Application Note, 1972.

9. Downham, E., Woods, R., "The Rationale of Monitoring Vibration on Rotating Machinery in Continuously Process Plant", ASME Paper No. 71, - Vib - 96, June 1971.

10. Vandiver, K. , "Detection of Structural Failure on Fixed Platforms by Measurement of Dynamic Response", *J. of Petroleum Technology*, March, 1977, pp. 305-308.

11. Tribolet, J. "Seismic Application of Homomorphic Signal Processing", ScD Thesis, Dept. of Elect. Eng., Mass. Inst. of Tech., May 1977.

12. Chung, J. Y., Crocker, M. J. and Hamilton, J. F., "Measurement of Frequency Response and the Multiple Coherence Function of the Noise Generation System of a Diesel Engine, *J. Acoust. Soc. Am.*, Vol. 58, No. 3, Sept. 1975, pp. 7-12.

REFERENCES (CONTINUED)

13. Oguchi, T., "Piston Slap Noise: Its Transfer Through an Internal Combustion Eng.", MSc Thesis, Mass. Inst. of Tech., Dept. of Mech. Eng., February 1979.

14. Obert, E. F. *Internal Combustion Engines and Air Pollution,* Harper and Row, 1973, Chapter 5.

15. Okamura, H. "Experiments on Transmission Paths and Dynamic Behavior of Engine Structure Vibration, Part I" *J. Acoust. Soc. Am.,* Vol. 67, No. 2, Feb., 1980.

16. Obert, E. F. *Internal Combustion Engines and Air Pollution,* Harper and Row, 1973, Chapter 15.

17. Lightly, L. C. *Combustion Engine Process,* McGraw Hill Book Co., New York, 1967.

18. Oppenheim, A. V. and Schafer, W. R. *Digital Signal Processing,* Prentice Hall, Inc., Englewood Cliff, N. J., 1975.

19. Cremer, L. and Heckl, M. *Structure Borne Sound,* Springer-Verlag, Berlin, 1973.

20. Slack, J. W. Personal Contact.

21. Bendat, J. S. and Piersol, A. G., *Random Data: Analysis and Measurement Procedure,* Wiley and Sons, Inc., New York 1971.

22. Cooley, J. W. and Dolan, M. T. "Fast Fourier Transform Subroutines", in *Programs for Digital Signal Processing,* IEEE Press, 1979.

23. DeJong, R. and Parsons, N. E., "High Frequency Vibration Transmission through the Moving Parts of an Engine", Paper submitted for publication.

24. Hickling, R., et al. "Knock Induced Cavity Resonances in Open Chamber Diesel Engine", *J. Acoust. Soc. Am., 65,* No. 6, June, 1979, pp. 1474-1480.

25. Tribolet, J. M. "A New Phase Unwrapping Algorithm", IEEE Trans. on ASSP, Vol. 25, No. 2, April 1977, pp. 170-177.

26. Claerbout, J. *Fundamentals of Geophysical Data Processing,* McGraw Hill, 1976.

REFERENCES (CONTINUED)

27. Kampble, B. "Estimation of Natural Frequencies and Damping Ratios of Off Shore Structures", PhD Thesis, Mass. Inst. of Tech., Dept. of Ocean Eng., May, 1980.

28. Makhoul, J., "Linear Prediction: A Tutorial Review", IEEE Trans. on ASSP, Vol. 63, April 1975, pp. 561-580.

29. Fletcher, R. and Powell, M.J.D., "A Rapidly Convergent Descent Method for Minimization", *Comput. J.*, Vol. 6, pp. 163-168, 1963.

30. Wu, Y. S., "Architectural Consideration of Signal Processor and Microprogram Control", 1972, Spring Joint Comput. Conf. Proc. Vol. 40, 1972, pp. 675-683.

31. Bergland, G. D., "Fast Fourier Transform Hardware Implementation -- an Overview", IEEE Trans., *Audio Electroacoustics*, Vol. Au-17, pp. 104-108, June, 1969.

32. Allen, J., Rabiner, L. R., "On Implementation of a Short Time Spectral Analysis Method for System Identification", IEEE Trans. on ASSP, April, 1980.

APPENDIX A: THE INSTRUMENTS USED

Transducers:

B & K 2 gram accelerometer model 4344

B & K 14 gram accelerometer model 43

Amplifers:

Preamplifers:

B & K charger amplifiers models: 2628, 2635

Itheco step amplifier model: 432, 451

Power Amplifier:

McIntosch model MC40

Tape Recorder:

Nagra model IV-SJ

Filters:

Itheco 1/3 octave bandpass filter model 4113

Shaker, Impedance head:

Wilcoxon model F7/F4

Noise Generator:

IVIE Electronics model IE208

APPENDIX B: ENGINE SPECIFICATIONS

Engine:	John Deer model 4219D
Type:	Naturally aspirated diesel engine
Usage:	Farming
Number of cylinders:	Four
Injection:	Direct
Compression ratio:	16.8:1
Bore:	102 cm
Stroke:	11 cm
Displacement:	35 90 cm^3
Rated Speed:	2500 rpm
Normal speed range:	1500-2500
Dimensions (WXHX L):	50.09 x 81.26 x 83 cm

APPENDIX C : PROGRAMS

PROCES

SUBROUTINES :

INP,PFFT,PIFFT,AFFT,CPICTR,DCOUT,SAVOUT

```
R

C       THIS PROGRAM IS PROC
        EXTERNAL OV1,OV2,OV3
        COMMON / / XT(4,256),XSC(256)
        COMMON/FREK/ XF(7,256)
        DIMENSION XAT(4),XAF(4),NFIL(7)
        DIMENSION NFIX(5,2),NFIY(5,2),ITITL(14) ,IOFLN(7)
        COMMON/PRJ/PI,NPTS,NPTSF,LN
        COMMON /PPO/ XAT,XAF,NL(40),NFIX,NFIY
        DATA PI,NPTS,NPTSF,LN/3.141592,256,256,9/
        DATA XAT(1),XAT(3),XAT(4),XAF(1)/0.,-1.,1.,0./
        DATA NFIX,NFIY/'FREQ (HZ)  TIME(MS) ','MAG. (DB)  PHASE          '/
        DO 110 I=1,40
110     NL(I)=0
        ICN=7
        CALL OVOPN(ICN,'PROCES.OL',IER)
1       WRITE(10,500)
500     FORMAT (1X,'ENTER PROCESSING FUNCTION : ',//,10X,
     &          'CONVOLUTION (Z=X.Y) ------ 1, DECONV. (Z=Y/X) ------ 2 ',/,m
```

```
      IF(IFU.EQ.3) IFP=4
      CALL DISKA(4,'FTEMP.DA')
      CALL DISKA(5,'TTEMP.DA')
      DO 215 I=1,4
      IB=(I-1)*2
      I1=I+1
      CALL RBLK(4,IB,XSC(1),2)
      CALL RVCOP(1.,0,XSC(1),2,XF(I1,1),14,256,1,0)
215   CONTINUE
      CALL DISKC(4)
      CALL RVCOP(XF(2,1),14,XF(4,1),14,XF(6,1),14,NPTSF,IFM,0)
      CALL RVCOP(XF(3,1),14,XF(5,1),14,XF(7,1),14,NPTSF,IFP,0)
      DO 320 I=1,NPTSF
      IF(XF(7,I).LT.-180.) XF(7,I)=XF(7,I)+360.
      IF(XF(7,I).GT.180.) XF(7,I)=XF(7,I)-360.
320   CONTINUE
      ACCEPT 'TYPE 1 IF YOU WANT IDFT OF OUTPU ',IDF
      IF(IDF.NE.1) GO TO 21
      CALL OVLOD(ICN,OV1,-1,IER)
       CALL PIFFT(-1)
C     CALL RVCOP(1.,0,XSC(1),2,XT(4,1),8,NPTS,1,0)
21    DO 30 J=1,256
30    XT(1,J)=DT*FLOAT(J-1)
      DO 225 I=1,3
      IB=(I-1)*2
      CALL RBLK(5,IB,XSC(1),2)
225   CALL RVCOP(1.,0,XSC(1),2,XT(I+1,1),8,256,1,0)
      CALL DISKC(5)
      DO 130 KJ=1,256
130   XF(1,KJ)=DF*FLOAT(KJ-1)
      IF (IFU.NE.3) GO TO 99
C                CALCULATING CORRELATION COEFF.
      X2=0.
      Y2=0.
      DO 220 J=1,NPTSF
      X2=X2+XT(2,J)*XT(2,J)
      Y2=Y2+XT(3,J)*XT(3,J)
220   CONTINUE
      X2=SQRT(X2/FLOAT(NPTSF))
      Y2=SQRT(Y2/FLOAT(NPTSF))
      RXY=1./(2.43576*X2*Y2)
      CALL RVCOP(RXY,0,XT(4,1),8,XT(4,1),8,NPTSF,1,0)
      AXY=Y2/X2
      DO 1005 I=1,NPTSF
      XA=XT(2,I)/X2-XT(3,I)/Y2
      XA=XA*XA
      PI3=(PI3*FLOAT(I-1)+XA)/FLOAT(I)
      IF(I.GT.NPTSF
```

```
                    F(NP.NE.1) GO TO 108
98      CALL OVLOD(ICN,OV2,-1,IER)
        WRITE (10,505)
505     FORMAT(1X,' ENTER TITLE FOR THE GRAPH : ',Z )
        READ (11,600) ITITL(1)
600     FORMAT(S27)
        CALL CPICTR
506     FORMAT (30X,S27,///)
        WRITE(10,506) ITITL(1)
        ACCEPT 'TYPE 1 IF YOU WANT ANOTHER PLOT ',IAP
        IF (IAP) 108,108,98
 108    ACCEPT 'TYPE 1 TO SAVE OUTPUT DATA  ',IOS
        IF (IOS.NE.1) GO TO 119
        CALL OVLOD(ICN,OV3,-1,IER)
        CALL SAVOUT
119     TYPE'ENTER NEXT STEP :'
        TYPE '        NEW INPUT X---1,NEW INPUT Y ---2 '
        TYPE '        NEW PROCES --- 3 ,QUIT -----4 '
        ACCEPT INS
        GO TO (77,78,1,109),INS
 109    CALL CLOSE(7,IER)
        STOP
        END
9
!BRFNFRice        #JIM87FRC.
:       HITC01SRccNASA1RB*`w
```

```
C
C       THIS IS SUBROUTINE INP(IX)
C               THIS SUBROUTINE WILL READ THE DATA IN FOR PROCESSING
C
C               A. ORDUBADI ,DEC. 1979
C
        SUBROUTINE INP(IX)
        EXTERNAL OV1,OV2,OV3
        DIMENSION NFIL(7),XFD(2,256),XS(256),IFX(7)
        COMMON / /XSE(512),XSC(256),XS,XFD
        COMMON/PRJ/PI,NPT,NPF,NL
        IXB=(IX-1)*4
        IXT=(IX-1)*2
        WRITE(10,101)
101     FORMAT(1X,'ENTER DATA FILE NAME :',Z)
        READ (11,201) NFIL(1)
201     FORMAT(S13)
        WRITE(10,102)
102     FORMAT(1X,'ENTER DATA FILE TYPE, TIME=1 ,FREQ=2 ,MOBILTY=3 :',Z)
        ACCEPT ITY
        GO TO (21,21,22),ITY
21      CALL OVLOD(7,OV1,-1,IER)
        IK=2-ITY
        CALL RFT(NFIL,IK)
        GO TO 23
22      CALL RFF(NFIL,1,IFX)
23      ACCEPT 'ENTER GAIN IN DB',GAIN
        GT=10**(GAIN/20.)
        GAIN=GAIN+40.5
        TYPE 'TYPE 1 IF YOU WANT TO TAKE OUT LINEAR PHASE(TIME DELAY) :'
        ACCEPT ITD
        IF (ITD.NE.1) GO TO 25
        ACCEPT 'ENTER TIME DELAY (MS) ',TD
        DFI=360.*TD*12.5/FLOAT(512)
        DO 100 I=1,NPF
        XFD(2,I)=XFD(2,I)-DFI*FLOAT(I-1)
        IF(XFD(2,I).LT.-180.) XFD(2,I)=360.+XFD(2,I)
        IF (XFD(2,I).GT.180.) XFD(2,I)=XFD(2,I)-360.
100
```

```
,IXB,XSC(1),2)
 CALL RVCOF(1.,0,XFD(2,1),4,XSC(1),2,NPF,1,0)
 IXB2=IXB+2
 CALL WBLK(4,IXB2,XSC(1),2)
 CALL RVCOF(GT,0,XS(1),2,XSC(1),2,NPT,2,0)
 CALL WBLK(5,IXT,XSC(1),2)
 CALL DISKC(4)
 CALL DISKC(5)
 RETURN
 END
R
```

```
      OVERLAY OV2
      SUBROUTINE CPICTR
      COMMON / /XT(4,256),ITITL(30,3)
      COMMON/FREK/XF(7,256)
      COMMON/AFF/KV(4),IX(4)
      COMMON/PPO/XAT(4),XAF(4),NL(40),NFIX(5,2),NFIY(5,2)
      DATA IX,KV/'1 2 3 4 ','A,B,C,D'/
      TYPE ' ENTER WHICH CURVES DO YOU WANT TO PLOT(UP TO 3) : '
      TYPE ' INPUT X(MAG)------- 1 , INPUT X (PHASE) -------- 2 '
      TYPE ' INPUT Y(MAG) -------- 3 , INPUT Y(PHASE) --------- 4'
      TYPE ' OUTPUT(MAG.) --------- 5 , OUTPUT (PHASE) -------- 6 '
      TYPE ' INPUT X(TIME) ------ 11  , INPUT Y (TIME) -------- 12'
      TYPE ' OUTPUT (TIME) ------ 13 '
      ACCEPT 'NP',NP1,NP2,NP3
      ACCEPT 'ENTER NO. OF LABEL LINES ',IL
      DO 50 I=1,IL
      WRITE(10,505),I
      READ(11,506) ITITL(1,I)
50    CONTINUE
505   FORMAT(1X,'ENTER LINE ',I4)
506   FORMAT(S59)
      IF(NP1.GT.10) GO TO 4
      NV=-1*2**NP1
      IF(NP2.NE.0) NV=NV-1*2**NP2
      IF(NP3.NE.0) NV=NV-1*2**NP3
      ACCEPT 'YMIN,YMAX ?',XAF(3),XAF(4)
      IK=((NP1/2)*2)-NP1+2
      DO 45 I=1,5
      NL(I+35)=NFIY(I,IK)
      NL(I+10)=NFIX(I,1)
45    CONTINUE
      CALL PICTR(XF,7,NL,XAF,NV,256,1,-1,-4,-2,FT,IX,KV)
      GO TO 6
4     NV=-1*2**(NP1-10)
      IF(NP2.NE.0) NV=NV-1*2**(NP2-10)
      IF(NP3.NE.0) NV=NV-1*2**(NP3-10)
      ACCEPT 'YMIN,YMAX ',XAT(3),XAT(4)
      DO 35 I=1,5
      NL(I+35)=0
35    NL(I+10)=NFIX(I,2)
      CALL PICTR(XT,4,NL,XAT,NV,256,1,-1,-4,-2,FT,IX,KV)
6     DO 100 I=1,IL
      WRITE(10,507) ITITL(1,I)
100   CONTINUE
507   FORMAT(15X,S59)
      RETURN
      END
R
```

CEPSTR

SUBROUTINS :

COMPCEP ,PHAUNW,PHCHK,SPCVAL

```
C
C                  PROGRAM CEPSTRUM
C
      EXTERNAL OV1,OV2,OV3,OV4,OV5
      COMMON / /AUX(512),XI(512),XNI(512),XF1(2,256),XF2(2,256)
      COMMON / PLOT/XAF(4),XAT(4),NL(40),DT,DF
      COMMON /PRJ/PI,NPTS,NPTF,LN
      COMMON /WIND/TW,TWM
      DATA NPTS,NPTF,LN/512,256,9/
      ICH=7
      CALL OVOPN(ICH,'CEPSTR.OL',IER)
      CALL OVLOD(7,OV1,-1,IER)
      CALL INOUTC(1,1)
      TYPE'ENTER FUNCTION ,REAL CEPST.=1, COMPLEX CEPS.=2'
      ACCEPT IFUNC
      NPTF1=NPTF+1
      ACCEPT 'SAMPLING FREQ.,TIME WINDOW ',SR,TW
      ACCEPT 'ENTER TIME WINDOW FOR PLOTTING  ',TWM
      DF=SR/512
      DT=TW/256
      XAF(1)=0.
      XAT(1)=-TWM
      XAT(2)=TWM
      IF(IFUNC.EQ.2) GO TO 71
      DO 130 J=1,NT=<k;k01(1,J)*XF1(1,J)+XF1(2,J)*XF1(2,J)
      XF1(1,J)=.5*ALOG(AMAG)
      XF1(2,J)=0.
130   CONTINUE
      GO TO 51
71    CALL OVLOD×VLOD(7,OV2,-1,IER)
      C
```

```
          hF (IPL.NE.1) GO TO 81
61        CALL OVLOD(7,OV3,-1,IER)
          CALL CPIC1(ID)
81        TYPE 'TYPE 1 IF YOU WANT TO WINDOW THE CEPSTRUM'
          ACCEPT IWC
          IF (IWC.NE.1) GO TO 91
          CALL OVLOD(7,OV2,-1,IER)
          CALL CEPSMOT
91        ACCEPT 'TYPE 1 IF YOU WANT ANOTHER PLOT ',IPA
          IF(IPA.EQ.1) GO TO 61
          TYPE 'DO YOU WANT TO SAVE OUTPUT ?'
          TYPE '     0=NO ,1=SAVE CEPST., 2=SAVE INV. CEPST.'
          ACCEPT ISAV
          IF (ISAV.EQ.0) GO TO 999
          CALL OVLOD(7,OV1,-1,IER)
          CALL INOUTC(2,ISAV)
999       CALL CLOSE(7,IER)
          STOP
          END
R
```

```
TYPE COMCEP.FR
C
C                SUBROUTINE COMCEP TO COMPUT COMPLEX CEPSTRUM
C       OF A SIGNAL
C                METHOD : TRIBOLET, QUATIERI
C
C
C                A. ORDUBADI ,DEC. 1979
C
        OVERLAY OV4
        SUBROUTINE COMCEP
        LOGICAL ISSUC
        COMMON/ / AUX(512),XS(512),XNS(512),XF1(2,256),XF2(2,256)
        COMMON/PRJ/ PI,NPTS,NPTF,LN
        COMMON/TRES/TWOPI,THLINC,THLCON,DVTMN2,N,L,H,H1
        DATA THLINC,THLCON/2.,1.2/
C
C                INITIALIZING
C
        TWOPI=PI*2.
        ISNX=1
        IF(XF1(1,1).LT.0.) ISNX=-1
        N=13
        L=2**N
        H=FLOAT(L)*FLOAT(NPTS)
        H1=PI/H
        ISSUC=.TRUE.
        XR1=XF1(1,1)
        XI1=XF1(2,1)
        XNR1=XF2(1,1)
        XNI1=XF2(2,1)
        AMAG=XR1*XR1+XI1*XI1
        PPDVT=PHADVT(XR1,XI1,XNR1,XNI1,AMAG)
        PPHASE=0.
        XF1(1,1)=.5*ALOG(AMAG)
        XF1(2,1)=0.
        PPV=PPVPHA(XR,XI,ISNX)
        DVTMN2=0.
C
        DO 50 I=2,NPTF
        XR=
```

```
T
      DVTMN2=DVTMN2+PDVT
50    CONTINUE
      DVTMN2=(2.*DVTMN2)/FLOAT(NPTF)
      TYPE 'DVTMN2 =', DVTMN2
      DO 100 I=2,NPTF
      PPV=PPVPHA(XF1(1,I),XF1(2,I),ISNX)
      PDVT=XF2(2,I)
      PHASE=PHAUNW(ISNX,I,PPHASE,PPDVT,PPV,PDVT,ISSUC)
      IF(ISSUC) GO TO 40
      TYPE 'PHASE UNW UNSU @ POINT',I, 'PHASE=',PPHASE
      ISO=ISO+1
      PHASE=PPHASE
40    PPDVT=PDVT
      PPHASE=PHASE
      XF1(1,I)=.5*XF2(1,I)
      XF1(2,I)=PHASE
100   CONTINUE
      IF(ISO.LE.4) GO TO 95
      TYPE 'PHASE UNWRAPPING UN SUCCESFUL  ',ISO
95    ISFX=(ABS(PPHASE/PI)+.1)
      IF(PPHASE.LT.0.) ISFX=-ISFX
      TYPE ''
      TYPE ' LINEAR PHASE = ',ISFX
      H=PPHASE/FLOAT(NPTF)
      ACCEPT'TYEP 1 IF YOU WANT TO TAKE LINEAR PHASE OUT ',ILP
      IF (ILP.NE.1) H=0.
      DO 120 I=1,NPTF
      AUX(I)=XF1(2,I)
      XF1(2,I)=XF1(2,I)-H*FLOAT(I-1)
      AUX(I)=AUX(I)*57.29578
      J=I+NPTF
      AUX(J)=XF1(2,I)*57.29578
120   CONTINUE
      CALL DISKA(3,'FTEMP.DA')
      CALL WBLK(3,0,AUX(1),4)
      CALL DISKC(3)
      RETURN
      END
R
```